Experimental and Simulation Studies of Industrial Scale Finishing Reactive Distillation Column

Thesis submitted

for the award of the degree

of

Doctor of Philosophy

by

Damandeep Singh
(Regn. No.: 90701508)

Under the guidance of

Dr. Raj Kumar Gupta
Associate Professor
Department of Chemical Engineering
Thapar University Patiala
Patiala-147004, India

Dr. Vineet Kumar
Professor
Department of Chemical Engineering
Indian School of Mines, Dhanbad
Dhanbad-826004, India

Department of Chemical Engineering
Thapar University Patiala
Patiala-147004, Punjab, INDIA
www.thapar.edu

CERTIFICATE

This is to certify that thesis entitled "**Experimental and Simulation Studies of Industrial Scale Finishing Reactive Distillation Column**", being submitted by Mr. Damandeep Singh, to the Department of Chemical Engineering, Thapar University, Patiala in partial fulfillment for the award of degree of **Doctor of Philosophy**, is a record of bonafide research work carried out by him. Mr. Damandeep Singh has worked under our guidance and supervision and has fulfilled the requirements for the submission of this thesis, which to our knowledge has reached the requisite standard.

The results embodied in the thesis have not been submitted in part or full to any other university or institute for the award of any diploma or degree.

Dr. Raj Kumar Gupta
Associate Professor
Department of Chemical Engineering
Thapar University Patiala
Patiala-147004, India

Dr. Vineet Kumar
Professor
Department of Chemical Engineering
Indian School of Mines
Dhanbad-826004, India

ACKNOWLEDGEMENTS

I am highly grateful to the authorities of Thapar University, Patiala and IOL Chemicals and Pharmaceuticals Limited, Barnala for providing this opportunity to carry out the present research work. I got the opportunity to get associated with **Dr. Raj Kumar Gupta** (Associate Professor, Department of Chemical Engineering, Thapar University, Patiala) and **Dr. Vineet Kumar (**Professor, Department of Chemical Engineering, Indian School of Mines, Dhanbad, India) as my supervisors. As outstanding teachers and researchers they have given me the benefit of their guidance throughout the course work. I am grateful to both for showing me all the angles of research life. Their deep insight into the problem and ability to provide constructive suggestions have been of immense value in improving the quality of my research work at all stages.

Heartful thanks are due to **Mr. Varinder Gupta** (MD, IOL Chemicals and Pharmaceutical, Barnala), for his encouragement and support during this research work. I expresses deep sense of gratitude to **Dr. Prakash Gopalan** (Director, Thapar University), **Dr. Susheel Mittal** (Deputy Director, Thapar University), **Dr. O. P. Pandey** (Dean, Research and Sponsored Projects, Thapar University), and **Dr. P.K. Bajpai** (former Dean, Research and Sponsored Projects, Thapar University), for their support at all stages.

I would like to express the gratitude to my doctoral committee members (**Dr. Susheel Mittal**, and **Dr. Rajeev Mehta**) for their valuable suggestions during the course of this work. Thanks are also due to all faculty, and staff of the Chemical Engineering Department, Thapar University, for their support.

I wish to thank **Mr. R.K. Thukral**, **Mr. Vijay Singla**, **Mr. Pankaj Adhikari**, **Mr. Narinder Singh**, **Mr. Kiran Panchal** and **Mr. Arun kumar** of IOL Chemicals and Pharmaceuticals Ltd. for providing all possible assistance and co-operation during the course of experimental work. I am also thankful to my friends **Dr. Gursewak Singh**, **Dr. Jyoti kaushal** ,**Pushpinder kansal**, and **Mr. Bhupinder S. Bhullar** who always encouraged me during difficult times. I am also thankful to the authors whose research work I have used in this work.

I express my gratitude to my wife **Manpreet Kaur**, sons **Harmandeep Singh** and **Guunveer Singh** and other family members for their patience, sacrifices and support throughout the research work. My firm faith in **God** has led me to overcome all difficulties that came my way. Last, but not the least, my **Mother** deserve most special mention for her love, affection and blessings and constant encouragement to undertake and successfully complete this work.

Date: 14.06.16 (Damandeep Singh)

Place: TU, Patiala

ABSTRACT

RD is the process developed by integrating two different operations (chemical reaction and multi-stage distillation) simultaneously in a single unit. Reactive distillation (RD) has been successfully implemented for the production of the Ethyl acetate (*EtAc).*The RD feature of shifting the equilibrium in the forward direction is useful for *EtAc* production by the reversible esterification reaction of acetic acid with ethanol.

The main advantages of using the RD with a pre-reactor for the production of the *EtAc* is that, the existing plants based on the conventional process can be easily revamped to use the RD technology. Also, in case of RD with pre-reactor, a smaller RD column (as compared to complete RD process) is required which reduces the capital investment. At IOL Chemicals and Pharmaceuticals Ltd., the *EtAc* is produced by the esterification of *HAc* with *EtOH* in the presence of the homogeneous acid catalyst (para-toluene-sulfonic acid) using RD with pre-reactor. Most of the reaction takes place in the reactor and the reacted mixture is fed to the column where simultaneous removal of product improves the conversion and product yield. The work reported in this thesis was aimed at generating the experimental data from an industrial scale RD column (situated at IOL Chemicals and Pharmaceuticals Limited, Trident Complex, Barnala, Punjab, India) and to compare the simulation results with this RD column data.

The provision for the collection of vapor and liquid samples from each tray was made during a scheduled shutdown of the plant. The simulation was carried out using the rate based model of Aspen Plus^{TM}, as the column hardware information was readily available. A new set of thermodynamic parameters for the NRTL model was established for the highly the non-ideal liquid mixture, of this reaction system, by regression of the vapor-liquid equilibrium data available in literature. Predicted vapor and liquid composition profiles are in good agreement with plant data. The simulation results indicate that stages 20 to 30 are the most active stages of the column from the hydrodynamic point of view.

Like a conventional distillation column, in this case too, an increase in organic reflux (keeping the distillate flow rate constant) causes an asymptotic increase in distillate purity (i.e., *EtAc* concentration). A linear increase in re-boiler duty and decrease in ethanol conversion was also observed with an increase in reflux flow rate. However, at high reflux flows, a higher *EtAc* concentration suppresses the forward reaction, thus, overall conversion in the column decreases.

The simulation results further show that the column is having more number of trays (about 6 trays) in the rectification section than required. The effect of feed stage location is also discussed to utilize these extra trays. The results show that re-boiler and condenser duties decrease on moving the feed stage up in the column (from stage 39 to stage 33). Also, the ethanol conversion increases as the reaction zone in the column increases with the shifting of feed stage from stage 39 to stage 33.

It is observed that the extra stages can be utilized in a more effective way by changing the feed location (moving the feed stage up in the column) so that reaction zone in the column increased; and by addition of a fresh feed of ethanol at stage 49 to improve the forward reaction. A fresh feed of ethanol (150 kg/h) is added in the down-comer of 49^{th} stage and the feed from the pre-reactor was introduced at stage 34. The ethanol conversion in the RD column increased from 17.43 kg to 93.44 kg, the ethanol conversion (wt%) increased to 39.94 % from 18.76%. The specific energy (kcal/kg of *EtAc*) requirement of re-boiler reduced from 1115 to 1054, and condenser duty (kcal/kg of *EtAc*) reduced from 684 to 654.

Comparison of the column composition profiles, for liquid and vapor phases, with EQ and rate-based model simulations show that, for all the components, the rate based model's predictions are far more superior to the EQ model predictions. The rate-based model predicted lower *EtAc* generation rates, than the EQ model, as introduction of mass transfer resistance reduced the reaction rates.

PUBLICATIONS

Publications in SCI Journals

1. **Singh, D.**, Gupta, R.K., Kumar, V. (2014) Experimental studies of industrial-scale reactive distillation finishing column producing ethyl acetate. *Industrial and Engineering Chemistry Research*, 53, 10448−10456.

2. **Singh, D.**, Gupta, R.K., Kumar, V. (2015). Simulation of a plant scale reactive distillation column for esterification of acetic acid. *Computers and Chemical Engineering*, 73, 70−81.

TABLE OF CONTENTS

LIST OF FIGURES

LIST OF TABLES

NOMENCLATURE

a_j	effective vapor-liquid interfacial area on the j^{th} tray (m^2/tray)
C_k	catalyst concentration (volume percent)
E_j^I	vapor to liquid residual heat transfer rate on j^{th} tray
E_j^L	liquid phase residual heat balance on j^{th} tray
E_j^V	vapor phase residual heat balance on the j^{th} tray
f_{ij}^l	liquid feed rate of i^{th}component on j^{th} tray (mol/s)
f_{ij}^v	vapor feed rate of i^{th}component on j^{th} tray (mol/s)
h_j^L	liquid phase heat transfer coefficient (J/m^2.s.K)
h_j^V	vapor phase heat transfer coefficient (J/m^2.s.K)
H_j^L	liquid phase molar enthalpy on j^{th} tray (J/mol)
H_j^{LF}	molar enthalpy of the liquid feed to the j^{th} tray (J/mol)
H_j^V	vapor phase molar enthalpy on j^{th} tray (J/mol)
H_j^{VF}	molar enthalpy of the vapor feed to the j^{th} tray (J/mol)
K	degree kelvin
k_1	forward reaction rate constant (l/mol.s)
k_2	backward reaction rate constant (l/mol.s)
K_C	reaction equilibrium constant
K_{ij}	equilibrium constant for distillation
$\bar{k}_{ij}^L$	diffusive mass transfer coefficient of binary *i*-*k* pair of components in the liquid phase ($mol/m^2 \cdot s$)
$\bar{k}_{ij}^V$	diffusive mass transfer coefficient of binary *i*-*k* pair of components in the vapor phase ($mol/m^2 \cdot s$)
l_{ij}	flow rate of component *i* in the liquid stream on j^{th} tray (mol/s)
L_j	total liquid flow rate exiting j^{th} tray (mol/s)
M_{ij}^L	material balance residual function of i^{th} component on j^{th} tray in liquid phase (mol/s)
M_{ij}^V	material balance residual function of i^{th} component on j^{th} tray in vapor phase (mol/s)
N_{ij}	mass transfer rate of i^{th} component from vapor to liquid phase on j^{th} tray (mol/s)

$\bar{N}_j^L$ mass transfer rate of i^{th} component from vapor-liquid interface to bulk liquid (mol/s)

$\bar{N}_j^V$ mass transfer rate of i^{th} component from bulk vapor to vapor-liquid interface (mol/s)

P pressure of j^{th} tray

p_{ij}^I partial pressure of ithcomponent at the interface on j^{th} tray

Q_{ij}^I phase equilibrium residual function of i^{th} component at the interface on j^{th} tray

r_{ij} rate of formation of component *i* due to the liquid phase reaction on j^{th} tray (mol/s)

R universal gas constant (J/kmol.K)

T temperature (K)

T_j^L bulk temperature of liquid phase on j^{th} tray (K)

T_j^I temperature at the interface on j^{th} tray (K)

T_j^V bulk temperature of vapor phase on j^{th} tray (K)

U_j liquid holdup on the j^{th} tray (l)

v_{ij} flow rate of component *i* in the vapor stream on the j^{th} tray (mol/s)

V_j total vapor flow rate exiting j^{th} tray (mol/s)

x mole fraction in liquid phase

x_{ij}^I liquid phase equilibrium mole fraction of i^{th} component at the interface

y_{ij} vapor phase mole fraction of i^{th} component on j^{th} tray

y mole fraction in vapor phase

y_{ij}^I vapor phase equilibrium mole fraction of i^{th} component at the interface

Greek letters

α_{im} NRTL binary non-randomness factor parameter

γ_i activity coefficient of component i

τ_{im} NRTL binary interaction energy parameter

$\widehat{\emptyset}_{ij}^I$ fugacity coefficient of component i

ABBREVIATIONS

AR	Analytical grade reagent
ASTM	American Standards for Testing and Materials
CSTR	Continuous stirred tank reactor
ETBE	Ethyl tertiary butyl ether
I.D.	Internal diameter
FI	Flow indicator
FIC	Flow indicator and controller
FID	Flame ionization detector
K_{EQ}	equilibrium constant
LIC	level indicator and controller
LR	Lab grade reagent
PIC	Pressure indicator and controller
MIBK	Methyl isobutyl ketone
MTBE	Methyl tertiary butyl ether
NRTL	Non random two liquids
O.D.	Outer diameter
TAME	Tertiary amyl methyl ether
wt%	weight percentage

Chapter 1
Introduction

Chemical industry requires large amount of energy to convert raw materials into useful products. The profitability of a chemical industry depends heavily on the efficient use of energy. The efficiency of a chemical plant may be improved by using the following strategies: implementing advanced control and optimization, improving the yield of desired products, and developing new processes. The word 'RD' (reactive distillation), which was coined in the early 20^{th} century is one of the techniques that may improve the energy efficiency and product quality of a chemical plant.

RD is the process developed by integrating two different operations (chemical reaction and multi-stage distillation) simultaneously in a single unit. Reactive distillation (RD) has been successfully implemented for the production of the Ethyl acetate (*EtAc).* Worldwide, CDTECH®,USA and Sulzer-Chemtech Ltd.,Switzerland are the technology providers for RD and have licensed more than 200 commercial scale processes successfully till 2006. Barriers and bottle-necking have also been removed by these companies for successful implementation of RD technology. Moreover, chemical manufacturing companies have also developed their own specific RD processes by their own research and development and/or in tie-ups [Harmsen,2007].

Ethyl acetate (*EtAc*) is an important colorless organic solvent with fruity smell and it is widely used in the production of varnishes, ink, synthetic resins, and adhesive agents. More importantly, the *EtAc* comes under Class 3 solvent (less toxic and of lower risk to human health) as per the ICH (International Conference on Harmonization) Q3 guidelines for the usages in pharmaceutical and food products. As it is having acceptable fruity odor, so it is more widely used as an extraction solvent in the production of the pharmaceuticals, food, as a carrier solvent for herbicides and in the lamination industry. It is slightly soluble in water and almost completely soluble in most of the other organic solvents.

Indian agriculture (sugar) industry is second largest in the world after Brazil and produces sufficient supplies of ethanol that could be used as renewable resource for *EtAc* feed-stocks as compared to the ethanol from petroleum route. Therefore, most commercial production units in India are based on the esterification of the acetic acid with organic ethanol [Dutia, 2004]. The major producers of the *EtAc* in India are IOL Chemicals and Pharmaceuticals Limited, Jubilant Organosys, Gujrat Narmada Fertilizer Corporation, and Laxmi Organics. Among these, IOL

Chemicals and Pharmaceuticals (IOLCP) Limited uses a pre-reactor and a finishing RD column. In the present work, performance of this finishing column at IOLCP is studied.

1.1 Reactive distillation (RD) and its importance

In the chemical process industry, the chemical reaction and separation of desired products by distillation are carried out in series of unit operations. In many cases, the performance of this conventional process structure can be significantly improved by integration of chemical reaction and distillation in a single multi-functional process unit. This integration concept is called RD (reactive distillation). It is the generic version of catalytic distillation because it covers both catalyzed and un-catalyzed reaction systems. The catalyst can be present in the system in the homogeneous or heterogeneous phase. RD with catalyst in homogenous phase was studied in early 20^{th} century by Backhaus [1921] and Keyes [1932] whereas RD with heterogeneous catalyst was first explored by Spes [1966]. Now, RD has emerged as a favorable alternative to conventional reactor-separator configurations.

As shown in the Figure1.1 (a) for conventional process, components A, B are the reactants and C, D are products. It is assumed that the boiling points of both the products is in between boiling points of reactants, i.e., boiling point of A<C<D<B. The fresh reaction mixture of components A and B along with the un-reacted recycle stream, is fed to the reactor, where the reaction takes place in the presence of a catalyst and reaches equilibrium. Thereafter, a distillation train (as shown in Figure 1.1(a)) is required to separate all the four components. But, in the case of RD as shown in Figure 1.1(b), a reactive section in the middle of the column with non-reactive rectifying and stripping sections at the top and bottom, respectively, would be sufficient. In this configuration of RD column, in the rectifying section reactant B is recovered from the product stream C, and in the stripping section, the reactant A is removed from the product stream D. In the reactive section, the products are separated in situ from the reactants and thus the equilibrium is driven to the forward direction to increase the conversion. The separation of products also suppresses the undesirable side reactions.

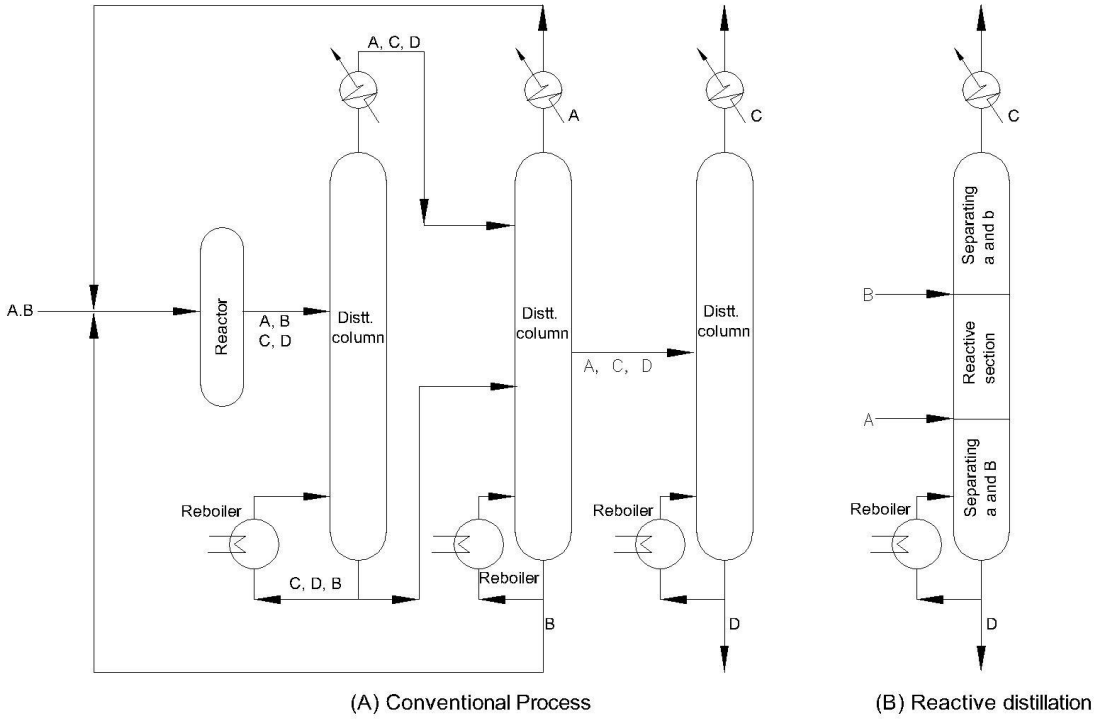

Figure1.1: (a) typical configuration of a conventional process consisting of a reactor followed by a distillation train (b) reactive distillation configuration [Source: Taylor and Krishna, 2000]

However, RD may not be applicable to all processes. A quick way of identifying reactive distillation as a feasible and attractive option is by using a qualitative graphical method provided by Schoenmakers *et al*. [2003] shown in Figure1.2.

Compared to the conventional processes (where reaction and separation occurs as two different unit operations in two different equipments), the resulting flow sheets with RD tends to be much simpler and have lesser recycle streams. But, their operation and design is much more complex than traditional distillation columns or reactors. There are many processes like esterification, trans-esterification, hydrolysis, alkylation, etherification, nitration, and amidation [Taylor and Krishna, 2000], where RD has been successfully implemented.

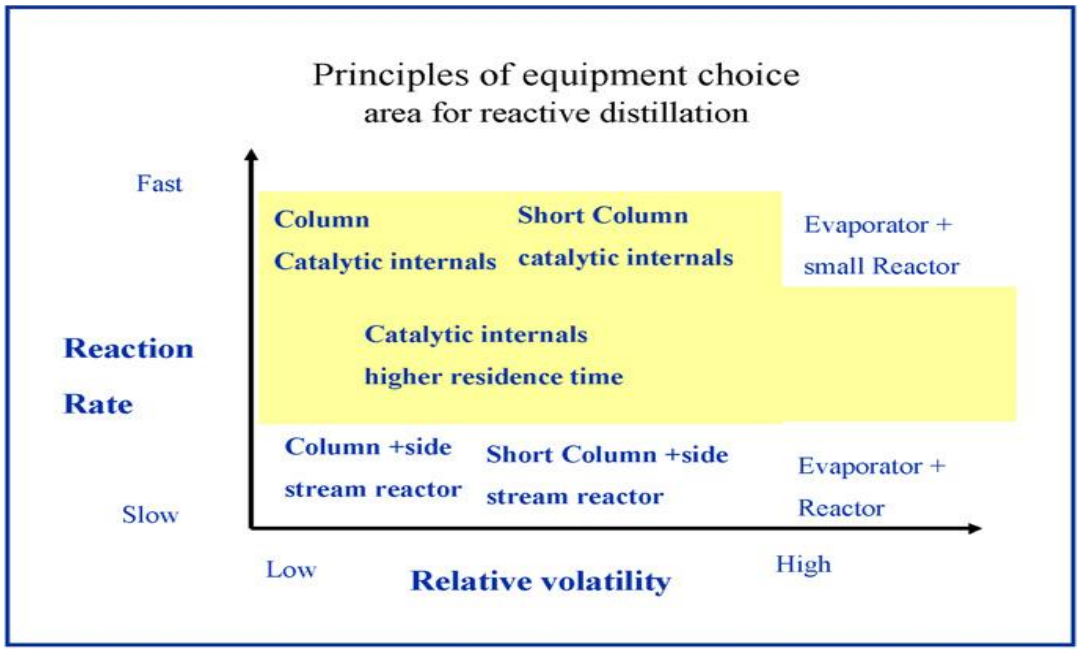

Figure 1.2: Principles of equipment choice reactor and distillation [*cf.* Harmsen, 2007]

The two most important industrial applications of RD are: famous Eastman chemical Co.'s process for the synthesis of methyl acetate in which a complex conventional flow sheet with 11 process units was replaced with a single hybrid RD column, and second example is that of the preparation of MTBE, TAME and ETBE (all fuel additives and ethers) [Sundmacher and Kienle, 2002]. RD can also be used for the recovery of valuable products like acetic acid, lactic acid, glycols and so on from the waste streams [Singh *et al*., 2007].

By applying the RD concept, one process unit (a separate reactor) can be eliminated or the size of the process unit can be reduced. This leads to a significant reduction in capital and operating costs. Other advantages of the RD are: overcoming equilibrium limitations on conversion, suppressing the side reactions to reduce the undesired by-products, overcoming azeotropic limitations on achievable separation, auxiliary solvents can be avoided, significantly improved economics, significantly reduced catalyst requirement for the same degree of conversion, reduced emissions, improved selectivity of products (lower impurities generation) and process intensification by energy integration between the reaction and separation systems, avoidance of hot spots and runaways using liquid vaporization as thermal fly wheel [Taylor and Krishna,2000]. Some of these advantages are realized by using reaction to improve separation; others are realized by separation to improve reaction.

1.2 Constraints and disadvantages of RD

RD offers numerous benefits; however, it cannot be used for every process that involves reaction and separation. RD has some constraints; generally, RD is not attractive for supercritical condition, gas-phase reactions, reactions that require high temperature and pressure conditions, and for the reactions where solid reactants or products are involved [Seader and Henley, 2006].

Reactive distillation can be considered as an alternative to the use of separate reactor and distillation vessels whenever the following holds [Alejski and Dupart, 1996; Taylor and Krishna, 2000; Frey and Johann, 1999]:

- Feasible temperature and pressure for the reaction and distillation are the same. i.e., reaction and separation rates are comparable. Considerable conversions are achieved at distillation temperature and pressure levels.
- The chemical reaction occurs in the liquid phase (homogeneously catalyzed and un-catalyzed reactions), or at the solid-liquid interface (heterogeneously catalyzed reactions).
- The reaction is equilibrium-limited so that in-situ removal of product(s) drives the reaction towards completion, and excess reactant is not required to achieve high conversions. This especially is advantageous for the systems where an azeotrope is formed and the recovery of excess reactant is difficult.
- Higher requirements on the quality of the design and control systems including more sophisticated controller designs and more complicated control structures.
- Reactions rates are reasonably fast so that very large hold-up on trays in distillation column is not required.
- The volatilities of the reactants and products should have sufficient difference in the reaction zone of the column so that the separation takes place easily.

Due to the interaction of reaction and distillation in one single unit, the steady state and dynamic operational behavior of RD is very complex. The scale up from the pilot plant, the experimental validation of a new process is well known for conventional distillation, but it becomes much more complex in case of an RD column. To overcome these problems, either reference plant experience on industrial scale or (if not available) further research is required [Sundmacher and Kienle, 2002].

1.3*'EtAc'* candidate for RD

The temperature and pressure conditions inside the distillation column for the separation of *EtAc* favor the *EtAc* reaction conditions. So RD has been successfully implemented for the production of the *EtAc.* Various studies have been done to develop a method for the implementation and solving the problems related to *EtAc* production via RD because of commercial benefits (due to high volumes of global production of *EtAc*) [Backhaus,1921; Keyes, 1932; Suzuki *et al.* 1971;Komatsu, 1977; Wayburn and Seader, 1987; Alejski *et al.*, 1988; Chang and Seader, 1988; Venkataraman *et al.*, 1990; Lee and Dudukovic, 1998; Kuo-Ching Wu and Yu-Wen Chen, 2003; Vora and Daoutidis, 2001; Tang *et al*., 2003; Tang *et al.*, 2005; Khaledi and Bishnoi, 2006; Kai and Matsumoto, 2013].

1.4 RD Modeling

RD modeling is the most important part for successful design and commercialization of RD technology. Therefore, careful attention should be given to the modeling aspects, including column dynamics, even at the conceptual design stage [Doherty and Buzad, 1992; Roat *et al*., 1986]. The RD could have the negative effects by improper choice of feed stage, reflux rate, catalyst percentage, re-boiler duty, etc. For example, the well known increased separation capability of a conventional column by increasing reflux rate is no longer valid for an RD column, as, in a RD column an increase in reflux flow could decrease process performance [Sneesby *et al*., 1998]. It is also possible that the conversion decreases on increasing the amount of catalyst under certain circumstances [Higler *et al*., 1999b].

Distillation column models can be broadly classified as rate-based models and equilibrium-stage models. Rate-based models are more complex because of the large number of parameters to be estimated. The rate based models (non-equilibrium models) where MERQ (material balance, energy balance, rate of inter-facial mass transfer, and equilibrium) equations are involved [Vora and Daoutidis, 2001] and equilibrium-stage models where MESH (material, equilibrium, summation and enthalpy) equations are considered [Taylor and Krishna, 2000]. The chemical reaction is incorporated into these model equations by adding the reaction kinetics in the component balances and the heat of formation in the enthalpy balance equations.

In the context of reactive distillation, new complexities arise in the determination of vapor-liquid equilibrium, vapor-liquid mass transfer, intra-catalyst diffusion (for heterogeneously catalyzed processes) and chemical kinetics [Taylor and Krishna, 2000]. Complexities arise due to the interactions between chemical reactions and distillation in the same vessel. The other factors which affect the modeling of RD column are – liquid-phase splitting that may occur on one or more stages within the reactive distillation column when highly non-ideal mixtures are processed, the inclusion of many equipment details and realistic descriptions of the physicochemical behavior of the materials processed, heat and mass transfer rates, etc. Expressions for the physicochemical properties of materials, such as fugacity or activity coefficients, are often long and intricate, and various screening tests are needed before assuming that a computational implementation is correct.

Short-cut procedures for RD cannot be made generic because of the many ways in which chemical reactions influence the process [Ciric and Spencer, 1995]. Bock and Wozny [1997] showed that the assumption of chemical equilibrium, often made in developing short cut methods, is inappropriate for many RD processes. So, their usefulness depends upon the system being considered, the physicochemical data concerning the VLE and reaction kinetics, and upon our knowledge of a given RD system. Each model has its place in the process development cycle. Residue curve maps are very useful for initial screening and flow-sheet development. EQ (equilibrium) models are more suited for preliminary designs. However, NEQ (non-equilibrium) or rate-based models give better results when employed for commercial RD plant design and simulation works.

1.5*EtAc* production via esterification of acetic acid with ethanol

EtAc is normally produced via the liquid-phase reversible esterification reaction of the *HAc* with *EtOH* in the presence of an acid catalyst in the homogeneous/heterogeneous phase as shown in equation 1.1,

$$\underset{\text{(Acetic Acid)}}{CH_3COOH} + \underset{\text{(Ethanol)}}{C_2H_5OH} \xleftrightarrow{\text{para toluenesulfonicacid/ Sulfuric Acid}} \underset{\text{(Ethyl Acetate)}}{CH_3COOC_2H_5} + \underset{\text{(Water)}}{H_2O} \qquad (1.1)$$

Due to the thermodynamics and equilibrium limitation of the esterification reaction, the overall yield of the *EtAc* is typically within 67% with equimolar reactants [Wu and Chen, 2003]. Consequently, 30% of un-reacted reactants are with azeotropic by-products of *EtOH–H_2O*, *EtOH-EtAc*, and *EtOH-H_2O-EtAc*. The RD feature of shifting the equilibrium in the forward direction has been successfully implemented for the production of the *EtAc* via esterification of acetic acid with ethanol.

The conventional process as one shown in the Figure1.3 consists of a separate reactor (for reaction of reactants) and a distillation column (for the separation of reactants and products) [Chien *et al*., 2005]. Fresh ethanol and acetic acid are fed to a reactor where, to ensure maximum conversion of the *EtOH* to *EtAc*, excess acetic acid concentration is maintained in the reactor.

From the reactor, unconverted reactants (*HAc* and *EtOH)* and products (*EtAc* and *H_2O*) in the vapor phase are fed to the distillation column where the products are separated out from the top of the column (which is further purified to obtain the pure *EtAc*) and heavy reactant (*HAc*) from the bottom of the column are recycled back to the reactor. This process is most commonly used in India.

The RD process can be used for *EtAc* production broadly by the following two methods:

i. Complete RD
ii. RD with pre-rector

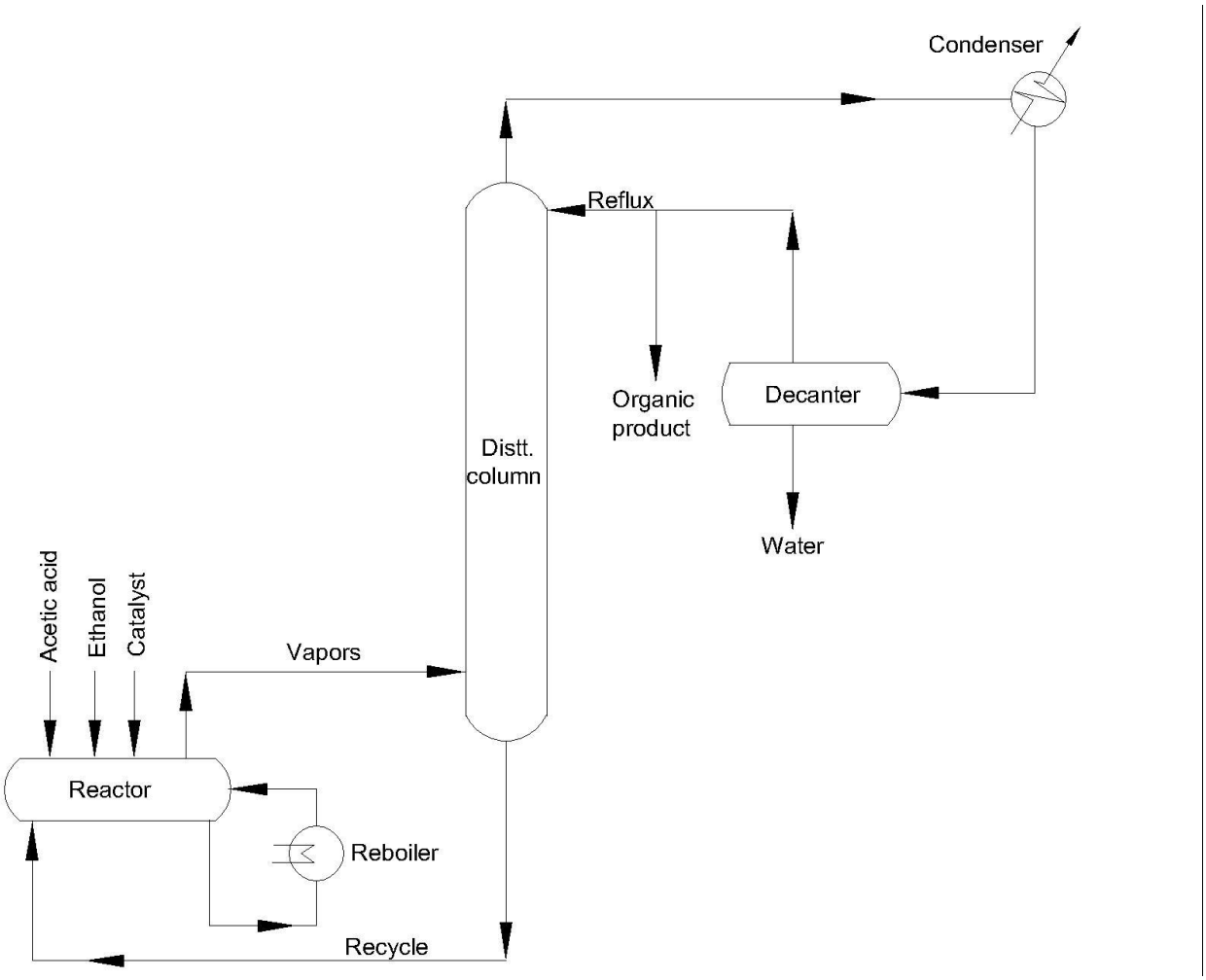

Figure 1.3: conventional process for *Et*Ac production

1.6 Complete RD

The complete RD can be implemented for *EtAc* production as proposed by Vora and Daoutidis [2001] and Tang *et al*. [2003], shown in the Figure1.4 (a) and (b). The high boiling point reactant (*HAc)* is added from top of the reactive zone and the low boiling point reactant (*EtOH)* from bottom of the reactive zone. The products *EtAc* (65 mol%), as the low boiling point azeotrope from the top of the RD column and the high boiling point mixture (*HAc, H_2O* and catalyst) from the bottom of the RD column are taken out.

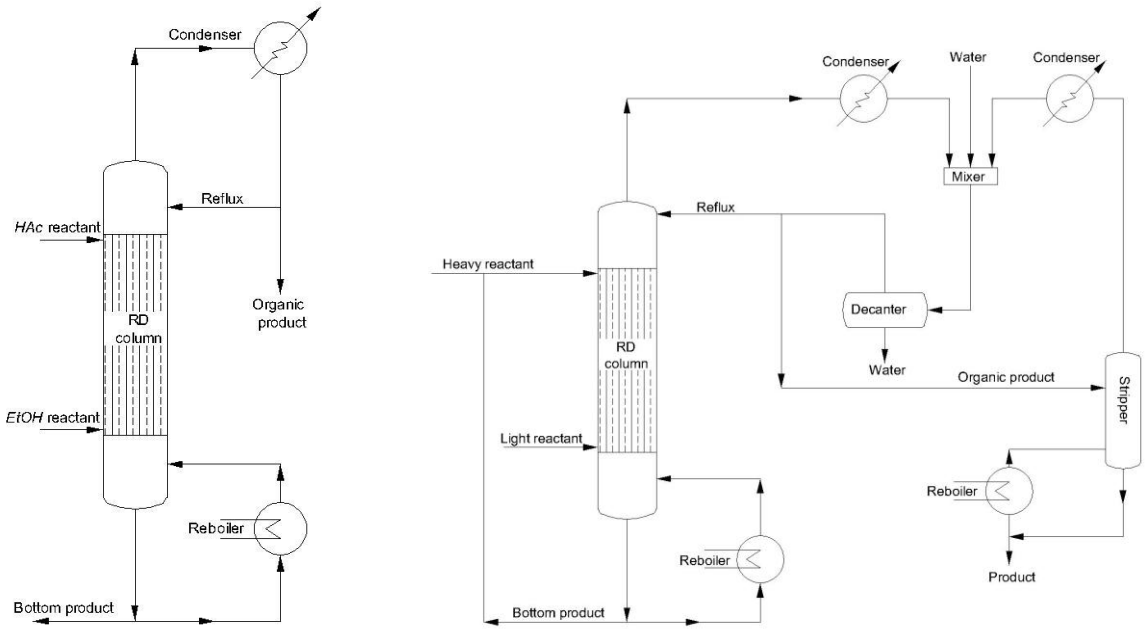

Figure1.4: Complete RD process, Source: (a) Vora and Daoutidis [2001] (b) Tang *et al*., [2003]

Heterogeneous catalysis use for complete RD process is a relatively recent development and was first described by Spes [1966], but due to high cost of catalyst and practical design problems of fixing the catalyst in the reaction zone [Sundmacher and Kienle, 2002], high cost of initial investment for resin (the heterogeneous catalyst) and its frequent replacement cost (as the catalyst gets de-natured with time, exposure to high temperature and due to impurities), high pressure drop in the catalytically packed reactive section. Due to above mentioned problems; the homogeneous catalysis is more favorable for RD. Moreover, if the catalyst undergoes deactivation, it is very difficult to remove the denatured catalyst and add the fresh catalyst, in the RD column and it requires shut down of the plant as on-stream removal of catalyst is not possible [Taylor and Krishna, 2000].

1.7 RD with pre-reactor

The *EtAc* production can be achieved by RD with pre-reactor (Figure1.5) as first proposed by Keyes [1932]. In this process configuration, most of the reaction occurs in the reactor, where excess amount of ethanol/acetic acid is maintained and homogeneous catalyst (H_2SO_4/PTSA) is used to increase the reaction rate. The mixture from reactor is fed to the RD column so that

reaction can take place beyond the equilibrium point of the pre-reactor [Steinigeweg and Gmehling, 2003]. The catalyst along with the bottom product is taken out of RD column (that can be re-cycled back) and products stream (*EtAc*) is taken out from the top of the RD column.

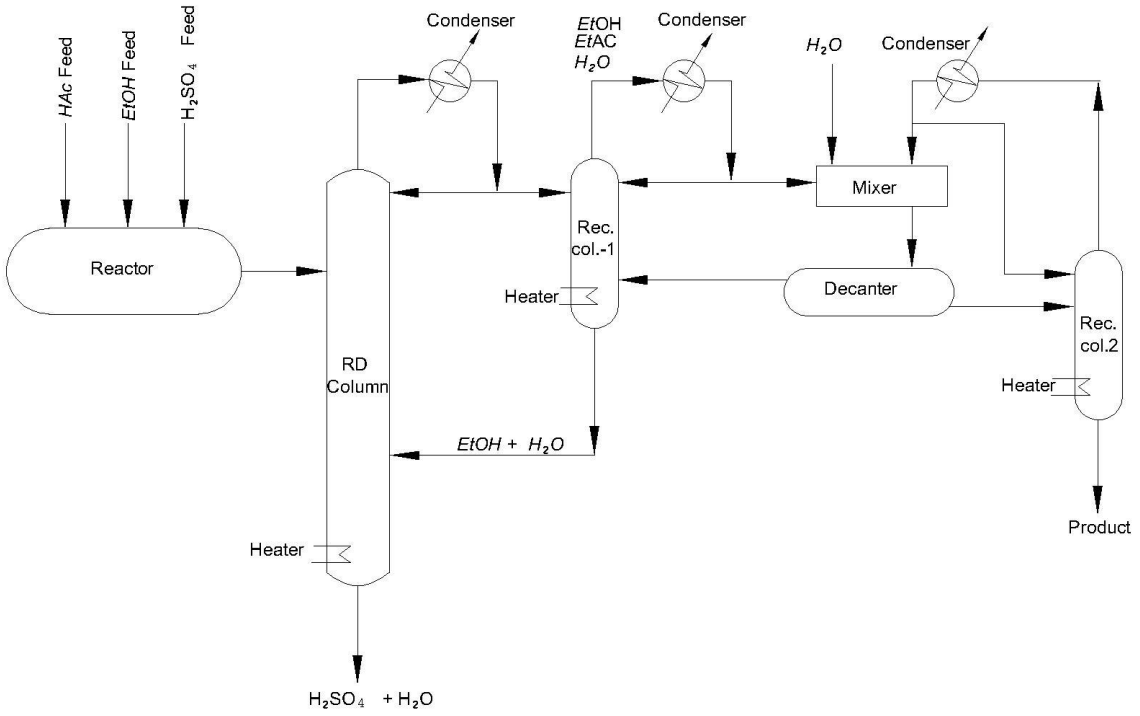

Figure1.5: RD with pre-reactor [Source: Keyes, 1932]

The main advantages of using the RD with pre-reactor for the production of the *EtAc* is that the existing plants based on the conventional process can be easily revamped to use the RD technology. Whereas the cost of converting an ordinary distillation into an RD column is low, there is a significant gain of about 25-30% conversion of residual *EtOH*. Also, in case of RD with pre-reactor, a smaller RD column (as compared to complete RD process) is required which reduces the capital investment. At IOLCP Barnala the *EtAc* is produced by the esterification of *HAc* with *EtOH* (equation 1.1) in the presence of the homogeneous acid catalyst (para-toluene-sulfonic acid) via RD with pre-reactor process (plant layout is shown in Figure1.6).

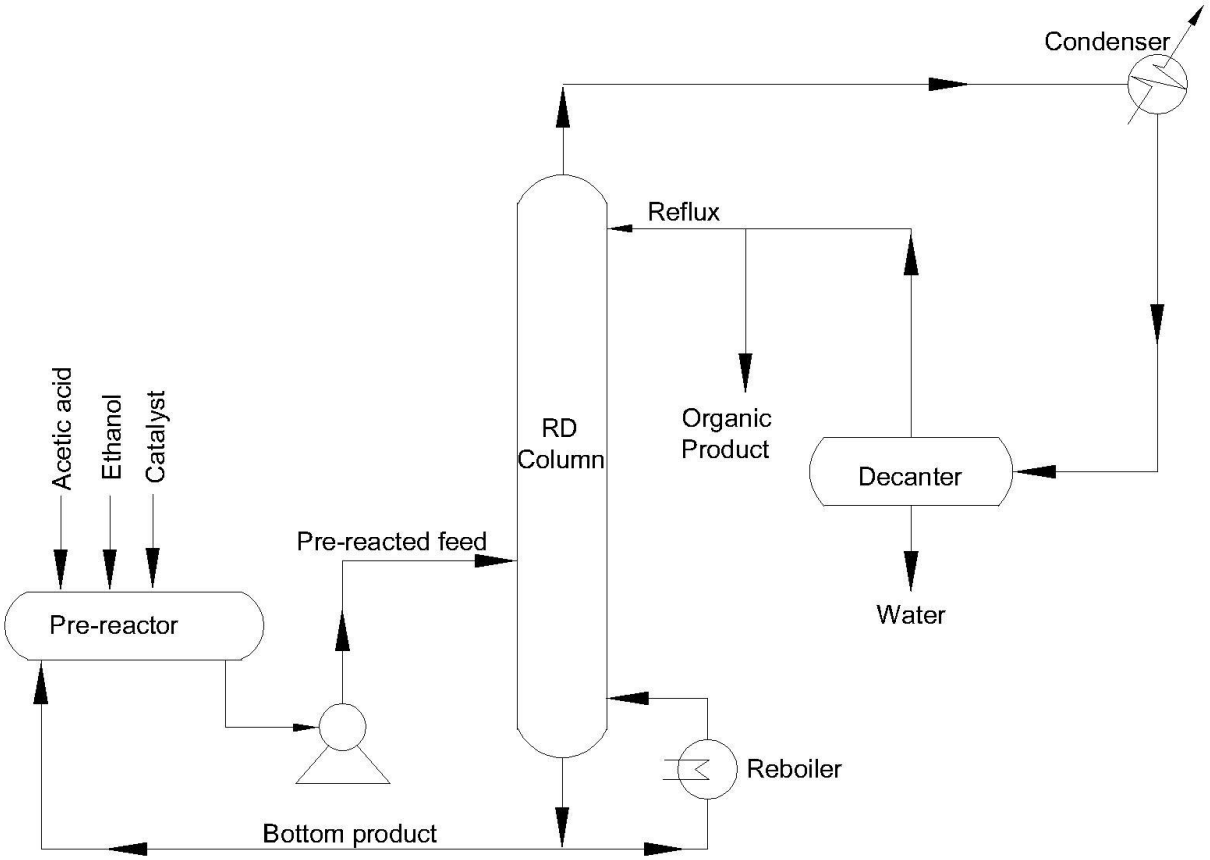

Figure1.6: RD with pre-reactor and recycle from the column bottom

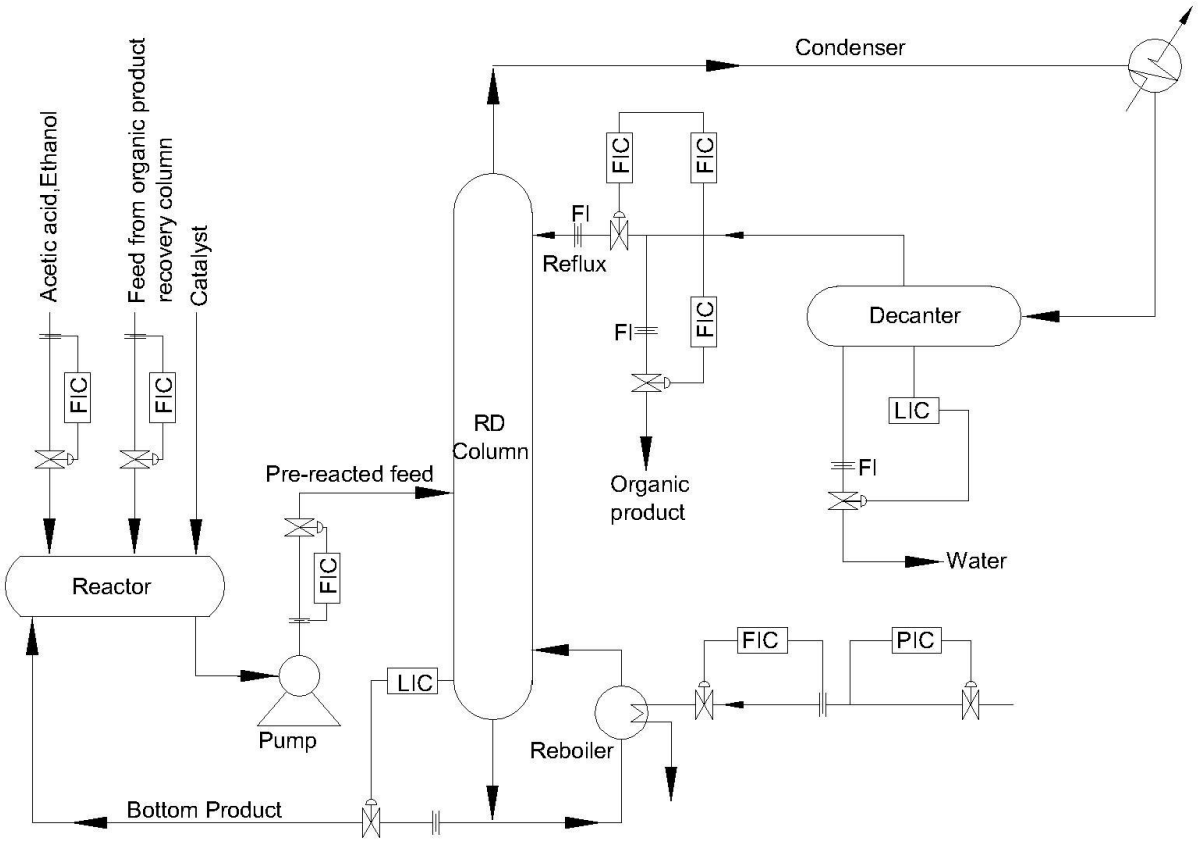

Figure 1.7: Instrumentation of RD with pre-reactor at IOLCP Barnala

The RD plant's instrumentation at IOLCP, Barnala is shown in Figure 1.7. There are four major units in the *EtAc* plant:(i) a pre-reactor (ii) a reactive distillation unit with a decanter (iii) a post fractionator and (iv) Recovery Column. The post fractionator and recovery column are not shown in the figure. The pre-reactor is a continuous reactor and is fed with fresh *HAc, EtOH,* make-up catalyst (PTSA), and a recycle stream (bottom stream from the RD column). The reactor temperature is maintained between 100 to 105 °C, so that most of the conversion of *EtOH* (90 to 94%) takes place in the pre-reactor. The partially reacted mixture is continuously supplied from the pre-reactor to the 38^{th} tray, counted from the top, of the RD Column. The RD column is having 48 bubble-cap trays, a condenser, a re-boiler, and a decanter for the phase splitting i.e., separating the aqueous phase and the organic phase. In the RD column, the rate of

reaction depends on the PTSA concentration on that particular tray, and it becomes negligibly small on trays where PTSA concentration is zero.

The organic vapors (a ternary azeotropic mixture of the *EtAc*, H_2O and *EtOH)* withdrawn from top of the RD column are condensed and fed to a gravity decanter which separates the product into organic and aqueous layers. One part of the organic product stream from the decanter is recycled to RD column and rest is taken as the organic product draw which is further purified to 99.90 wt% in the post fractionator. The aqueous stream from the decanter is fed to the organic product recovery column where organic material is recovered and re-cycled back to the pre-reactor. The bottom product stream from the RD column (93-95 wt% excess acetic acid) is sent back to the pre-reactor.

1.8 Motivation for the present work

The present work was aimed at generating the experimental (sampling and analysis) data from an industrial scale RD column (situated at IOL Chemicals and Pharmaceuticals Limited, Trident Complex, Barnala, Punjab, India) and simulation of this column. IOLCP Barnala is presently a leading manufacturer of bulk chemicals and API's having a standalone turnover of $150 million. The *EtAc* production capacity of this RD unit is 60 tons per day. The motivation to undertake the present work was due to the following reasons:

- No data is available in the open literature for the large industrial RD column (such as having 48 trays of 1800 mm diameter).
- In India the demand for *EtAc* is increasing very rapidly, the investigations on RD with pre-reactor will be helpful for revamping of existing plants to meet the demand and become competitive by reducing the energy cost and improving the equipment life.
- Organic route of synthesis is directly related to agriculture (source of the raw material is the renewable sugar cane). Use of ethanol for economical production of ethyl acetate will help the agrarian economy.

Chapter 2

Literature review

Reactive distillation combines two operations (reaction and distillation) in a single unit. The concept of RD (simultaneous reaction and separation) can fulfill many process objectives. All the reacting processes may not be suitable for RD implementation. Columns are suitable only for the reactions that are fast enough to achieve considerable conversions in reasonable residence time. The most important example of RD implementation is methyl acetate production process. After the commissioning of large-scale plants for the production of MTBE and methyl acetate, the RD concept has become important. The production of methyl acetate by Eastman Kodak process with near stoichiometric ratio of reactants in the RD column feed led to a simpler process configuration as compared to the conventional process. Siirola[1995] noted that conventional methyl acetate production process required one reactor and nine distillation columns. RD implementation of this process required only one column giving about 100% conversion of the reactant. The use of RD for the production of ethers has resulted into many patents.

The RD process has attracted considerable attention of researchers due to its potential as an effective process intensification operation. Malone and Dohrethy [2000] presented a commentary on the various aspects of reactive distillation: feasibility and alternatives, conceptual design and evaluation, equipment selection and hardware design, and operation and control. Taylor and Krishna [2000] have presented a detailed review on the modeling of reactive distillation. Sharma and Mahajani [2003] and Hiwale *et al*. [2004] presented reviews on the industrial applications of RD.

Ethyl acetate production by esterification of acetic acid with ethanol is one of the processes where RD is successfully implemented. One of the early studies on simultaneous reaction and distillation for the production of ethyl acetate is by Keyes [1932]. He used a pre-reactor, two recovery columns, and one decanter. The combination resulted in savings in energy consumption and decreased investment cost.

Several technologies have been commercialized for the production of ethyl acetate. The Avada process, employed at BP Chemicals, Salt End, U. K., uses ethylene and acetic acid with solid acid catalyst, whereas ethanol is dehydrogenated to acetaldehyde, which further reacts to form ethyl acetate at Sasol, SA. Most commercial production units, however, are based on esterification of acetic acid with ethanol in the presence of a catalyst. The two major advantages of adopting esterification of acetic acid with RD are (i) plants can be set up from very small

capacities to very large capacities with power cogeneration and (ii) an existing plant can easily be revamped to use the RD technology.

Perhaps, because RD is a relatively new field of research interest, only limited number of review paper has come up. Taylor and Krishna [2000] in their review discussed the RD phenomena and various modeling approaches in detail. They discussed the EQ models and their algorithms, and modeling approaches for homogeneous and heterogeneous RD. Authors concluded that there are a variety of models available for the RD columns aimed at analyzing, designing, or optimizing the column. They stressed the need for experimental work, where parameters should be measured along the height of the column, for the validation of RD column models. Harmsen [2007] reviewed the application areas of commercial scale reactive distillations, advantages of RD, and scale-up and design methods for RD. Sharma *et al.*[2010] presented a critical review on the controllability aspects of an RD column. On the other hand, many papers highlighting different feature of RD process are available in open literature.

2.1 Phase and Chemical Equilibrium

This four-component system (*HAc, EtOH, EtAc, H_2O*) has several azeotropes. The normal boiling points of the pure components and the azeotropes and compositions of the azeotropes are given in Table 2.1[Siirola, 1995]. Calculation of vapor-liquid equilibrium for this highly non-ideal mixture has received a lot of attention in the literature. Kang *et al*. [1992] obtained the vapor-liquid equilibrium with simultaneous esterification of acetic acid and ethanol to produce ethyl acetate using para-toluene sulfonic acid (PTSA) catalyst under chemical equilibrium condition. The authors used 2 wt% catalyst for quickly obtaining the reaction equilibrium. Hirata and Komatsu [1966] have measured the vapor-liquid equilibrium values for the esterification of a quaternary system of acetic acid-ethanol-ethyl acetate-water. They showed that the vapor-liquid equilibrium constants could be correlated with the reaction temperature and the compositions in the liquid phase at hypothetical conversion ranging from 0 to 100%.

Table 2.1: Normal boiling points of the pure components and azeotropes and composition of the azeotropes of the ethyl acetate system [Source:Siirola, 1995]

			mol %	mol %	mol %	T (^{0}C)	Azeotrope type
EtAc	*EtOH*	*H_2O*	58.7	15.9	25.4	70.1	MI
EtAc	*H_2O*		69	31		70.6	MIH
EtAc	*EtOH*		55.4	44.6		71.8	MI
EtAc						77.1	
EtOH	*H_2O*		90.8	9.2		78.2	MI
EtOH						78.4	
H_2O						100	
AcOH						117.9	

MI – Minimum boiling azeotrope; MIH- Minimum boiling heterogeneous azeotrope

In the literature, various liquid-phase activity models were employed for the model simulation of ethyl acetate RD columns. Pillavachi *et al*. [1997] studied the sensitivity of model parameters on the reactive distillation column simulation and design. The authors compared the results obtained by using various liquid phase activity coefficient models for the ethyl acetate RD process.

Alejski and Dupart [1996] presented a dynamic model for RD for kinetically controlled reaction. The authors compared the model results with the pilot-plant scale 20 stage, 0.075 m internal diameter bubble cap column with a plate spacing of 0.08 m for the esterification of acetic acid with ethanol using sulfuric acid as homogeneous catalyst. Authors attributed the differences between experimental and simulation results due to the simplification in the model, inaccuracy of kinetic and vapor-liquid equilibrium description for highly non-ideal mixture, and precision of experimental measurements. Peres-Cisneros *et al*. [1996] studied the various aspects related to the simulation design and operation of RD processes. The authors presented their results using the case studies for the production of MTBE and ethyl acetate. They observed that the experimental data of Suzuki *et al*. [1971] was difficult to match unless the fitted activity coefficient model proposed by them is used together with the expression for reaction kinetics. They concluded that the simulations using Aspen Plus could provide the best match with the

experimental data using the combination of UNIFAC model for the liquid phase, Virial equation for the vapor phase, and the Venkataraman *et al*. [1990] expression for reaction rate. They also concluded that compared to transformed variable approach, the elemental mass balance approach was a promising alternative.

Okur and Bayramoglu [2001] studied the effect of liquid-phase activity model on the simulation of esterification of acetic acid with ethanol in a homogeneous RD column. They used the EQ model for the plate distillation column and compared the simulation results obtained by using the four liquid phase activity models (UNIQUAC, UNIFAC: Dortmund, UNIFAC: Lyngby, and empirical). The authors concluded that the selection of liquid phase activity model was the most crucial aspect in reactive distillation modeling and the best activity model can be selected by comparing the model results with the experimental data. Tang *et al*. [2003] regressed the binary vapor liquid equilibrium data available in literature for the component pairs *EtOH-EtAc*, *EtOH-H_2O*, and *EtAc-H_2O* to obtain the parameters for NRTL model. Other binary model parameters for *HAc-EtOH, HAc-EtAc*, and *HAc-H_2O* were obtained from Aspen Plus. Using this NRTL model parameter set they were able to predict the compositions and temperature of the four azeotropes of the system with close agreement to the experimental data.

It is a known fact that interactions between reaction and separation complicate the design of RD columns. These interactions originate from vapor-liquid-liquid equilibria, vapor-liquid mass transfer, intra-catalyst diffusion (in case of heterogeneous RD) and chemical kinetics. Chemical reactions can cause the formation of azeotropes (called reactive azeotropes) which limit the range of product composition from a reactive distillation column in the same way as the ordinary azeotropes do for the conventional distillation column. In some cases, the chemical reaction eliminates the azeotropes that are present in the un-catalysed non-reacting systems [Ung and Dohrethy, 1995a]. Barbosa and Doherty [1987] studied the effect of single chemical reaction on phase diagram of multi-component mixtures. Ung and Dohrethy [1995b] studied the effect of multiple reactions and the presence of inert components on the phase diagrams of multi-component mixtures. Mahajani and Kolah [1996] extended the approach of Barbosa and Doherty [1988a, b] to the packed RD columns. The authors studied the influence of various design parameters on the feasibility of design for kinetically controlled and equilibrium controlled reactions using a hypothetical three-component system. Venimadhavan *et al.* [1994] discussed

the effect of homogeneous reaction kinetics on the vapor liquid equilibrium and reactive azeotropes. Venimadhavan *et al.*[1999] used bifurcation analysis to study the feasibility of reactive distillation in the presence of multiple reactions.

Perez-Cisneros *et al.* [1997] presented new algorithms for the calculation of simultaneous chemical and physical equilibrium. These elements balance approach algorithms reduce the number of variables involved in the analysis and allow the visualization of phase diagrams in multi-component reactive system in two and three dimensions. The authors presented the example of reactive flash calculations for the esterification of acetic acid with ethanol to produce ethyl acetate. Bessling *et al.* [1997] applied the concept of reactive distillation lines for the feasibility study of reactive distillation. Authors concluded that by the reaction space analysis it can be decided whether a reactive distillation must be combined with a nonreactive distillation, and the characteristics of the distillation line diagram provide hints on the basic column design and necessity of two feed stages can be predicted.

2.2 Models for *EtAc* RD column solution

EQ and NEQ Models

Equilibrium (EQ) stage model for reactive distillation are the extension of simple multi-component distillation models with an additional reaction term. In the EQ stage model the vapor and liquid streams leaving a stage [Figure 2.1(a)] are assumed to be in equilibrium. MESH (material balance, equilibrium, summation, and energy balance) equations are used to model equilibrium stages. However, it is well known that the real distillation columns do not operate at equilibrium. To account for the deviation from equilibrium, conventional way is to introduce a sage efficiency in the model equations. Practical application of EQ models by means of stage efficiencies have always been suspect for complex multi-component separation problems. Seader [1989] discussed the EQ model for multi-component distillation and advocated the use of rate-based models for non-ideal multi-component distillation in order to avoid uncertainties associated with the tray efficiencies. Taylor and Krishna [1993] have noted that with three or more species, the component efficiencies are almost always unequal to one another and these can routinely assume values greater than unity or less than zero. For packed columns HETP (height equivalent to a theoretical plate) is used in place of stage efficiency.

There are no fundamentally sound methods for estimating either efficiencies or HETPs in RD operations, in which the presence of chemical reactions will have an influence on the component efficiencies [Sundmacher and Kienle, 2002]. In reactive distillation operations we invariably have to deal with multi-component mixtures exhibiting large thermodynamic non-idealities. Furthermore, in-situ reactions with separation could significantly influence inter-phase transport and column composition profiles [Baur et al., 2000 CEJ]. In these processes the rate of mass and heat transfer often limit the separation. NEQ stage models (or rate-based models) do not use efficiencies but model the mass transfer process directly thereby avoiding the uncertainty associated with the use of efficiencies. Schematic of a non-equilibrium stage (Taylor et al., 2003) is shown in Figure 2.1(b).The component compositions are not in the equilibrium. Also, the temperatures of the phases are different. The MERQ (material balance, energy balance, rate of inter-facial mass transfer, and equilibrium) equations are used for NEQ models. In a rate based model separate equations are written for each phase. The use of a rate-based model, however, requires reliable predictions of mass transfer coefficients, interfacial areas, and diffusion coefficients.

Lee and Dudukovic [1998] presented models and computational algorithms for a reactive distillation tray column to compare equilibrium (EQ) and non-equilibrium (NEQ) models. The authors used the homogeneous liquid phase reversible reaction between acetic acid and ethanol in the production of ethyl acetate for the comparison. They found significant differences in the simulation results for the production rate of ethyl acetate and the re-boiler heat duty between the EQ and NEQ models. They also showed that the conventional prediction of Murphree efficiency, from an empirical correlation, may not be reliable for multi-component systems. The authors advocated the use of NEQ model for the simulation of a tray reactive distillation column, because the accurate prediction of individual Murphree tray efficiencies is very difficult in the case of simultaneous multi-component separation and reaction. They further showed that the magnitude of the reaction rate is the main factor that affects the behavior of a reactive distillation column. With the increase in exothermic reaction rate, the more heat is produced by reaction in the column, the less heat duty of the re-boiler, and the lower tray temperatures under the given set of operating conditions.

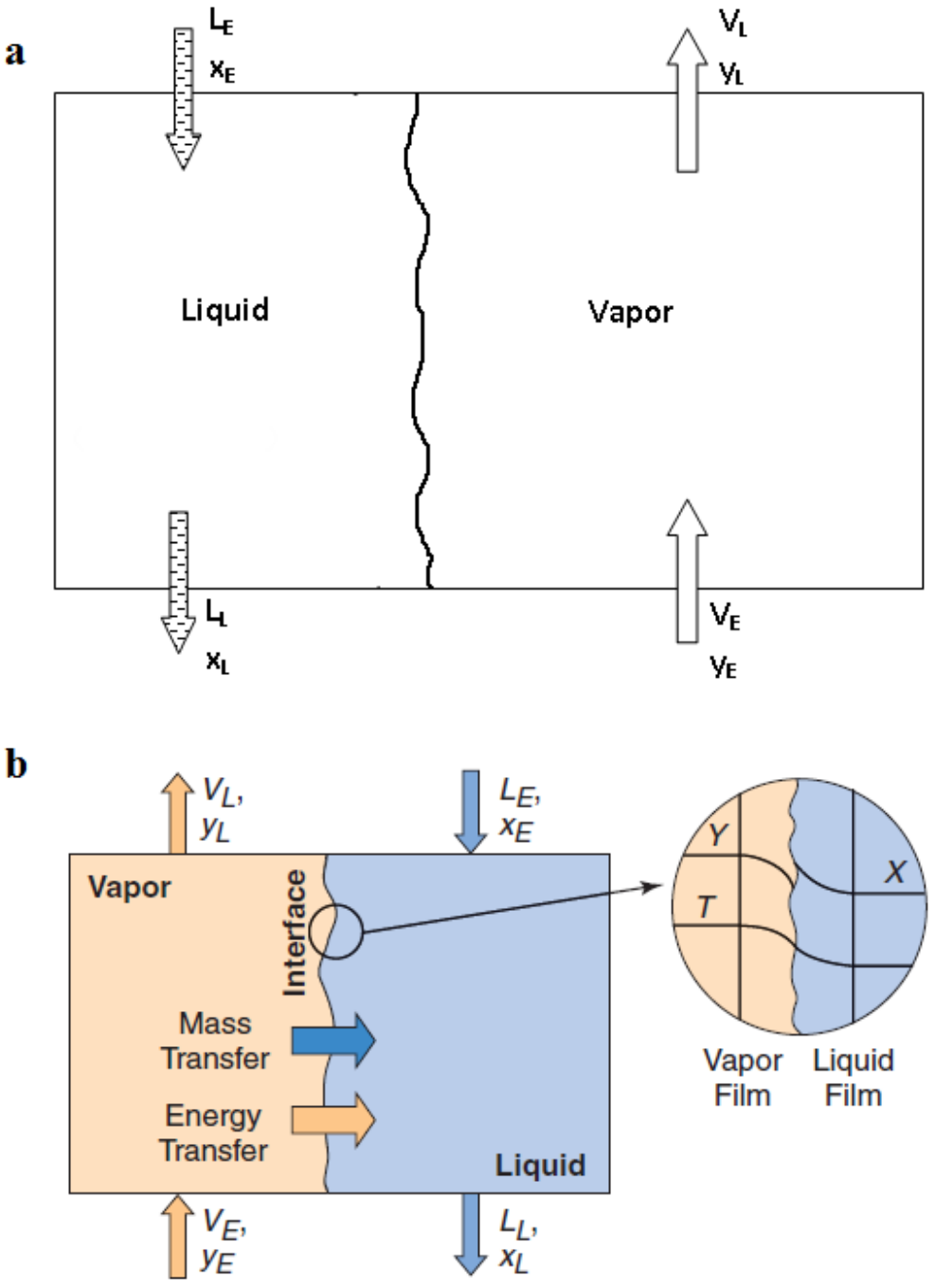

Figure 2.1 Schematic of (a) EQ stage (b) NEQ stage [Source: Taylor et al., 2003]

Higler *et al.*[1998] developed a NEQ model for simulation of homogeneous reactive distillation column. Authors studied the RD process for the production of ethyl acetate in the 13 stage column of Suzuki *et al.*[1971].The authors compared the EQ model results with the NEQ model. They concluded that reactions could have a significant effect on component efficiencies, and rate-based models are better for reactive distillation. Their study of parametric sensitivity showed that the effects of operational and design parameters on column behavior can be very complicated for the reactive distillation. They developed another generic NEQ model [Higler *et al.*, 1999a] for the reactive distillation tray column for arbitrary liquid-phase reactions. Authors used Maxwell-Stefan equations for mass transfer, considered reactions in film and bulk, and adopted a multi-cell modeling approach in the direction of liquid and vapor flows. Using the case study for hydration of ethylene oxide to ethylene glycol, they demonstrated the importance of tray hardware design on the selectivity. Kreul *et al.*[1999] discussed the adequate model complexity for the reactive separation processes in packed columns. The authors investigated the differences caused by the basic model assumptions such as equilibrium and kinetic concepts from the complete rate-based model.

Baur *et al.*[2000] compared the EQ stage models, in which the vapor and liquid phases are assumed to be in thermodynamic equilibrium and NEQ models in which the finite mass transfer rates across the vapor–liquid interface are used, for the RD columns. The authors used the case studies of MTBE synthesis and hydration of ethylene oxide to ethylene glycol. The multiple steady states were predicted by the NEQ model for a shorter range of process parameters as compared to EQ models. Another important conclusion that can be drawn from their work is that the hardware design can have a significant influence on the conversion and selectivity. Authors recommended the use of NEQ models for design of reactive distillation columns. Taylor and Krishna [2000] concluded that EQ models are suitable for preliminary designs. However, due to shortcoming of the EQ models, NEQ models are used for commercial RD plant design and simulation. Kenig *et al.*[2001] presented an experimental and modeling study for ethyl acetate synthesis by homogeneously catalyzed reactive distillation. The experiments were performed in a glass column having 80 bubble cup trays, a total height of 4 m and an internal diameter of 50 mm. They used effective diffusion coefficients in the rate based model and used a rate-based simulator ‘DESIGNER’ for the solution of the model equations. The model simulation results agreed well with the experimental data. Taylor *et al.*[2003] discussed the rate based modeling

approach for the multi-component separations. The authors discussed the need for rigorous Maxwell-Stefan based non-equilibrium models by comparing the NEQ and EQ models for the water-ethanol and acetone system in a bubble cap tray column. They observed that the differences in column composition profiles predicted by a rigorous NEQ model that incorporates the MS equations may differ significantly from those predicted by an equilibrium stage model. They showed that for the water-ethanol and acetone system the non-equilibrium model was able to follow the experimentally observed column trajectories much better than the equilibrium model. The differences in the column composition trajectories are due to differences in the component Murphree efficiencies.

2.3 Simulation strategies for ethyl acetate RD process

Many workers addressed the development of algorithms for solving distillation problems involving chemical reaction. Early modeling works on the ethyl acetate production by esterification are by Suzuki *et al.*[1970], Suzuki *et al.*[1971], and Komatsu [1970, 1977]. Suzuki *et al.*[1970] obtained the quaternary vapor-liquid equilibrium data for the mixture of acetic acid, ethanol, water, and ethyl acetate, with simultaneous esterification from the binary data. The Wilson's model was used for fitting the model parameters of the quaternary system. Suzuki *et al.*[1971] solved rigorous model comprising of linearized equations for a 13-stage column using modified Muller's method for the convergence of column temperature profile. They performed calculations by assuming the vapor-liquid equilibrium ratio as a function of temperature only, and by using activity coefficient model of Suzuki *et al.*[1970] for the vapor-liquid equilibrium. The authors have shown a very good match of the calculated profiles with the experimental data of Komatsu [1970].Muller's method is extended using the θ method of convergence proposed by Holland [1963] for solving the model equations of the reactive distillation column [Komatsu and Holland, 1977].

Relaxation methods involve writing the MESH equations in unsteady-state form and integrating numerically until the steady-state solution is found. Komatsu [1977] used the relaxation method of convergence of model equations and compared the converged results with the experimental data from a RD column for ethyl acetate, having a single bubble cap plate made of pyrex glass. The authors proposed a correction method for their numerical procedure for matching the experimental column composition profiles with the plant data.

Researchers have proposed various solution strategies for the models of this RD process. Simandl and Svrcek [1991] have summarized the works that simulated steady state multistage equilibrium model solutions for tower with and without chemical reactions **(**Table 2.2**)**. Homotopy-continuation methods are employed most often for solving problems that are considered very difficult to solve with other methods. Chang and Seader [1988] proposed a numerical procedure that makes use of homotopy-continuation, for the simulation of reactive distillation involving highly non-ideal liquid mixtures. The authors used this method for ethyl acetate RD column, using cases of single saturated feed and two saturated feeds, for an 11 plate column and a condenser and re-boiler. For the single feed case the same specifications as of Suzuki *et al.*[1971] were used. The calculations showed negative reaction rates for the top four stages for the single feed case. For the two feeds case (acetic acid fed to stage 6 and ethanol fed to stage 12) the separation and reaction rate did not improve. Lee and Dudukovic [1998] used both the Newton-Raphson and homotopy-continuation methods to solve the model equations for the esterification of acetic acid with ethanol in a distillation column. They solved both EQ and NEQ model equations and concluded that the homotopy-continuation was superior for the NEQ model, although, it required longer computational time. Alejski *et al.*[1988]proposed an error minimization function method, for RD column models, that does not depend upon the estimates of the starting points. The author studied the esterification of acetic acid with ethanol for the 8 plate column of Komatsu [1977]. The simulation results varied considerably from the experimental data of Komatsu [1977]. The authors concluded that the method is useful for the estimations of the concentration and temperature profiles in RD columns for which the heat balance can be neglected.

Table 2.2: Summary of the works that simulated steady state multistage equilibrium model solutions for towers with and without chemical reactions [Source: Simandl and Svrcek, 1991]

Simultaneous correction method	
Distillation:	*Reactive distillation:*
Napthali and Sandholm [1971]	Murthy [1974]
Ishii and Otto [1973]	Simandl and Svrcek [1985]
	Simandl [1988]
Relaxation method	
Rose *et al.*[1958]	Jelinek and Hlavacek [1976]
Ketchum [1979]	Komatsu [1977]
Continuation-homotopy methods	
Bhargava and Hlavacek [1984]	Chang and Seader [1988]
Salgovic *et al.*[198 1]	
Byrne and Baird [1985]	
Vickery and Taylor [1986]	
Wayburn [1983]	
Tearing or equation decoupling methods	
Sequential and simultaneous modular. stage to stage:	
Thiele and Gedda [1933]	Davies et al. [1979] (unsucessful)
Lewis and Matheson [1932]	
Fonyo *et al.*[1983]	
Equation solving:	
Wang and Henke [1966]	Suzuki *et al.*[1971]
Tomich [1970]	Nelson [1971]
	Tiemey and Riquehne [1982]
	Kinoshita *et al.*[1983]
	Holland [1981]
	Izarraz *et al.*[1980]
	Komatsu and Holland [1977]
Inside-out:	
Boston [1970, 1980]	Simandl and Svrcek [1987]
Russell [1983]	Simandl [1988]
Chimowitz *et al. [1983]*	
Saegerand Bishnoi [1986]	

Solving all of the model equations simultaneously using Newton's method (or a variant of Newton's method) is an approach used widely by authors [Pilavachi, *et al.*, 1997; Lee and Dudukovic, 1998]. Venkataraman *et al*,[1990] proposed an extension of inside-out approach of Boston [1978] that combines Newton's method with inside-out approach very effectively. In this approach the complex physical properties are solved in the outer loop using Broyden's method while the model equations are solved in the inner loop using Newton's method. They solved the 13-stage column example of the esterification for ethyl acetate production given in Holland [1981] using RADFRAC module of Aspen Plus. Simandl and Svreck [1991] used the simultaneous correction and inside-out method to the 13 stage ethyl acetate RD column. They used Wilson's model with parameters from Barbosa and Doherty [1988c]. The authors compared the simulation results with the experimental data of Komatsu [1970]. Between the two methods studied, the inside out method converged faster. There was considerable deviation of the simulation results from the experimental data. Authors commented that due to the suitability of RD only for the reactions that occur at suitable separation conditions there is a dearth of experimental data for RD systems.

Recently, Alfradique *et al.*[2005]presented an extension of a computer algebra (CA) program, *Thermath*, originally developed for the automatic implementation of physical property calculations, for the simulation of steady-state reactive distillation columns. Their procedure required the simultaneous solution (using the Newton–Raphson method) of material and energy balances, phase equilibrium, chemical equilibrium or rates of reaction equations with an additional equation to match the number of degrees of freedom. The authors presented the example of esterification of acetic acid with ethanol and used Wilson model [Wilson, 1964] for the liquid phase activity. The model parameters were obtained from Barbosa and Doherty [1988c]. They compared the model results (composition and temperature profiles) with the experimental data of Komatsu [1977] and the results of Alejski *et al.*[1988] and showed that their model results matched better with the experimental data as compared to that of Alejski *et al.*[1988].

Dalaouti and Seferlis [2006] presented a modeling approach for staged reactive processes that combines the rate-based balance equations with the model-order reduction properties of orthogonal collocation on finite elements (OCFE) approximation techniques. The model involves

the rigorous description of mass and heat transfer phenomena, phase equilibrium relations and chemical reactions in both gas and liquid phases in a limited number of collocation points. In addition, polynomial approximation as implemented in the OCFE techniques, transforms the staged column domain into a continuous analog thus, making the formulation more compact than the equivalent tray-by-tray model. Apart from other examples, the authors used the esterification of acetic acid with ethanol in the RD column for the comparison of their proposed model results with the full-scale (tray-by tray) model results. The results of their proposed formulation were in excellent agreement with the full-scale tray-by-tray formulation results. Khaledi and Bishnoi [2006] proposed an algorithm for the steady-state simulation of two- and three-phase multistage reactive distillation processes with equilibrium chemical reactions. In this method, the liquid-phase splitting is allowed at each stage, the phase stability test, and the phase and chemical reaction equilibrium calculations, are conducted simultaneously. Authors showed the ability of the algorithm in determining the phase pattern within the reactive distillation column in the cyclohexanol reactive column by changing the column operating conditions.

2.4Ethyl acetate process studies

Tang *et al.*[2003] studied the esterication of acetic acid with ethanol using sulfuric acid catalyst for ethyl acetate production. The authors designed a complete RD system for the process. They proposed a flow sheet that contained an overhead decanter with the RD column to obtain high purity ethyl acetate by splitting the top product form the RD column into the organic and aqueous phases in the decanter. The bottom product rich in acetic acid was recycled to the column by mixing with the fresh feed of acetic acid to the column. To meet the ethyl acetate product purity required in the industry they proposed a second column (stripper) to obtain a bottom product having ethyl acetate purity >99.5 wt%. Top product from the stripper was recycled to the decanter. They showed that their process was simpler than the process of Keyes [1932] and produces high purity ethyl acetate than that could be produced in the process proposed by Vora and Daoutidis [2001]. Tang *et al.*[2005]studied the esterification of acetic acid with five different alcohols, ranging from C_1 to C_5. The process flow sheets were classified into type I, II, and III for the five systems that were studied. They used a design procedure to optimize the design based on the total annual cost and identified major design variables for the different flow sheets. They showed that it was possible to systemize the design of reactive

distillation by qualitatively generating flow sheet from phase equilibria and by quantitatively completing the process flow diagram using a sequential design procedure.

Wu and Chen [2003] presented an interesting experimental study in which they investigated the temperature dependence on the yields and the effect of temperature on the equilibrium constant in the two-phase (liquid and vapor) regimes. They kept the experimental operation regime between liquid-vapor phases and defined the vapor-liquid system as the one conducted at a pressure of 1 atmosphere and a temperature between 393 K (vapor-phase operation) and 353 K (liquid-phase operation), in which two-phase operation is plausible and in equilibrium. They used NRTL-Hayden-O'Connell model to simulate the two-phase esterification reaction system. They concluded that the two-phase reaction system could significantly improve the yield. In the coexistence of vapor and liquid phases, the esterification reaction with equimolar feeds has one-pass conversion of 85mol% while the ethanol concentration in the products flow decreased to 6.5 wt%. The reduction of the ethanol concentration is advantageous for further purification processes.

Keller and Gorak [2013] presented the modeling study of homogeneously catalyzed RD processes in a packed column. The authors compared the results of different modeling approaches for homogeneous RD processes with experimental data. The four different modeling approaches were compared: the NEQ stage models using the Maxwell–Stefan (MS) equations, the NEQ stage models using the effective diffusion coefficients, the EQ stage models including reaction kinetics, and the EQ stage models assuming chemical equilibrium. They presented the case of the homogeneously catalyzed trans-esterification of dimethyl carbonate with ethanol and compared the results with the experimental data obtained by Keller *et al.*[2012].Their study showed that the equilibrium-stage model assuming chemical equilibrium was not sufficient for a proper description of the experiments. Consideration of the reaction kinetics significantly improved the accuracy of the simulation results. The best agreement between experimental and simulated data was obtained by using a NEQ stage model. Identical results were obtained with NEQ stage models, either using effective diffusion coefficients or applying the MS equations.

Kaymak and Luyben [2004] explored the effect of the chemical equilibrium constant on the design of reactive distillation columns. Authors concluded that with decrease in K_{EQ} value the higher numbers of reactive trays are required and operating pressures are lower. Also, the total

annual cost is higher because energy consumption increases and the number of reactive stages increase.

Chien *et al.*[2005] studied the design and control aspects of coupled reactor/ distillation configuration for ethyl acetate production. The authors proposed a continuous stirred tank reactor (CSTR) coupled with rectifier, a decanter, another stripper and a recycle stream for the overall optimum design. Lv *et al.*[2012] proposed a reactive distillation (RD) − pervaporation (PV) coupled process for ethyl acetate production. In this process the PV membrane is located in the bottom stream in order to selectively remove the water from the re-boiler and recycle the acetic acid into the feed. They studied the effects of PV operating temperature and acetic acid/ethanol molar ratio on the RD performance in detail. The authors claimed that due to the water removal and acetic acid recycle from the re-boiler, both the ethanol conversion and ethyl acetate purity were remarkably improved, from 82.4 to 85.6 wt% and from 81.3 to 84.8%, respectively. Smejkal *et al.*[2009] presented a study that involved the coupling of a fixed-bed reactor and a reactive distillation column for acetic acid and ethanol esterification utilizing strong acidic ion-exchange resin as catalyst. The authors experimentally studied (14 stages with 1 reaction stage) the effect of catalyst loading on reaction conversion in the fixed-bed reactor at reaction temperature ranging from 60 to 120 °C. They proposed partial separation of products in the form of their azeotropic mixture by the flash distillation that increased the reaction conversion above chemical equilibrium.

Kloker *et al.*[2004]presented a theoretical and experimental study of ethyl acetate production using different catalytic packing. A laboratory scale column (50 mm diameter column with a packing height of 3 m) and at semi-industrial scale column (162 mm diameter column with a packing height of 12 m) were used for experiments. They used commercially available packing (KATAPAK®-S and two different variants of MULTIPAK®). The authors investigated the influence of the selected catalytic internal on conversion and product purity. Weng and Lee [2013] studied the effects of tray efficiency and catalysts on the number of trays for the ethyl acetate RD process. Authors used three catalysts, Purolite CT179 [Hangx *et al.*, 2001], Amberlyst 35 [Tsai, 2007] and Amberlite 120 [Savkovic-Stevanovic*et al.*, 1992] in ethyl acetate esterification reaction. Their results show that trays of rectifying section increase more than two times, and the trays of reactive section are less than two times when the tray efficiencies is

changed from1.0 to 0.5.

2.5 RD model solution using Aspen Plus

In many recent modeling studies, the commercial simulation package (Aspen Plus™) is used. Both, equilibrium and rate-based, approaches for the modeling of RD columns are available in Aspen PLus™. Venkataraman *et al.*[1990] demonstrated the ability of Aspen Plus™ for the simulation of RD columns with inside-out algorithm. Perez-Cisneros *et al.*[1996] used the equilibrium (EQ) stage model of Aspen Plus™ for the esterification simulations and concluded that the data of Suzuki *et al.*[1971] is difficult to match unless specially chosen values are used to define activity coefficient and the reaction kinetics. Pilavachi *et al.*[1997] also used an EQ stage model of Aspen Plus™ and showed that the thermodynamic model selection plays an important role in the design of RD columns. More recently, Tang *et al.*[2003] proposed the design for the ethyl acetate reactive distillation column using Aspen Plus™. Tang *et al.*[2005] further extended this work and proposed design configurations for reactive distillations of acetic acid esterification processes. Lai *et al.*[2008] simulated a pilot plant scale RD column for the production of ethyl acetate using EQ stage model of Aspen Plus™. Kenig *et al.*[2004]implemented the rate-based approach in ASPEN Custom Modeler™ for the solution of the model equations for the lab and pilot scale catalytic RD columns for ethyl acetate production. Smejkal *et al.*[2009] simulated a Coupled fixed-bed reactor and a reactive distillation column for ethyl acetate production strong acidic ion-exchange resin as catalyst. The authors compared their experimental results with the results of numerical simulations by using Aspen Plus™.

Chapter 3
Data collection and analysis

Ethyl acetate(*EtAc*) plant at IOLCP Barnala consists of four major units: a pre-reactor, a reactive distillation unit with a decanter, a post fractionator and a recovery column. Two of these units (pre-reactor and reactive distillation unit) are shown schematically in Figure3.1. The pre-reactor is a continuous reactor of volume 100 m^3. The reactor temperature is maintained between 100 to 105 °C and it is equipped with a condenser (to recover heat of reaction) and a purging device. A circulation pump is used for the mixing of the contents of the reactor and the pump outlet and inlets are connected to the specially designed spargers for proper mixing. The space velocity of the reactor is 0.0086 per second (30.96 per hour).

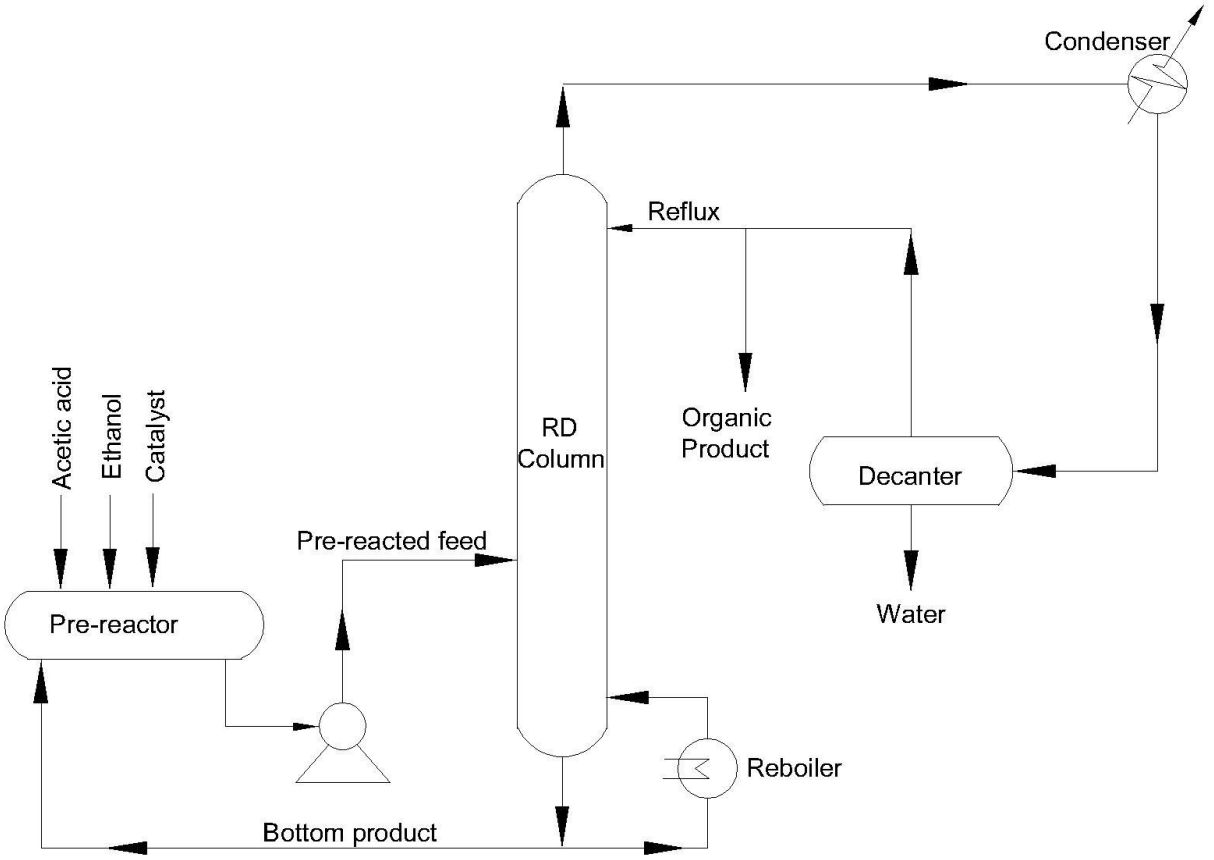

Figure 3.1: Schematic of RD column with pre-reactor at IOLCP Barnala

The feed to RD column, containing mixture of ethanol and acetic acid in the molar ratio 1:160 to 1:170, is supplied continuously from the pre-reactors. Due to reversible nature of the reaction,90 to 94% conversion of ethanol takes place in the pre-reactor and about 25 to 30% of the remaining ethanol (that happens to be about 2 to 3% of the total ethanol used) is converted in the RD column (leading to an enhanced production of about 1.5-2.0 TPD of ethyl acetate). The reactive distillation column has 48 bubble-cap trays, a total condenser and a thermo-siphon type re-boiler, and a decanter for the separation of aqueous phase from the organic phase (Figure3.1). The organic layer (top layer) from the decanter is divided into two parts and one part is pumped back to the column as reflux. The column hardware specifications are given in Table 3.1. Condenser and re-boiler hardware specifications are given in Table 3.2. The partially reacted mixture containing acetic acid (*HAc*), ethanol (*EtOH*), ethyl acetate (*EtAc*), water (H_2O) and para-toluene-sulfonic acid (PTSA) is fed at the 38^{th} tray (39^{th}stage including condenser counted from the top) of the column. Due to the reversible nature of the reaction, the reaction is never complete in the pre-reactor and continues in the RD column. The reversible reaction shown is in equation (1.1) continues in the liquid phase on all stages of the column. The reaction may be catalyzed or un-catalyzed depending on the availability of the catalyst on a particular tray. For the trays on which the catalyst is present, the rate of reaction, however, depends on the catalyst concentration on that particular tray.

Table 3.1: Tray design of the RD column

Parameter		Value
Column diameter (internal)		1800 mm
Total tray area (m^2)		2.5434
Number of flow passes		Single
Number of bubble cap trays		48
Tray spacing [mm]	from top tray 1 to tray 37	337.5
	from tray 38 to tray 48	400
Height of the Column (m)		20
Number of bubble caps on each tray		77
Holdup on each tray (l)		112
Holdup of bottom kettle (l)		5000
Liquid flow path length		1345 [mm]
Active area		2.168 [m^2]
Net area		2.3057[m^2]
Total hole area		0.255 [m^2]
Down-comer area		0.1377 [m^2]
Percentage area of risers		10.99 %
Percentage area of down-comers		8.39 %
Percentage area of trough		10.91 %
Hole diameter [Nominal Bore]		65 [mm]
Hole pitch		147 [mm]
Weir length		1083 [mm]
Weir height		50 [mm]
Weir type (e.g. segmental)		"V" notch
Down-comer clearance		60 [mm]
Deck thickness		5 [mm]
Down-comer sloping		90 0
Down-comer length	from top tray 1 to 37 tray	387[mm]
	from tray 38 to 48 tray	452 [mm]
Cap diameter		103 [mm]
Slot area (all caps)		0.2021 [m^2]
Riser area		0.255 [m^2]
Annular area		0.3046 [m^2]
Slot height		15 [mm]
Slot width		5 [mm]
Skirt clearance		12 [mm]

Table 3.2: Re-boiler and condenser details

Re-boiler (2 No., Thermo siphon Type)		
	Re-boiler -1	*Re-boiler -2*
Type of exchanger	Thermo-siphon (shell and tube)	Thermo-siphon (shell and tube)
Number of tubes/plates	376	950
Tube O.D [mm]	25.4 [mm]	25.4 [mm]
Tube I.D [mm]	21.4 [mm]	21.4 [mm]
Tube length [mm]	2000 [mm]	2000 [mm]
Tube pitch	34 [mm]	34 [mm]
Pitch type	Triangular	Triangular
Shell I.D [mm]	750 [mm]	1145 [mm]
No. of Baffles	3	3
Baffle cut (%)	25	25
Process media	Process liquid	Process liquid
Heating media	Saturated steam	Saturated steam
Heat transfer area [m^2]	60	150
Condenser (2 No., identical, Plate Type)		
Type of exchanger	Corrugated Plate type heat exchanger	
Number of plates	194	
Number of twins	97	
Plate thickness [mm]	0.6	
No. of passes	1:1	
Process media	Process vapor	
Plate material	Alloy SS-316	
Cooling media	Cooling tower water	
Relative direction of the fluids	Countercurrent	
Heat transfer area [m^2]	160	
Connection diameter [mm]	200	
Design temperature (^{0}C)	90	
Design pressure (atmg)	6	

3.1 Objectives and outlines

- To generate data from an industrial scale reactive distillation column producing ethyl acetate using ethanol and acetic acid through liquid-phase esterification reaction using para toluene sulfonic acid as catalyst.
- Thermodynamic modeling of the reactive distillation column for better understanding of the RD process.
- To analyze the data with respect to operating conditions and the thermodynamic model.
- To simulate the column using a process flow sheet simulator.

With these in view, the plant data was generated using following steps:

- Sampling and analysis of the liquid and Vapor composition of all the trays, condenser and re-boiler of the RD Column.
- Temperature measurement of all the trays, condenser and re-boiler of the RD Column.
- Pressure measurement of all the trays, condenser and re-boiler of the RD Column.
- Input and output flow measurement of the RD Column.

3.2Data collection

For detailed analysis of plant behavior, it was decided that in addition to the data available through DCS (distributed control system), data for space velocity of reactor, temperature, pressure and composition (both vapor and liquid phases) on each tray of RD column should be obtained. Major bottlenecks of direct data acquisition from plant arise from the continuous operation, and no provision for sampling from intermediate trays of the column. The data generation required that sampling ports for collecting vapor and liquid samples be provided on each tray. The following difficulties were foreseen in making the provision for samples collections and simultaneous analysis of the collected samples:

1) Capital investment and scheduling of plant shut down were required for providing liquid and vapor phase sample collection ports along with provision for temperature and pressure sensors on each end every tray for online recording.
2) Identification of a standard condition of operation and maintaining the process parameters during the sampling time.
3) Simultaneous analytical checking for chemical acidity and moisture of all the samples during sampling.
4) A team of 6-7 persons was required to assist in the simultaneous sample collection procedure.

To overcome these difficulties, it was decided that, because of safety concerns due to the highly flammable nature of the ethanol and ethyl acetate, the installation of sampling port should be carried out in one phase during a scheduled shutdown of the plant. For collecting the liquid samples, sampling ports made of stainless steel tubes (SS317L) were provided in the down-comer at 10 mm above the bottom of the seal-pot. This location of the sampling port ensures that any vapor bubbles in the liquid on a tray, and froth at the top of the down-comer do not come in the liquid sample at the time of sample collection; also, the sampling ports do not get choked any time due to stagnation of flows or during long shutdowns of plant. Similarly, to avoid contamination of vapor samples by entrained liquid droplets, vapor sample collection ports were provided at the top of the disengaging space above the tray. Vertical 500 mm long stainless steel pipes of 13 mm ID and 15 mm OD were pierced through the bottom of the tray to collect samples of vapor emanating from the tray just below it. High density polyethylene (HDPE) transparent hose pipes were connected to the upper end of this tube. The vertical steel pipe was

filled with glass beads. Function of the vertical stainless steel pipe was to minimize the entrainment of liquid along with vapor. In case of any accidental liquid carryover, the transparent HDPE hosepipe was proved to be very useful for manual observation (Figure3.2). A drawing of the device used for sampling is given in appendix A (Figure A.1).

Figure 3.2: Sampling in ice-cooled containers

To make the provision for online recording of temperature, thermo-wells were provided in each down-comer with RTD (resistance temperature detector) installed. Similarly, pressure point sockets were installed in the disengaging space above every tray for the installation of pressure

transmitters and pressure gauges. It took about 900 man-hours in fabrications of these sampling ports. A shutdown was required for installing all these probes. A team of 15 members were deputed who looked after the insulation, instrumentation, mechanical and safety aspects for this job. It took additional 720 man-hours to complete the activity of providing sampling ports in a single shut-down of the plant. Temperature and pressure transmitters were used for continuous recording of temperature and pressure through DCS (ABB make, Freelance 2000). The analog signals were transmitted through DC output in the range 4 to 20 mA at 24 V and recorded digitally in the DCS memory.

3.2.1 Sampling schedule and strategy

There were total 104 sampling points on the RD column. Vapor and liquid samples were collected manually from all the points in glass ice-baths (Figure3.2). These ice-baths were used to prevent flashing of the hot liquid and to stop the reaction, if any, due to the high temperature of the sample. Similarly, vapor samples were also collected in similar glass ice-baths where the vapor after coming in contact with the cold surface condensed. Cold samples were then transferred to HDPE bottles for storage in a refrigerator for further analysis. Samples were labeled as L or V (liquid or vapor, respectively) followed by a two digit number representing stage number from where the sample had originated.

All the liquid and vapor samples from all the trays were collected as quickly as possible. However, it took about eight hours in collecting samples from all points. Also, essentially all process parameters were required to be maintained at a desired value listed in the Table 3.3 till all the samples for one set of data were collected. Two sets of data at two different settings (by about a 2.3% decrease in the reflux ratio, from 4.09 to 4.0, by decreasing the reflux flow rate from 13700 kg/hr to 13000 kg/hr) were collected. A larger variation in the reflux ratio (or any other parameter) was not permitted due to very dynamic nature of an industrial scale column (which is always operated under pseudo-steady state condition). To operate the column with this changed reflux ratio, other parameters were adjusted according to the operator's heuristic experience.

If during sampling there was a deviation in the process parameters, which were indicated by the alarms in the DCS, then the sampling was abandoned and fresh sampling was re-done on another

day. Typically it took about 3-4 attempts to collect one set of the sample from all the trays in one go (without DCS alarm). After making several attempts, two sets of data (reported as Case-1 and Case-2) were collected successfully.

Table 3.3: Two settings of the set-points while collecting samples

Parameter	**Case-1**		**Case-2**	
	Set point	Actual range	Set point	Actual range
Feed to column (kg/hr)	24200	23800-24200	24200	23800-24200
Reflux to RD column(kg/hr)	13000	12900-13200	13700	13500-13900
Top draw from column(kg/hr)	2550	2500 - 2600	2700	2650 - 2750
Water draw from decanter (kg/hr)	700	650-750	650	600-700
Bottom flow from RD column(kg/hr)	20900	20850-20950	20775	20650-20900
Steam flow to re-boiler (kg/hr)	4500	4400-4600	4700	4600-4800
Bottom level of RD column (%)	65	60 - 70	65	60 – 70
Top temperature (°C)	74	73.8 – 74.5	74	73.8 – 74.5
Bottom temperature (°C)	117	116 - 118	117	116 – 118
11^{th} Tray middle top temperature (°C)	78	78-79	78	78-79
26^{th} Tray middle temperature (°C)	90	90-92	90	90 – 92
35^{th} Tray middle bottom temperature (°C)	94	94-96	94	94 – 96
Top pressure [$kg/cm^2(g)$]	0.2	0.2 -0.25	0.2	0.2 -0.25
Bottom pressure [$kg/cm^2(g)$]	0.35	0.35-0.40	0.35	0.35-0.40

Chemical testing for acidity and moisture was done during the sample collection as it cannot be delayed because of two major reasons. First, in case of any human error during sample collection, it can be detected and rectified simultaneously (by taking another sample). Otherwise, it is very difficult to bring the system back to the desired conditions (Table 3.3) after a long gap. Secondly, to verify that there is no any damage to a sample during storage by comparing with the chemical analysis done prior to GC analysis. It took around 10 days to get chromatographic analysis of all the samples on GC as the required time for testing one sample was about 1 hour and in a day total 10 to 12 sample could be analyzed. Only a few samples were found defective, and these have not been reported in the data presented in Tables A.1 and A.2 given in the Appendix A.

3.2.2 Laboratory analysis

Analytical testing for acidity

This test was performed as per ASTM D 1613 standards. Samples were titrated with 0.1 N (normal) solution of sodium hydroxide (NaOH) for weight/weight (w/w) analysis for the determination of their acidity. Ethanol sample, 50 milliliter (ml),was taken in a 250 ml flask and titrated with 0.1 N NaOH standard solution (using phenolphthalein as the indicator) to neutralize the acetic acid present in ethanol. First of all burette reading was recorded for blank titration reading (BR). Then 1 gram of the test sample was added to the neutral solution and titrated with a 0.1 N sodium hydroxide solution till the color of the sample changed from colorless to light pink. Acidity of sample was calculated using the following equation.

$$Acidity\ (\ \%\ ^{w}/_{w}, as\ acetic\ acid) = \frac{(TV-BR)\times 6.005\times Normality\ \ of\ \ 0.1\ \text{N}\ NaOH}{Weig\,ht\ of\ \ test\ \ Sample\ \ \ in\ gram} \quad (3.1)$$

where TV and BR are the volumes of the 0.1 N NaOH consumed for titrating the test sample and consumed for the blank titration (ml).The NaOH solution was prepared as per the Indian Pharmacopeia (2010).

Moisture Content

The test for moisture content was performed as per ASTM D 1364 standards. For w/w analysis of moisture (water) content in unknown samples, the samples were titrated with calibrated Karl Fischer (KF) autotitrator (Make: VIGO; Model: Matric D). 50 ml of solvent (methanol) was placed in the titration vessel so that the electrodes are dipped in the solvent. The solvent was titrated against KF reagent. The test sample, 10 g, was added to the titration vessel and it was titrated once again against KF reagent to the electrometric endpoint. Moisture content was recorded as,

$$Water\ (\ \%\ ^{w}/_{w}) = \frac{BR\times K.F.factor\ \times 100}{Weig\,ht\ of\ \ test\ \ Sample\ \ \ in\ gram\ \times 1000} \quad (3.2)$$

where BR = volume of KF reagent consumed in test sample titration (ml)

KF = water equivalence factor of the KF reagent (mg/ml)

w = weight of test sample (gm)

Testing for the catalyst

De-mineralized (DM) water, 25 ml, was taken in a conical flask. To this 10 ml of test sample was added after weighing. The flask was then heated to 80 ^{0}C for the proper dissolution of the test sample in the DM water. Then the sample was cooled to the room temperature. $BaCl_2$ solution 10% (w/w), 10 ml, was added and the mixture was left for 4 to 5 hours. The precipitate is removed by filtering the sample through pre-weighed Whatman filter paper (no. 42 i.e. ash less).The retentate was taken in a silica crucible and keep in the muffle furnace at 650 ^{0}C for 2 hours and then cooled down to room temperature and the residue was weighed. The PTSA content in each sample wascalculated using the relation as shown below and the values are given in Table (3.4).

$$\text{PTSA } (\%\, {}^{w}/_{w}) = \frac{weig\,ht\ of\ residue\ \ in\ gram \times 0.1375 \times 100}{weig\,ht\ of\ test\ sample\ \ in\ gram \times 1000} \qquad (3.3)$$

Table 3.4**:** Catalyst concentration on each stage

Stage number	**Catalyst (wt %)**	**Catalyst (vol %)**
1 to 32	**0.00**	**0.00**
33	0.008	0.01
34	0.016	0.02
35	0.09	0.11
36	0.09	0.11
37	0.25	0.31
38	0.31	0.38
39 (Feed)	0.49	0.61
40	0.4	0.49
41	0.47	0.58
42	0.41	0.50
43	0.59	0.72
44	0.37	0.45
45	0.34	0.42
46	0.31	0.38
47	0.29	0.36
48	0.26	0.32
49	0.23	0.28
50 (re-boiler)	0.25	0.31

Gas chromatography:

Gas chromatography (GC), is a common type of chromatography used in analytical chemistry for separating and analyzing compounds that can be vaporized without decomposition. Typical uses of GC include testing the purity of a particular substance, or separating the different components of a mixture (the relative amounts of such components can also be determined). In gas chromatography, the mobile phase (or "moving phase") is a carrier gas, usually an inert gas such as helium or nitrogen. The stationary phase is a microscopic layer of liquid or polymer on an inert solid support, inside a piece of glass or metal tubing called a column. The instrument used to perform gas chromatography is called a gas chromatograph.

The gaseous compounds being analyzed interact with the walls of the column, which is coated with the stationary phase. This causes each compound to elute at a different time, known as the retention time of the compound. The sample is analyzed on the basis of comparison of retention times.

Exploratory testing for GC method development:

The following points are to be considered for the sample analysis method development using GC:

- Selection of GC machine
- Selection of column
- Selection of diluting solvent, dilution ratio
- Selection of internal standard
- Selection of program of GC
- Injection volume of sample

It took number of test trials and literature references for the development of method for unknown samples obtained from the trays of RD column. The unknown samples were a mixture of polar and non-polar compounds, and the concentration of the components in the sample (w/w) was varying in the range of 0.1 percent to 94 percent.

In the first attempt, the samples taken from the RD column were directly injected in the GC. First of all, we tried direct injection of unknown samples on GC's of different make like Nucon, Shimazu, and Agilent. This was tried for the GC's of various makes like Nucon, Shimazu, and Agilent. Various columns having different stationary phase, column I.D., film thickness, and column length as suggested by the respective manufacturers, e.g., HP-5, DB-624, DB-5 and GS-Alumina, DB-Wax were also tried for the sample analysis. But the major difficulty observed was merging of the peaks of ethyl acetate and acetic acid.

On the basis of information available in GC manufacturer's guides and some other standard texts [Vogel *et al.*, 1989; J&W GC and GC/MS Column selection Guide], several preliminary trials were conducted. Finally, it was decided to use acetone as a dilutant in the ratio of 1:30 (sample to acetone dilution ratios) and Agilent's DB-624 column (Table 3.5). Results were reproducible, no peaks were getting merged, and predicted acetic acid percentage was in close agreement with analytical results. For the quantitative analysis, MIBK was selected as internal standard and program for oven temperature was set after many trial runs on GC. The best program was to have 1 min hold-time at 40°C followed by increasing the temperature at a rate of 10°C/min up to 130°C, thereafter 15°C/min up to 220°C. Run time was set to be16 minutes.Figure3.3presents a typical chromatogram of a sample.

Table 3.5: GC column specifications

Column	DB-624
Length	30 m
Diameter	0.53 mm
Film thickness	3.0 μm
Film composition	6 % cynanopropyl-phenyl, 94 % dimethyl-polusiloxane
Oven equilibration time	0.5 min
Gas used	Nitrogen
Flow	4 ml/min
Average velocity	31.57 cm/s

For the analysis of the unknown samples, multi-level standardization of GC was done. Seventeen samples of known compositions (Table 3.6) were prepared in the expected range of composition from the plant data. A gas chromatograph (GC 7820 A, Agilent, Germany) equipped with a flame ionization detector (FID) was used for sample analysis. All analyses were carried out using a DB-624 column with nitrogen as a carrier gas at a flow rate of 30 ml/min. The oven temperature was varied from 40 ^{0}C to 220 ^{0}C.

Table 3.6: Samples composition (w/w) for multi-level standardization of GC

Sample No.	Acetic Acid	Ethanol	Ethyl Acetate	Water
1	95	0.4	2.5	1.5
2	90	0.3	7.1	3.35
3	83	0.6	12	4.82
4	77	0.96	17.0	4.04
5	71	1.6	19.4	7.35
6	67	1.6	22	9.12
7	63	1.85	23.4	10
8	53	1.71	29.90	14.7
9	48	2	36	14.4
10	43	1.7	43	11
11	38	1.7	47	11
12	31.5	1.8	49.6	16
13	27.5	1.8	58.5	10
14	21.5	1.5	72	3.8
15	14.3	1.0	84	1.64
16	8.3	1.0	87	2.4
17	3.8	0.75	92	1.2

Internal Standard Report

Data File: D:\EZChrom Elite\Enterprise\Projects\ETHYL ACETATE\Data\mix\VAPOURS-3\13080105.dat
Method: D:\EZChrom Elite\Enterprise\Common\Methods\Acetic Anhydride Asper IOLCP-1.met
Acquired: 14/08/2010 1:18:27 AM
Printed: 14/08/2010 4:04:33 AM

Sample Amt: 4.2325
Internal Std. Amt: 1.0271
Multiplier: 4.9662

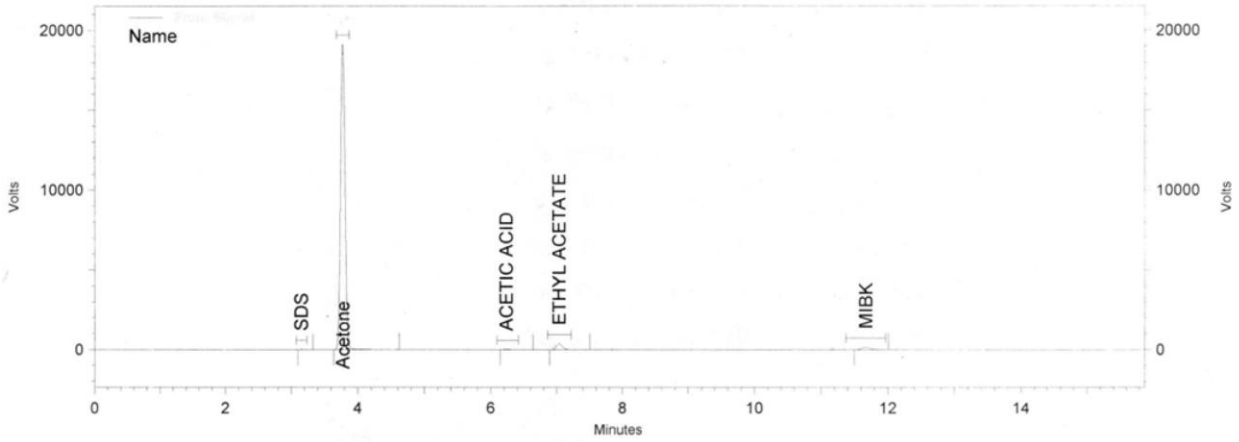

Channel A

Front Signal Results

Name		Time	Area	Amount	**Average RF**
SDS	3.155	236255	1.113		39.13328
Acetone	3.777	685995849	26.138		0.31681
ACETIC ACID	6.236	868199	5.487		53.52627
ETHYL ACETATE	7.039	18657083	81.508		34.89545
MIBK	11.674	9829529	1.205		1.00000
WATER			0.000 BDL		
Totals		715586915	115.452		

Figure 3.3: Typical chromatogram

Sample preparation and calculation

The reagents used for preparing the standards were lab reagent (LR) grade of acetone (99%) and ethyl acetate (99.9%) whereas acetic acid (99.9%), ethyl alcohol (99.9%), and MIBK (99.9%) were of analytical reagent (AR) grade.

For preparing a mixture to be injected in the GC, 5 g of a sample was mixed with 1 g of MIBK (as internal standard) giving 6 g of the sample (mixed with MIBK). One gram of this mixture was mixed with 30 g of acetone (dilutant), out of this 31 g mixture, 0.2 μL was injected in the GC, using auto sampler, for quantification. GC was kept under specified conditions for four hours before injecting the samples. Testing was repeated twice on two different days to check the reproducibility of the results. After confirming reproducibility, internal standard) correction factors were determined. Thereafter, the final weight percentages of the components were determined. Table 3.7 presents a sample calculation for predicting weight percent of ethyl acetate, acetic acid, ethyl alcohol, and water using GC.

Table 3.7: Sample calculation for determining composition (wt%)

Ethyl acetate		
Quantity as per GC	Quantity as per internal standard	Percentage
A	G=A*(E/F)	$\frac{G * 100}{(G + H + I)/(1 - 0.01 * D)}$
53.39	49.25	55.66
Acetic acid		
Quantity as per GC	Quantity as per internal standard	Percentage
B	H=B*(E/F)	$\frac{H * 100}{(G + H + I)/(1 - 0.01 * D)}$
33.22	30.64	34.63
Ethyl alcohol		
Quantity as per GC	Quantity as per internal standard	Percentage
C	I=C*(E/F)	$\frac{I * 100}{(G + H + I)/(1 - 0.01 * D)}$
1.28	1.18	1.33
Water (wt%)		
D		
8.38		
MIBK		
Quantity added	Quantity as per GC	
E	F	
1.14	1.24	

3.3Data analysis

The complete set of concentration, temperature and pressure data obtained in the present study is presented in Appendix A. Overall material balance of the column on the basis of concentrations measured in the laboratory and the flow rate obtained from DCS, and for two cases of operating conditions (Table 3.3) is given in Table 3.8. As thermo siphon re-boiler (50^{th} stage) evaporates the boil-up stream and returns the vapor to the column, therefore, the overall material balances across the column were made using recycle stream to the pre-reactor, feed to the column, organic distillate, and water decant streams (Figure3.1). It is seen from the table that, although, there is a

perfect match in the overall mass flow rates, however, a considerable difference in the mass balance of individual components is observed due to conversion of components through chemical reactions (Table 3.8). However, this rate of generation or consumption of each component is not in tune with the stoichiometry of the esterification reaction (e.g., to produce 392 kg of Ethyl acetate, only 180 kg Acetic acid is required).

Table 3.8: Component mass flow rates (kg/hr)

Component	*Feed*	*Bottom Product (49^{th} stage)*	*Water (Decant)*	*Top Product (Distillate)*	*Rate of Generation*
Case-1					
Ethyl acetate	2751.54	530.9	65.7	2455	392
Acetic acid	19916.6	19631.6	0.4	0	-415.3
Ethanol	91.96	6	28.1	29.9	-13.4
Water	1439.9	731.5	630.8	90.1	36.7
Total	**24200**	**20900**	**725**	**2575**	**0.0**
Case-2					
Ethyl acetate	2751.54	455	68.3	2544.6	316.36
Acetic acid	19916.6	19478.6	0.4	0	-437.6
Ethanol	91.96	12.5	29.3	33.2	-16.96
Water	1439.9	828.9	655.7	93.2	137.9
Total	**24200**	**20775**	**753.7**	**2671.1**	**-0.2**

This discrepancy may be due to pseudo-steady state behavior of large scale columns where all the key parameters are continuously monitored by the DCS and proper corrective control action is taken continuously to maintain all key parameters close to their respective set points. A close agreement in the overall mass balance indicates that during the investigation period there all the control actions were smooth and there was no drift in the set points. On the other hand, even a minor controlling action (required to maintain the operating conditions) is sufficient to disturb internal equilibrium conditions in such a way that all parameters remain fluctuating about a mean value, but the mean value of any parameter does not change with time (the pseudo-steady state). Thus data presented in Table 3.8 indicate that plant was running satisfactorily in the pseudo-steady state condition during data collection period.

Concentration profiles of *HAc* and *EtAc* obtained after laboratory analysis for the two cases (Table 3.3) are shown in Figures3.4(a) and 3.4(b). The figures indicate that the RD column is very sensitive to reflux ratio. For a 2.25 percent increase in reflux ratio from 4.00 (Case-1) to 4.09 (Case-2), there is a drastic change in ethyl acetate concentration profile in the column. By comparing Figures. 3.4(a) and 3.4(b), it appears, as if, an increase in reflux ratio has pushed the rectification zone downwards in the column. In Figure3.4(a) rectification of *EtAc* takes place between 10^{th} and 23^{rd} stages, whereas in Figure3.4(b) rectification begins right from the feed stage (39^{th} stage) to about up to the 17^{th} stage. This ultimately leads to a slight increase in the purity of ethyl acetate from 94.12% to 94.53% (w/w) in the distillate stream.

Increase in purity of distillate with increasing reflux ratio is in agreement with the behavior of conventional distillation columns. However, this similarity may not be observed in an RD column when the change in reflux ratio is large. Tang *et al*. (2005) showed this phenomenon for methyl acetate synthesis in a RD column. Distillate purity in an RD column depends on two factors – degree of separation, and the rate of reaction. An increase in reflux ratio leads to greater separation but at the same time it also increases product (*EtAc*) concentration on the lower trays (Figure 3.4b) favoring backward reaction (or retarding forward reaction). The reduction in forward reaction by increasing the reflux ratio is evident from the increase in rate of consumption of alcohol (the limiting reactant) from 13.4 to 16.96 kg/h (Table 3.8). The total initial mass of alcohol in the feed was 91.96 kg/h and the total alcohol in the products was 75 kg/h which is equivalent to reduction in alcohol conversion from 30.4% to 18.44% (Table 3.8). In the present RD system, with increase in reflux ratio from 4.0 to 4.09, the component separation overcomes the reduction in rate of formation.

Although there is significant change in the gradient of concentration profile (with a minor change in reflux ratio) leading to considerable change in reaction rate on many trays, but the temperature profile of the column remains smooth and almost unchanged (Figure 3.5). This is due to the fact that for the esterification reaction of acetic acid with ethanol, heat of reaction is negligibly small, and the pseudo-steady-state condition keeps all the internal flow rates fluctuating about a mean value. Such fluctuations may lead to level out any steep change in temperature profile inside the column.

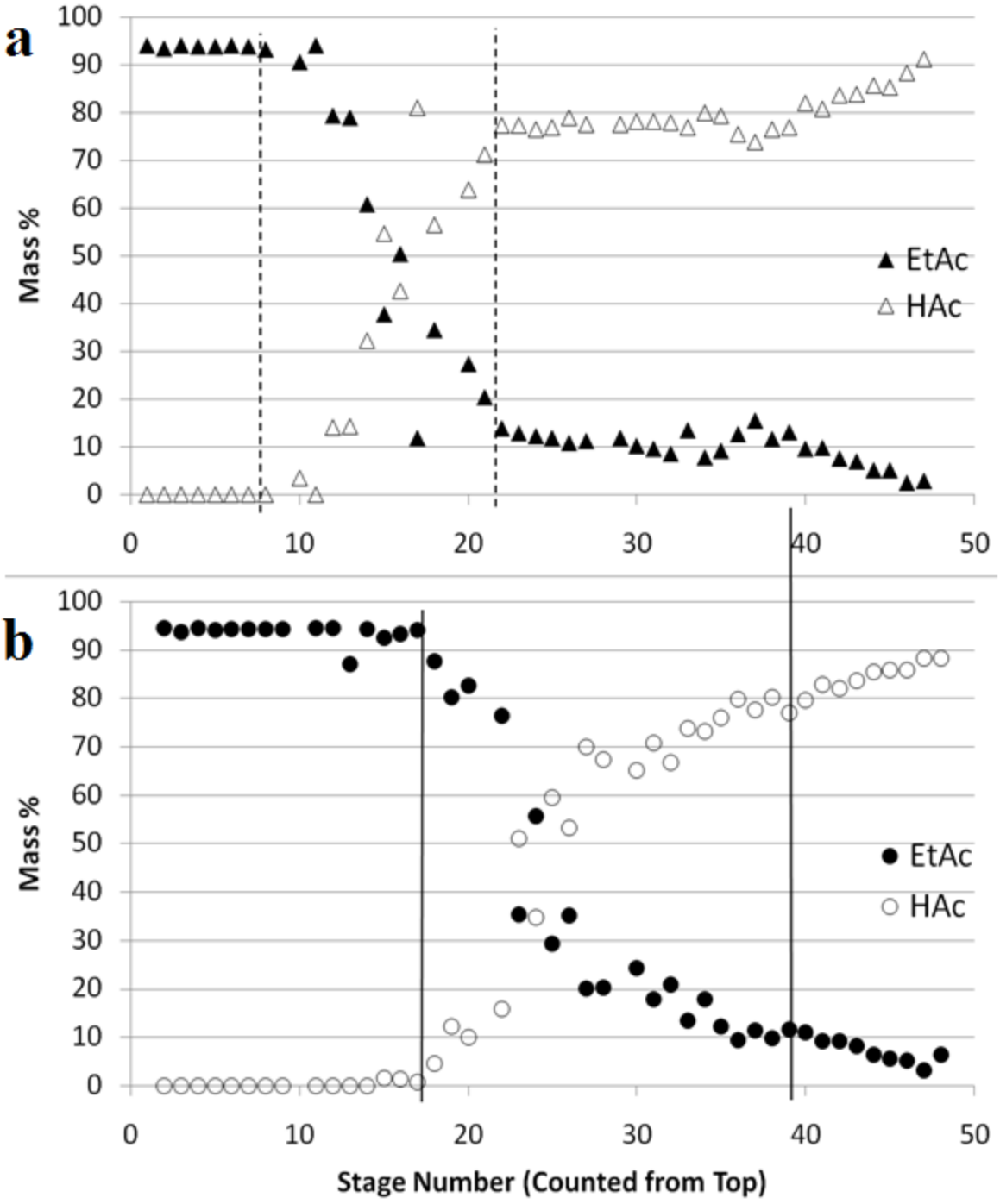

Figure 3.4: Concentration profiles (weight percent) of ethyl acetate (product) and acetic acid (reactant) (a) Case-1, (b) Case-2

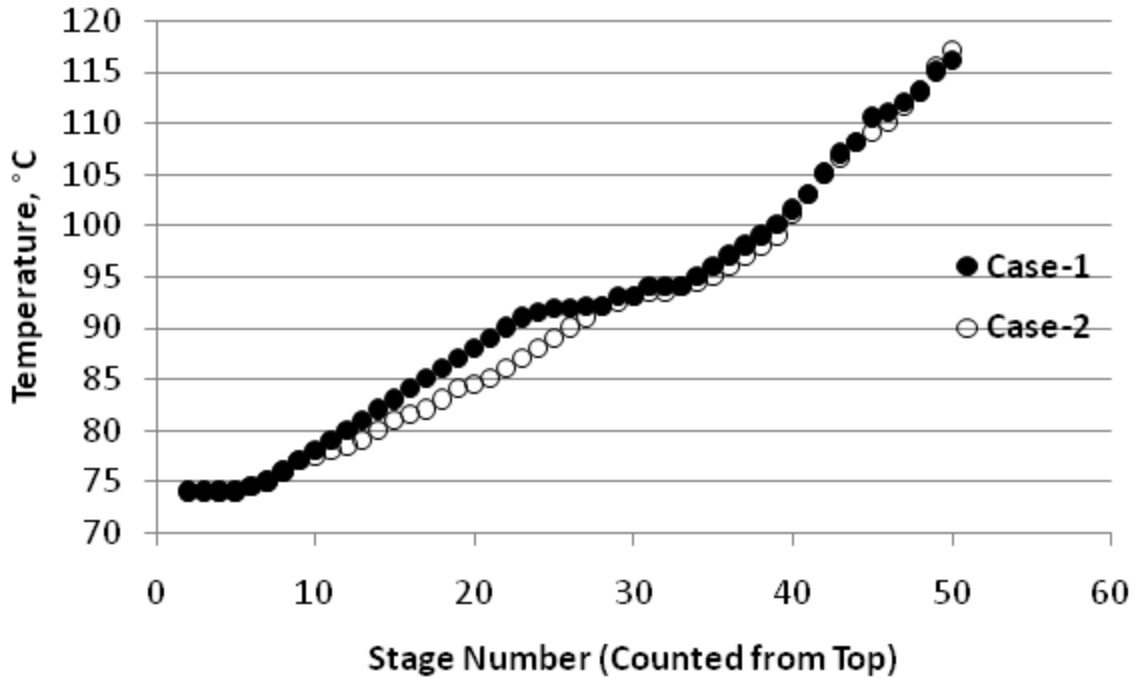

Figure 3.5: Temperature profile of the RD column for the two cases

Chapter 4

RD Column Model

The schematic of plant scale RD finishing column (capacity 60 tons per day) simulated in the present study is shown in Figure 4.1. The plant has a pre-reactor (not shown in the figure), an RD column with a decanter and a thermo-siphon re-boiler as discussed in the previous section. The pre-reacted, sub-cooled feed at about 101 °C from the reactor is pumped at a pressure of 304 kPa on the 39th stage (counted from the top, including total condenser) in the flash zone of the column at about 130 kPa. The feed is a mixture of acetic acid (*HAc*), ethanol (*EtOH*), ethyl acetate (*EtAc*), water (H_2O) and PTSA (para toluene sulfonic acid, the catalyst in the homogeneous phase). The reversible esterification reaction (catalyzed/uncatalyzed) occurring in the reactor as well as in the RD column can be represented as:

$$HAc + EtOH \underset{k_2}{\overset{k_1}{\rightleftharpoons}} EtAc + H_2O \qquad (4.1)$$

In the pre-reactor, excess of acetic acid (*HAc*) is used to ensure maximum conversion of *EtOH*, the extra *HAc* coming out from the bottom of the RD column is recycled back to the pre-reactor. The top vapor product from the column is condensed and sub-cooled to about 20 °C in a total condenser. Vapor stream emerging from the top of the column is condensed and separated into layers of water and organic phases in the decanter. One part of the organic layer is recycled as reflux to the column at the same temperature (20 °C) and the other part is withdrawn as a product for further purification. The water layer is sent for the recovery of *EtAc* and *EtOH*. The bottom product of the column, rich in *HAc*, comes from the lowermost tray (49th stage). One part of the bottom product is sent back to the pre-reactor and the other part to the thermo-siphon re-boiler for total vaporization. In the present work, RD column and decanter (Figure 4.1) are simulated and results are compared with the plant data.

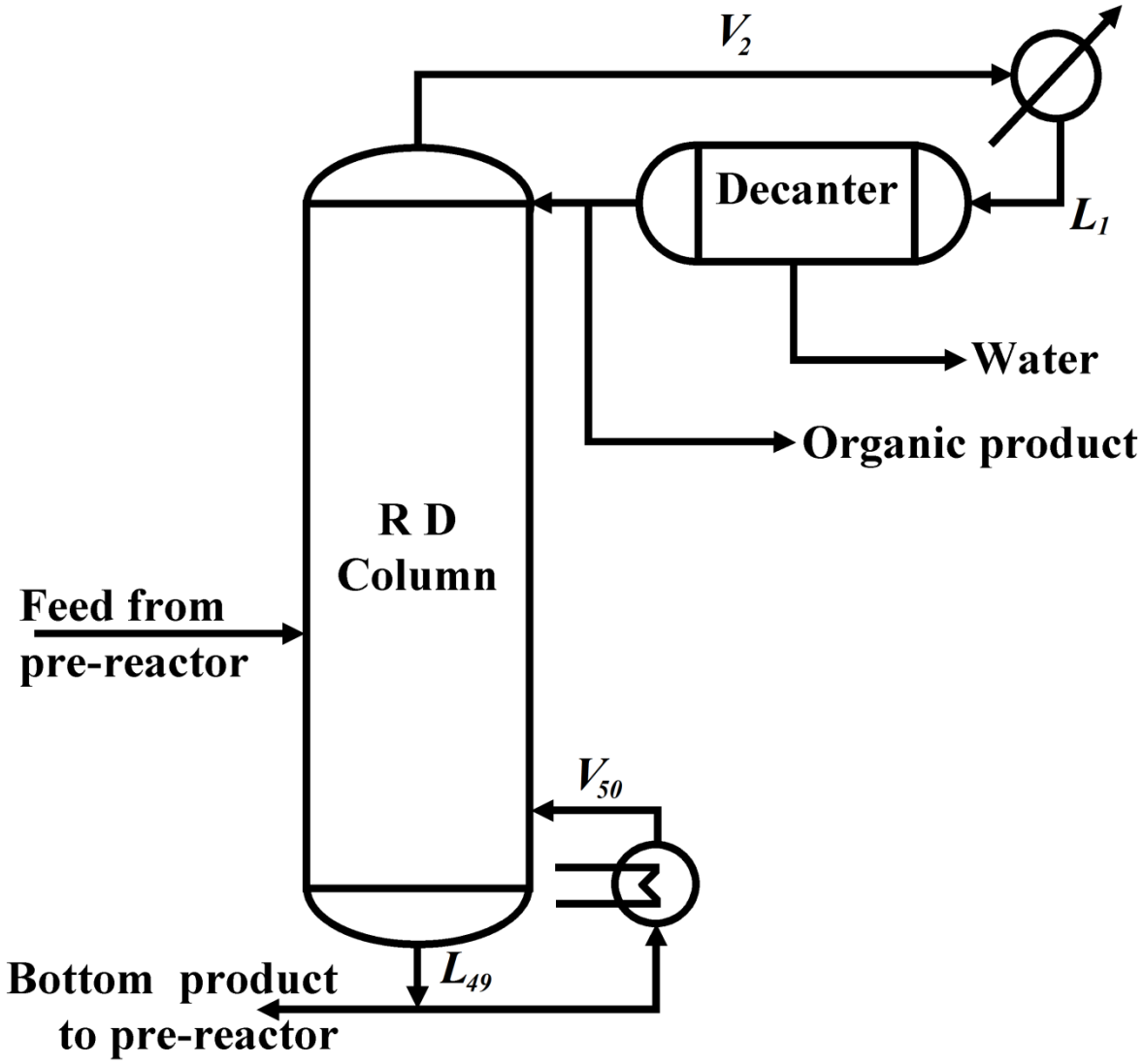

Figure 4.1: Schematic of RD column and decanter simulated in the present study

4.1Model for tray column simulation

The simulation was carried out using the rate based model of Aspen Plus™. Many authors have advocated the use of rate-based model for the RD columns. In the literature, the works based on rate-based model have used hypothetical values for tray hold-up. In this work, the rate based-model was used with the actual holdup data as the column hardware information was readily available. The rate-based model performs interphase mass and heat transfer calculations using transport equations rather than the idealized representation of equilibrium (theoretical) stages. Rate-based model also accounts for the multi-component interactions between simultaneously diffusing species, and assumes vapor-liquid equilibrium to exist only at the interface. The chemical reaction (equations4 and 5), is considered to take place in the liquid phase having reactor volume equal to the liquid holdup of the tray. The rate of formation of the i^{th} component on the j^{th} tray (r_{ij}) is estimated by adopting a suitable reaction kinetic model.

Based on the observation made by Liang *et al.*[2008] that the activities of sulfuric acid and PTSA are same, in the present work, the kinetic parameters reported for reaction rates with sulfuric acid catalyzed reaction [Alejski and Duprat, 1996]are used for PTSA. The overall reaction rate in the presence of a catalyst is expressed as:

$$-r_{HAc} = -r_{EtOH} = r_{EtAc} = r_{H2O} = k_1 C_{HAc} C_{EtOH} - \frac{k_1}{K_C} C_{EtAc} C_{H_2O} \quad (4.2)$$

where

$$k_1 = (4.195C_k + 0.08815)\exp(-6500.1/T) \quad (4.3)$$

and

$$K_C = 7.558 - 0.012T. \quad (4.4)$$

In case of un-catalyzed reaction, the rate expression reduces to[Venkataraman *et al.*, 1990]:

$$-r_{HAc} = -r_{EtOH} = r_{EtAc} = r_{H2O} = k_1 C_{HAc} C_{EtOH} - k_2 C_{EtAc} C_{H_2O}, \quad (4.5)$$

however, in this case forward and backward rate constants are given respectively by

$$k_1 = 483.33 \exp(-59445100/RT), \quad (4.6)$$

and

$$k_2 = 123 \exp(-59445100/RT), \quad (4.7)$$

wherek_1 and k_2 are in l/mol.s, *E*is in J/kmol and *R* is in J/kmol.K. Sensitivity analysis of these reaction models on the simulation results were done by evaluating forward and backward

reaction rates with ±20% deviation in rate constant values. Only about ±1% change in the predicted conversion was observed, suggesting that for the present work the conversion was not strongly dependent on the rate constant, therefore, using sulfuric acid kinetic parameters is safe.

Contrary to the equilibrium stage models where conventional MESH equations are solved for the overall material and energy balance on each stage [Kumar *et al.*, 2001], in the rate-based models these balance equations are applied separately for each phase on a stage. Apart from the phase material balances, phase energy balances, equilibrium equations, summation equations; the mass transfer in vapor phase, mass transfer in liquid phase and energy transfer across the interphase are used in the rate-based models.

The rate based model of Aspen Plus™ used in the present work is depicted in Figure 4.2. The figure shows a generalized schematic diagram of a typical non-equilibrium tray (j^{th} tray, counted from the top). In this figure, flow directions of inter-tray liquid and vapor streams along with vapor and liquid feed on the tray, and internal inter-phase material and energy exchange streams are shown. Within the stage, the i^{th} component's mass transfer occurring across the phase boundary is equal to the mass transfer rate of i^{th} component approaching the interface from the bulk of vapor on the j^{th} stage, N_{ij}^{V}, and the rate of mass transfer from interface to the bulk of liquid, N_{ij}^{L} (moles per second). The positive sign of N_{ij} $(= N_{ij}^{V} = N_{ij}^{L})$ indicates mass transfer from vapor to the liquid phase. Similarly, the heat transfer rate is also estimated in two parts, i.e., from the bulk of vapor to the interface and from the interface to the bulk of liquid. Reactions are assumed to occur in the liquid phase alone at a rate of r_{ij}. This assumption is justified as the vapor hold-up is very small as compared to the liquid hold-up on a tray.

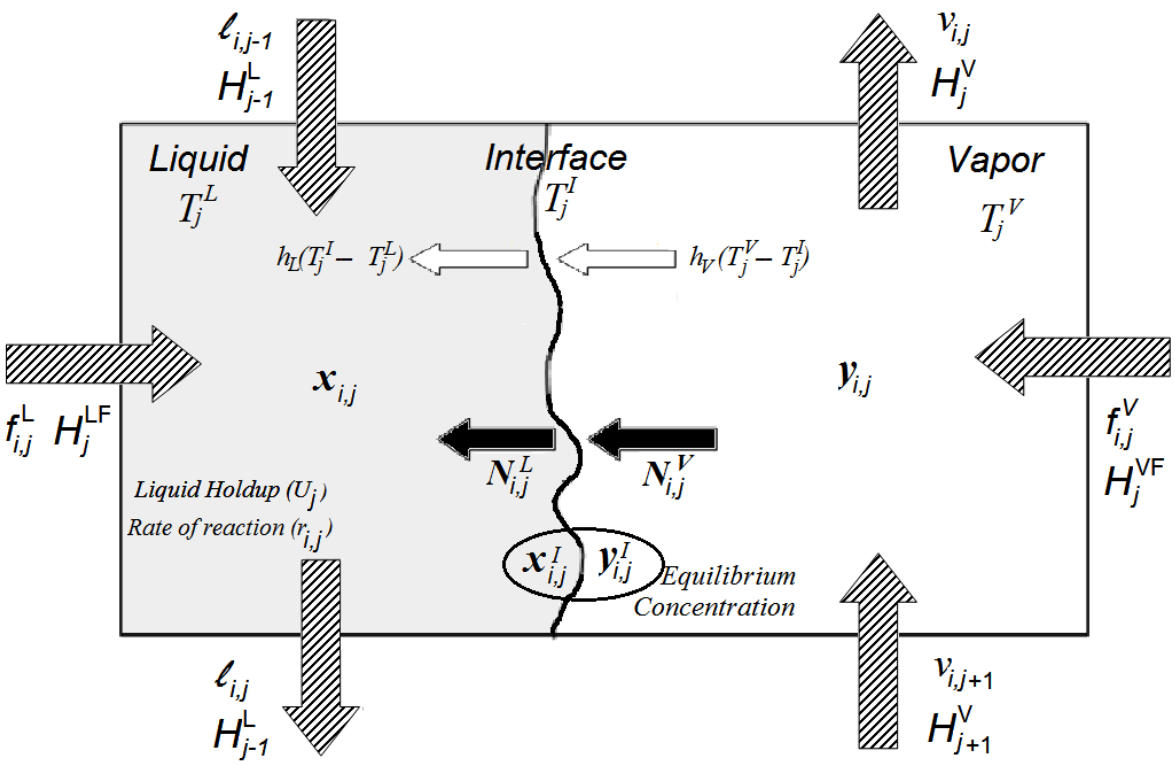

Figure 4.2: Schematic representation of rate-based model of non-equilibrium tray

4.2 Model equations

The non-equilibrium tray model equations in residual form are explained in the following paragraphs. For solving these equations concurrently, Aspen Plus™ uses Newton-based simultaneous correction approach to reduce all residuals to zero. The residual form of the molar balance equation may be represented as:

$$M^L_{ij} \equiv l_{ij-1} - l_{ij} + f^L_{ij} - N^L_{ij} + r_{ij} U_j = 0 \qquad (4.8)$$

where, U_j is the liquid holdup on j^{th} stage, and N^L_{ij} is the inter-phase mass transfer rate (mol/s) of i^{th} component (from the vapour-liquid interface to the bulk liquid), given by

$$N^L_{ij} = \bar{k}^L_{ij}\, a_j \left(x^I_{ij} - x_{kj}\right) + x^I_{ij}\, \bar{N}^L_j. \qquad (4.9)$$

Since the binary diffusive mass transfer coefficient, k_i of the component i, cannot be applied in case of a multi-component system, the effective mass transfer coefficient, $\bar{k}^L_{ij}$ is used in the above equation (4.9). An elaborate discussion with examples for predicting the effective mass

transfer coefficient of the component *i* in the liquid as well as in the vapour phases is presented by Taylor and Krishna [1993].

Similarly the material balance for vapour phase on j^{th} stage is represented as

$$M_{ij}^{V} \equiv v_{ij+1} - v_{ij} + f_{ij}^{V} - N_{ij}^{V} = 0 \quad (4.10)$$

where,

$$N_{ij}^{V} = \bar{k}_{ij}^{V} a_j \left(y_{ij} - y_{ij}^{I}\right) + y_{ij}^{I} \bar{N}_j^{V}, \quad (4.11)$$

is the total molar flux from bulk of vapour phase to the interface, and the energy balance equation for vapour and liquid phases are

$$E_j^{V} \equiv V_{j+1} H_{j+1}^{V} + \left(\sum_{i=1}^{c} f_{ij}^{V}\right) H_j^{VF} - V_j H_j^{V} - h_j^{V} a_j \left(T_j^{V} - T_j^{I}\right) - \bar{N}_j^{V} H_j^{V} = 0 \quad (4.12)$$

and

$$E_j^{L} \equiv L_{j-1} H_{j-1}^{L} + \left(\sum_{i=1}^{c} f_{ij}^{L}\right) H_j^{LF} - L_j H_j^{L} + h_j^{L} a_j \left(T_j^{I} - T_j^{L}\right) + \bar{N}_j^{L} H_j^{L} = 0, \quad (4.13)$$

respectively. To ensure equality of material and energy transport between the phases (i.e., across the phase boundary) following additional constraints are imposed.

$$M_{ij}^{I} \equiv N_{ij}^{L} - N_{ij}^{V} = 0, \text{ and} \quad (4.14)$$

$$E_j^{I} \equiv h_j^{V} \left(T_j^{V} - T_j^{I}\right) - h_j^{L} \left(T_j^{I} - T_j^{L}\right) + \bar{N}_j^{V} H_j^{V} - \bar{N}_j^{L} H_j^{L} = 0. \quad (4.15)$$

It is commonly assumed that mole fractions at the interface are in equilibrium with each other Hence, the equilibrium composition on the two sides of the interface are related by,

$$Q_{ij}^{I} \equiv K_{ij} x_{ij}^{I} - y_{ij}^{I} = 0. \quad (4.16)$$

In the above equation, K_{ij} is the vapor-liquid equilibrium ratio for component *i* at stage *j*. These K_{ij} values are computed at the interface conditions (compositions and temperature) using the same thermodynamic models which are used for the equilibrium models.

Only the molar balance equation for bulk liquid (equation 4.8) contains reaction term since reaction is considered in the liquid phase only. As far as energy balance is concerned, a standard state reference temperature based enthalpy balance accounts for all the thermodynamic heat effects such as heat of formation and heat of reaction. Therefore, additional heat of reaction term in equation (4.13) is not needed. The above-discussed rate based model calculates the binary mass transfer coefficients and the interfacial area using the empirical correlations. For bubble cap

trays, the most widely used correlation is the AIChE method [Seader *et al.*, 2011], and the same is used in the present work.

The heat transfer coefficients are calculated from Chilton-Colburn analogy [King, 1980]. Other suitable correlations for the estimation of the mass transfer coefficients of multi-component systems are given by Lee and Dudukovic [1998] and Taylor and Krishna [1993]. The estimation of the vapor-liquid equilibrium constant, K_{ij}, appearing in the equation (4.16) is, however, the major bottleneck in using these model equations for multi-component systems (particularly when the number of components is more than three). Applying rigorous thermodynamic analysis [De Nevers, 2012], K_{ij} can be expressed as

$$K_{ij} = \frac{y_{ij}^I}{x_{ij}^I} = \frac{\gamma_{ij}^I p_{ij}^I}{\widehat{\phi}_{ij}^I P}. \tag{4.17}$$

At low to moderate pressure, above equation reduces to

$$K_{ij} = \frac{\gamma_{ij}^I p_{ij}^I}{P}. \tag{4.18}$$

Superscript *I* in above equations refers to the properties at the vapor-liquid interface on a tray, as, in the present model, vapor-liquid equilibrium exists only at the interface. Clearly, accuracy of predicted vapor-liquid equilibrium depends on the accuracy of activity coefficient, γ_{ij}^I. Many correlations such as Margules, van Laar, Wilson, NRTL, etc. have been proposed to estimate activity coefficient which are selected on the basis of suitability of the model for a particular system.

Considering the liquid mixture (acetic acid, ethanol, ethyl acetate, and water) to be highly non-ideal, many authors have attempted to study the effect of liquid phase activity. Various activity coefficient models such as WILSON [Simandl and Svrcek, 1991], NRTL [Giessler *et al.*, 2001], UNIFAC [Kiatkittipong *et al.*, 2011] were used by researchers for the 13-stage column example of Suzuki *et al.*[1971]. NRTL (Non-Random Two Liquid model) is one of the most successful among them, which is recommended for highly non-ideal chemical systems, and can be used for VLE and LLE applications [Aspen Plus, 2010]. The same is being used in the present study. The activity coefficient of the i^{th} component in a mixture within the specified temperature range ($T_{low}<T<T_{high}$) is given by the following equation

$$\ln \gamma_i = \frac{\sum_{m=1}^{c} x_m \tau_{mi} G_{mi}}{\sum_{m=1}^{c} x_m G_{mi}} + \sum_{m=1}^{c} \frac{x_i G_{im}}{\sum_{k=1}^{c} x_k G_{km}} \left(\tau_{im} - \frac{\sum_{r=1}^{c} x_r \tau_{rm} G_{rm}}{\sum_{k=1}^{c} x_k G_{km}} \right), \quad (4.19)$$

where

$$G_{im} = \exp(-\alpha_{im} \tau_{im}), \quad (4.20)$$

$$\tau_{im} = a_{im} + \frac{b_{im}}{T} + e_{im} \ln T + f_{im} T, \quad (4.21)$$

$$\alpha_{im} = c_{im} + d_{im} (T - 273.15), \quad (4.22)$$

$$\tau_{ii} = 0, \quad (4.23)$$

and

$$G_{ii} = 1. \quad (4.24)$$

The binary parameters a_{im}, b_{im}, e_{im} and f_{im} appearing in equation (4.21) are unsymmetrical whereas c_{im} and d_{im} of equation (4.22) are symmetrical.

The equation is well suited for binary mixtures giving excellent prediction even for highly non-ideal solutions; however, for solutions having more than two components, the binary interaction parameters are affected by the presence of other component(s). To account for this issue, and also to retain the sanctity of the binary parameters, some modified NRTL equations have been proposed with additional ternary parameters, τ_{imk} [Nagata and Nakajima, 1991]. However, only limited application of such equation appeared in literature perhaps due to unavailability of the ternary parameter in a wider operating range and (to some extent) the complexity of the equation.

Chapter 5

Results and Discussion

This chapter is divided into two parts: thermodynamic model selection and validation, and RD process analysis. Column specifications and process parameters given in Table 5.1and Table 5.2, respectively, were used for all simulation runs of the present work. The catalyst (PTSA) concentration (vol%) on each stage was determined experimentally at least three times and no appreciable variation was detected. Considering this the average PTSA concentration (Table 3.4) was taken as constant and used in the rate expression of the corresponding tray. On stages 1 to 32, catalyst was not detected, therefore, uncatalyzed rate expressions were used for these trays. Condenser, re-boiler, and the decanter are modeled as equilibrium stages. The organic phase from the decanter was divided into reflux and product using a stream splitter.

Table 5.1: RD column specifications

Parameter	**Value**
Internal diameter (m)	1.8
Height of the Column (m)	20
Number of bubble cap trays	48
Holdup on each tray (l)	112
Holdup of bottom kettle (l)	5000
Number of bubble caps on each tray	77
Tray spacing from tray 1 to tray 37 (mm)	337
Tray spacing from tray 38 to tray 48 (mm)	400
Percentage area of risers	10.99 %
Percentage area of down-comers	8.39 %
Percentage area of trough	10.91 %

Table 5.2:Process parameters used for simulations

Parameter	**Value**
Pre-reacted feed (kg/h)	24150-24250
Pre-reacted feed composition (mass fraction)	*HAc* = 0.8362 *EtOH* = 0.00384 *EtAc*= 0.1159 H_2O = 0.044
Feed Temperature (K)	374-378
Feed Pressure (kPa)	304
Bottoms rate (kg/h)	20650-20900
Decanter temperature (K)	293
Organic reflux rate (kg/h)	13600-13800

5.1 Thermodynamic model selection

For the selection of a suitable thermodynamic model, in the present work, three activity coefficient models (WILSON, NRTL, and UNIFAC) were tried, but none of them gave a satisfactory result with their available values of binary parameters (Figure 5.1). For all the models, the top and bottom compositions matched with the plant data due to overall material and energy balance according to problem specification. However, large deviations are observed on the stages in the middle of the column. The poor predictions of UNIFAC and NRTL models below the top 15 stages may be attributed to the presence of highly non-ideal quaternary system showing complex phase behaviour with the number of azeotropes (binary and ternary). Therefore, it becomes very difficult to predict phase behavior by any existing thermodynamic models mostly suited for binary mixtures. So, the selection of the form of thermodynamic model and evaluation of its parameters became very crucial.

Considering the above facts, Tang *et al.*[2003] established a set of suitable binary parameters of the NRTL model to calculate liquid activity coefficients for the four azeotropes in this system using the experimental data available in literature. These parameters are subsequently used in many works. In the present work, the simulation runs even with these parameters gave a poor prediction of the composition profile for ethyl acetate observed in the plant (Figure 5.1).

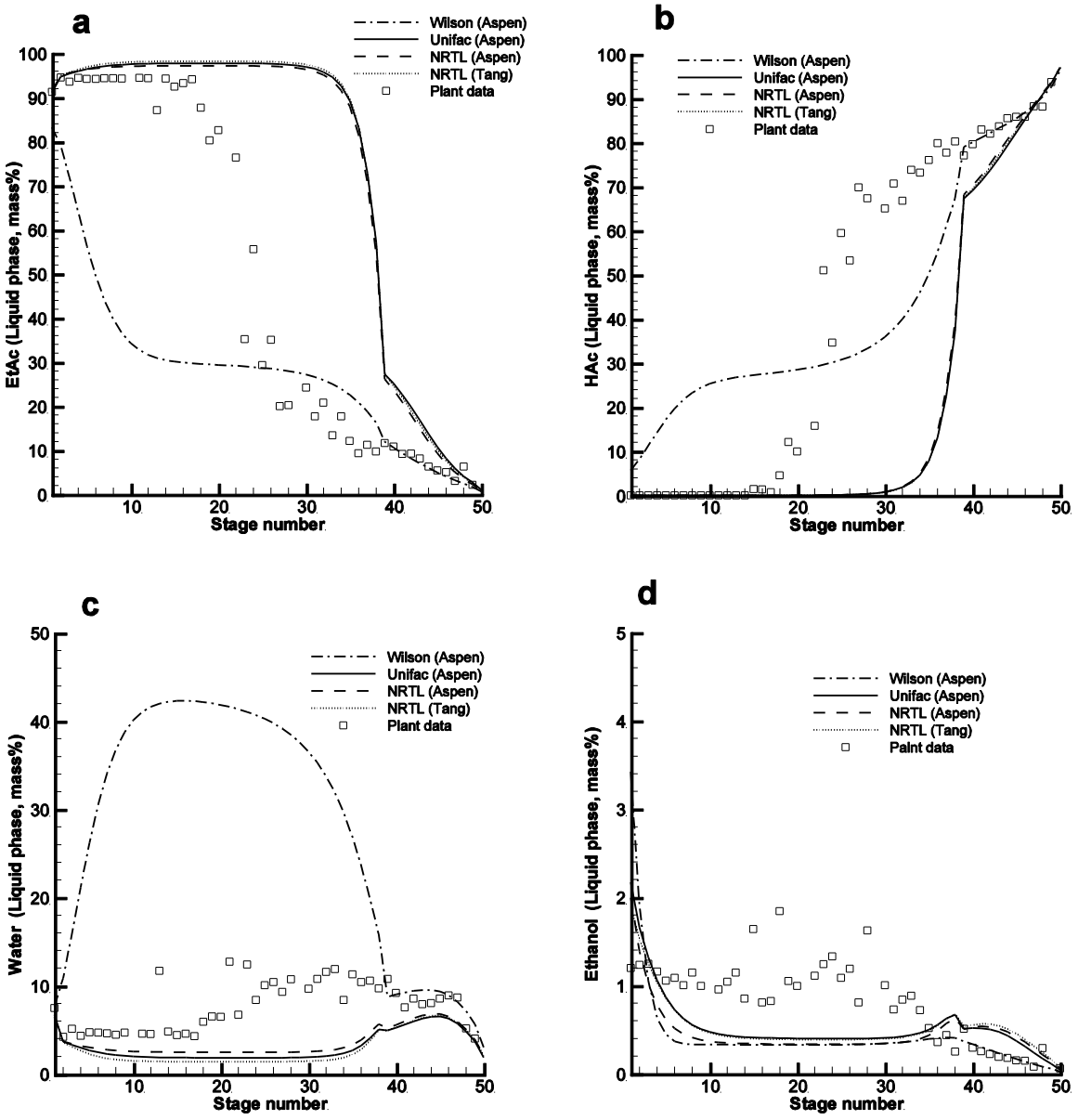

Figure 5.1: Comparison of Liquid phase concentration profile obtained from plant data with simulation results predicted using inbuilt Wilson, Unifac, and NRTL activity models for (a) *EtAc*; (b) *HAc*; (c) H_2O; (d) *EtOH*

Due to the existence of four azeotropes: *EtOH-EtAc*, *EtOH-H_2O*, *EtOH-EtAc-H_2O*, and *EtAc-H_2O*, in the system; the selection of model parameters becomes crucial. In this work, to improve the simulation results, a new set of thermodynamic parameters for the NRTL model was obtained by regression of the vapor-liquid equilibrium data available in literature. The binary parameters required for the NRTL model for the pairs *EtOH-EtAc* and *EtOH-H_2O* were taken from the Aspen Plus library, whereas, these parameters were evaluated by regressing experimental data obtained from literature for other binary pairs *EtOH-HAc* [Macarron, 1959], *HAc-H_2O* [Calvar *et al.*, 2005], *HAc-EtAc*[Pearce, 1954] and *EtAc-H_2O*[Ellis and Garbett, 1960]. The regression is done using the data regression module of Aspen Plus™. The complete set of binary NRTL model parameters used in present work is given in Table 5.3 and the comparison between experimental and predicted compositions of four azeotropes and their respective temperatures are given in Table 5.4.

Table 5.3: NRTL model parameters

Component *i*	*EtAc**	*HAc*	*HAc*	*EtAc*	*H_2O*	*EtOH**
Component *j*	*EtOH*	*EtOH*	*H_2O*	*HAc*	*EtAc*	*H_2O*
Temperature units**	K	F	K	K	K	K
Source	VLE-RK	***Fig 5.2(a)***	***Fig 5.2(b)***	***Fig 5.2(c)***	***Fig 5.2(d)***	VLE-IG
a_{ij}	-0.4331	0	3.557569	0.641522	15.04462	-0.8009
a_{ji}	-1.1015	0	1.202909	0.423308	-17.9925	3.4578
b_{ij}	336.9451	-700	274.3911	-660.233	-4188.59	246.18
b_{ji}	512.1041	350	-2071.47	-329.322	6800.702	-586.0809
c_{ij}	0.3	0.3	0.181587	-5.24E-01	0.414773	0.3
d_{ij}	0	0	-1.87E-03	1.00E-04	-1.68E-04	0
e_{ij}	0	0	3.91E-06	0.142193	-1.14E-03	0
e_{ji}	0	0	4.98E-06	0.132027	-0.03249	0
f_{ij}	0	0	0	0	0	0
f_{ji}	0	0	0	0	0	0
Temp. lower	313.15	373.15	0	0	273.15	298.14
Temp. upper	351.6	800	1000	1000	343.55	373.15

* Obtained from APV84-Aspen Plus™ data bank; **temperature units in equation 4.21

Table 5.4: Predicted compositions and temperatures of the azeotropes

Components	**Experimental compositions (mol fraction)**	**Experimental temperature (^{0}C)**	**Computed compositions (mol fraction)**	**Computed temperature (^{0}C)**
EtOH- EtAc	(0.462,0.538)	71.81	(0.4479,0.5521)	71.92
EtAc-H_2O	(0.6885,0.3115)	70.38	(0.6940,0.3060)	70.56
EtOH-H_2O	(0.9037,0.0963)	78.174	(0.8952,0.1048)	78.15
EtOH- EtAc-H_2O	(0.1126,0.5789, 0.3085)	70.23	(0.1181,0.6216, 0.2603)	70.37

The statistical data related to each regressed binary pair is given in Appendix B (TablesB.1 to B.4). The parity plots between x-y experimental data and the regressed parameters are given in Appendix B (Figure B.1).The sensitivity of the composition profile of *EtAc* to the regressed parameters is shown in FiguresB.2 and B.3.

5.2Validation of selected thermodynamic model

The binary molar *x-y* and *T-x-y* diagrams predicted using the new set of parameters after regressing experimental data (close to the atmospheric pressure) obtained from various sources is given in Figure 5.2(a-d). However, the two pairs of experimental data points (x=0.0049, y=0.5910) and (x=0.0086, y=0.6680) of Figure 5.2(d) were ignored as the regression module did not converge in the desired tolerance limits when these points were considered. Perhaps due to this, these points were not considered in the works of Tang *et al.*[2003 and 2005]. The figures show significant improvement in the match between experimental and predicted data, particularly for lower ethyl acetate concentration for the *EtAc*-water system. This improvement may play a vital role in the RD column simulation as in the lower section of the column, *EtAC* concentration is low. The predicted ternary two and three phase behavior of *HAc-EtAc-H_2O* and the residue curve map (RCM) of *H_2O-EtOH-EtAc* at the decanter pressure are presented in Figures 5.3(a) and 5.3(b), respectively.

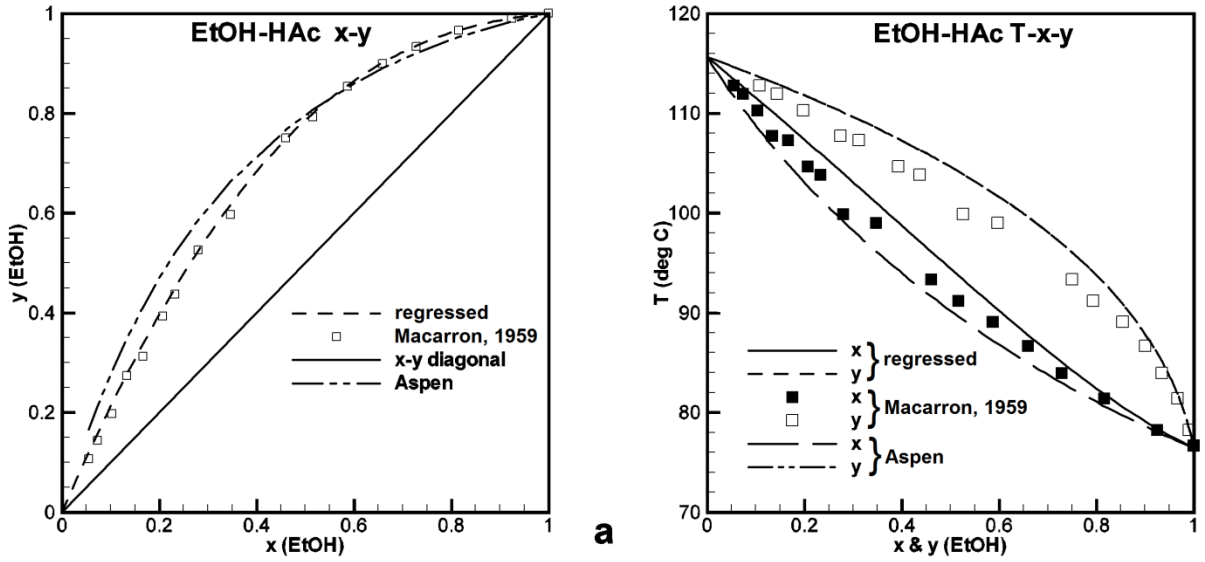

Figure 5.2(a): Comparison of experimental and predicted *T–x–y* diagram for *EtOH-HAC*[Source: Macarron, 1959]

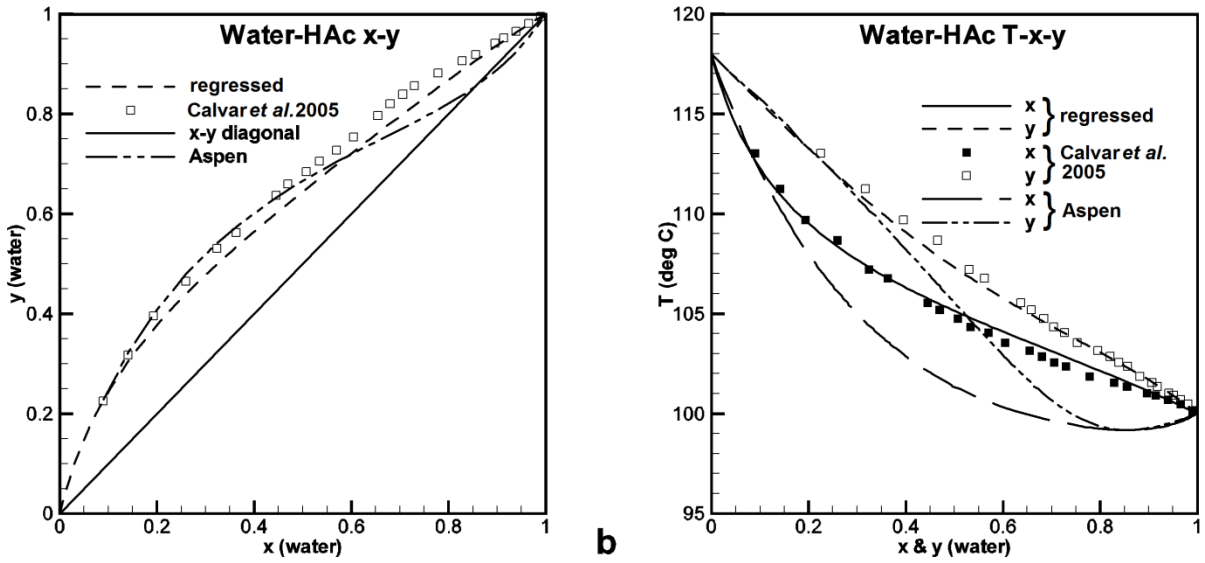

Figure 5.2(b): Comparison of experimental and predicted *T–x–y* diagram for *HAc-H_2O*[Source: Calvar *et al.*, 2005]

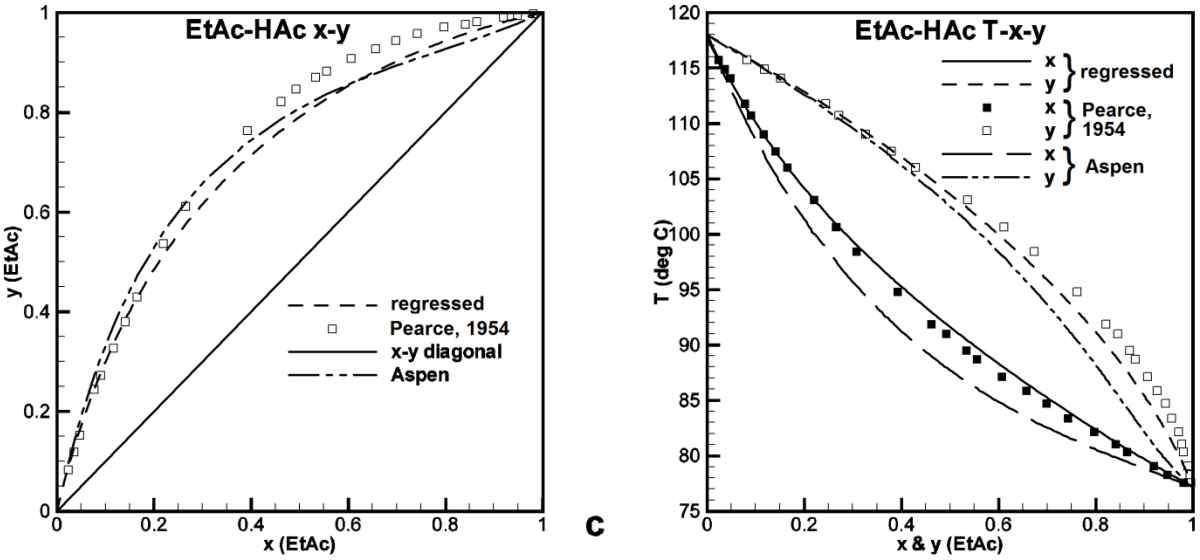

Figure 5.2(c): Comparison of experimental and predicted *T–x–y* diagram for *EtAc-HAc*[Source: Calvar *et al.*, 2005]

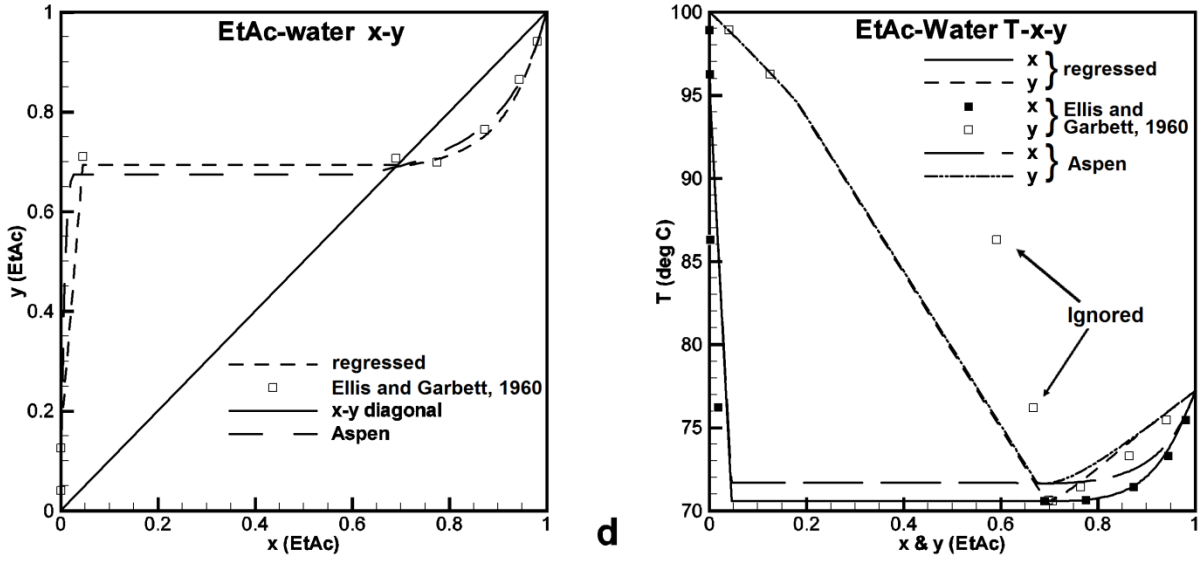

Figure 5.2(d): Comparison of experimental and predicted *T–x–y* diagram for *EtAc-H_2O*[Source: Ellis and Garbett, 1960]

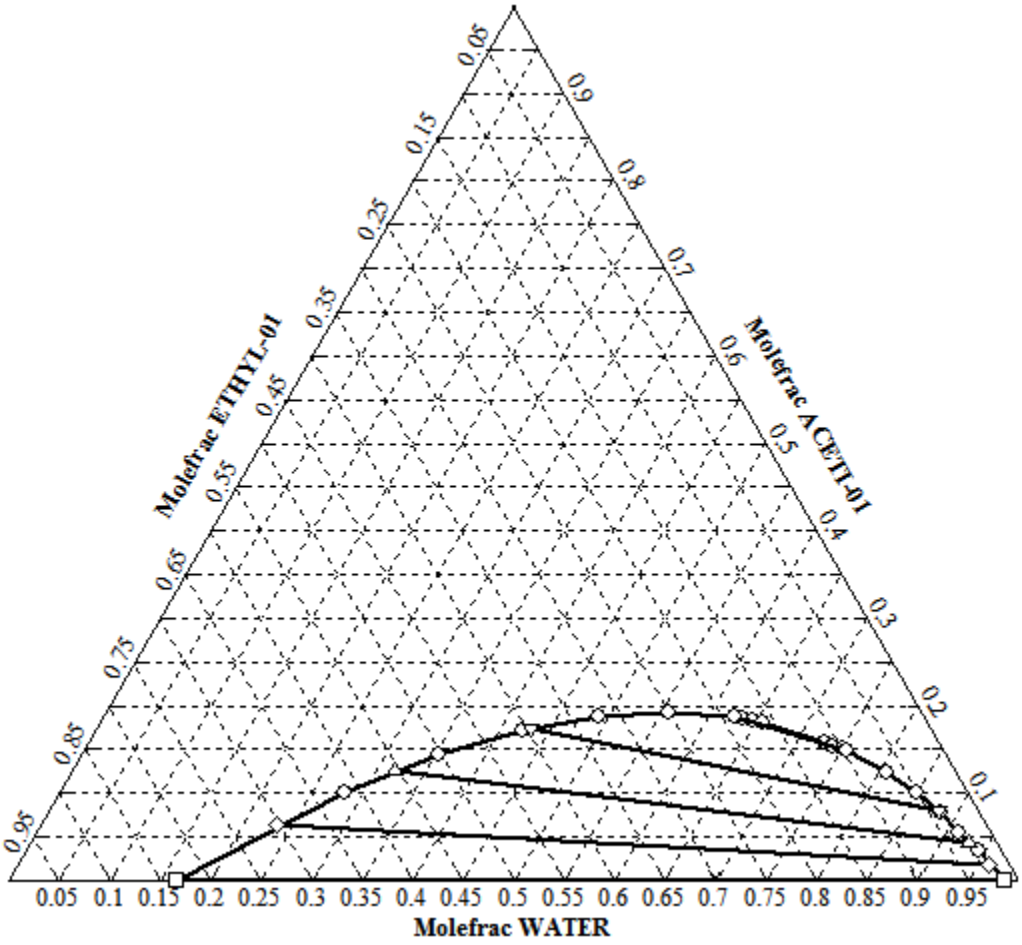

Figure 5.3(a): Ternary diagram for water – acetic acid (ACETI-01) – ethyl acetate (ETHYL-01)

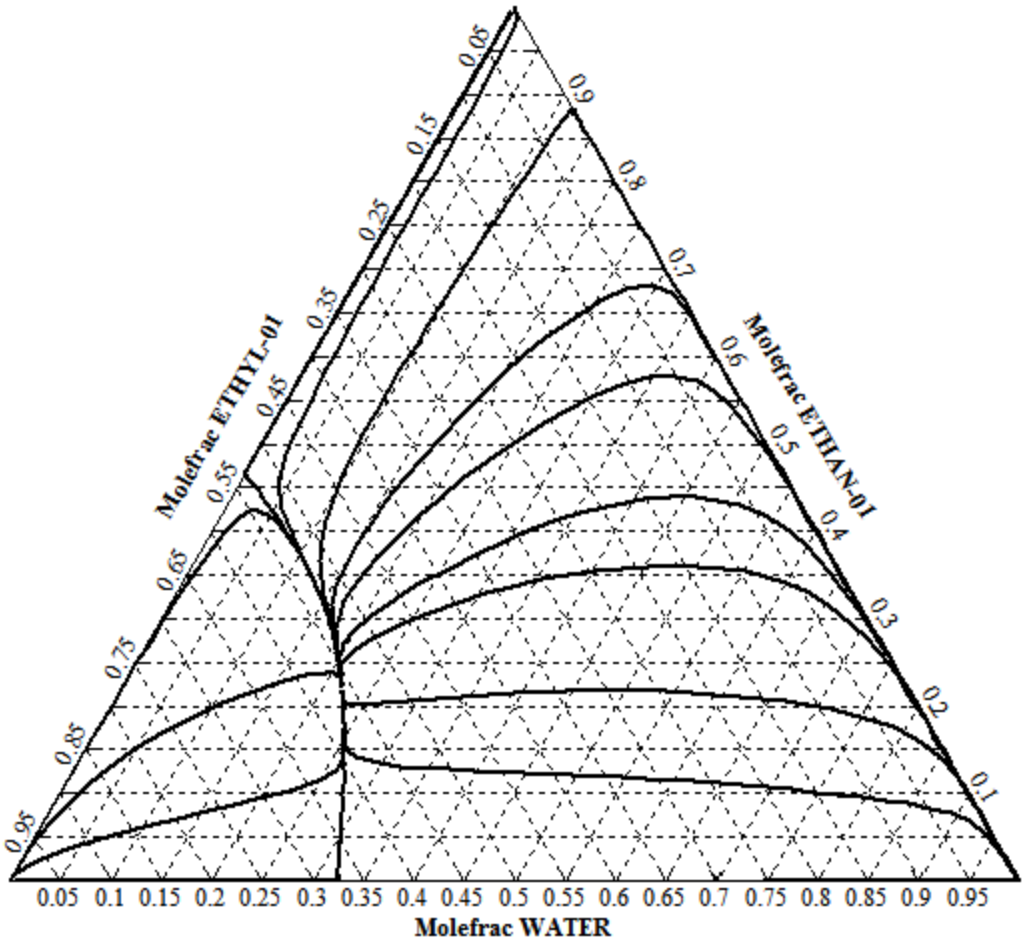

Figure 5.3(b): Residue curve map for water – ethanol (ETHAN-01) – ethyl acetate (ETHYL-01)

The various models for the liquid and vapor phase properties, with NRTL as base property method, used for the Aspen Plus simulation are given in Appendix C (Table C.1). Comparison of the predicted compositions of product streams, using simulation discussed in previous chapter and the modified thermodynamic parameters, with the plant data for these streams are reported in Table 5.5. Evidently, the predicted results are in good agreement with the plant data, which indicates overall material transport within the column and the specifications used for simulation are in tune with the actual plant.

Table 5.5:The comparison of predicted stream compositions (mass %) with the plant data

Component	Bottom product (49^{th} stage)		Top product		Organic product		Water	
	Plant	Aspen	Plant	Aspen	Plant	Aspen	Plant	Aspen
EtAc	2.19	2.64	91.30	91.48	95.27	95.49	9.06	8.52
HAc	93.76	94.13	0.00	0.0001	0.00	0.0001	0.05	0.001
EtOH	0.06	0.17	1.20	1.33	1.24	1.24	3.88	3.29
H_2O	3.99	3.06	7.5	7.19	3.49	3.27	86.99	88.19

5.3 Process analysis

Liquid and vapor phase composition profiles obtained for all four components, by using the new set of binary parameters, are compared with the plant data in Figure 5.4(a-d). Predicted vapor and liquid composition profiles of *EtAc* and *HAc* are in good agreement with plant data. However, the predicted change in concentration along the height of the column is slightly steeper than the plant data between stage numbers 20 and 30. A similar, but sharper, change in predicted temperature profile is also observed on these trays as compared to the observed plant data (Figure 5.5). These discrepancies may be due to one single difference, i.e., the strict steady-state condition in the flow sheet simulation and the pseudo-steady-state condition of the industrial column.

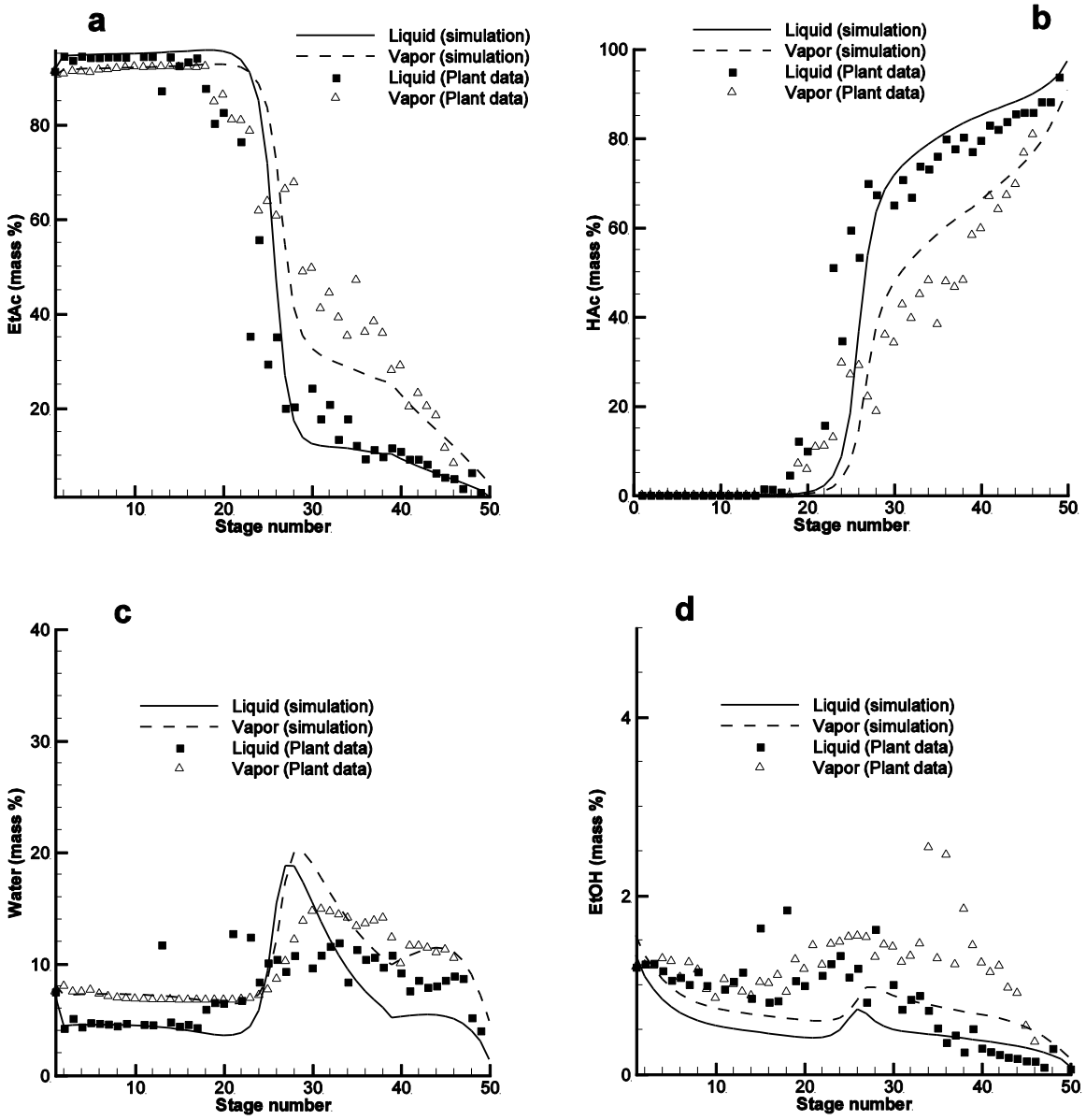

Figure 5.4: Comparison of vapor and liquid phase plant data with simulation results using NRTL model with regressed binary interaction parameters (a) EtAC; (b) HAc; (c) H_2O;(d) EtOH

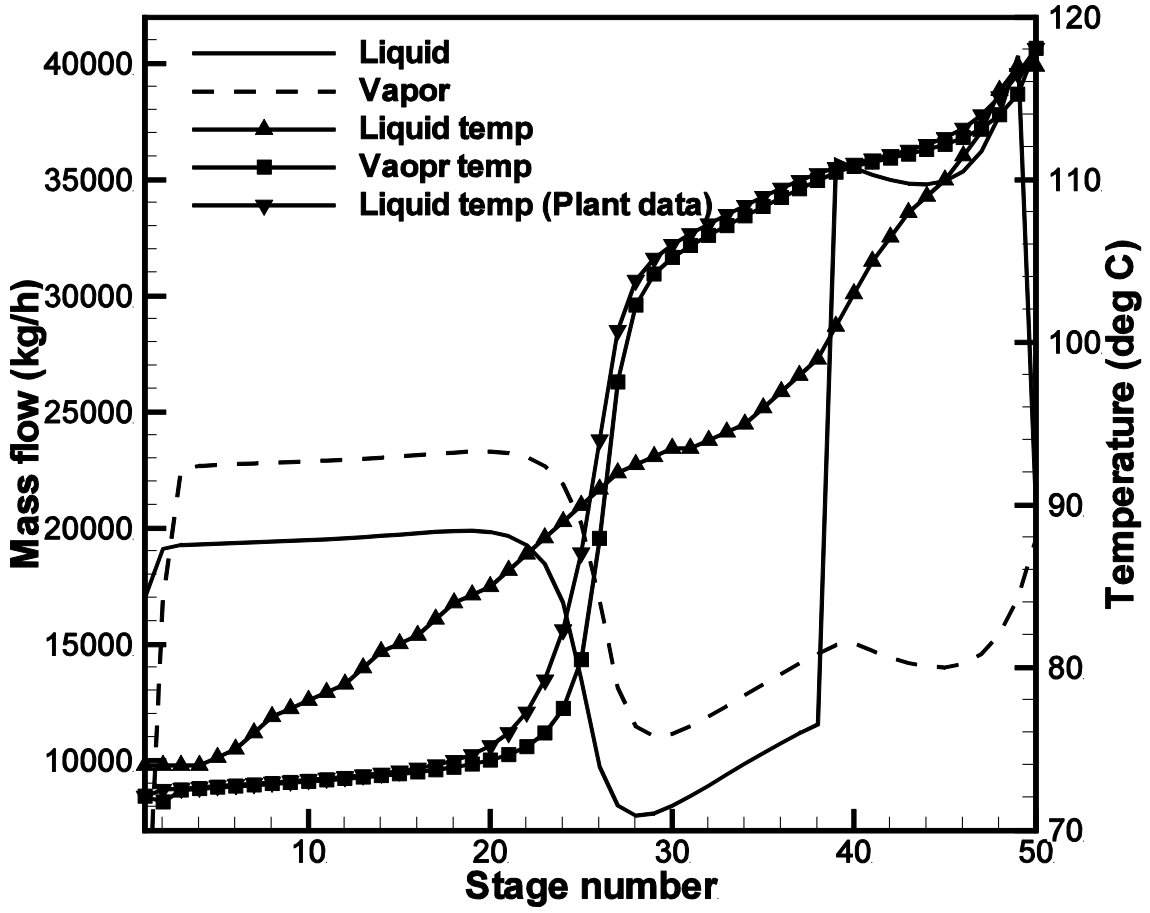

Figure 5.5: Mass flow rates and temperature profiles of vapor and liquid phases

In a large scale column, all the key parameters are continuously monitored and proper corrective action is taken to maintain them close to their respective desired steady-state value using a distributed control system (DCS). This controller action ultimately leads to fluctuations in variable parameters such as reflux ratio, boil-up ratio, liquid and vapor flow rates on each tray, etc. Such fluctuation about a mean value (set-point) may lead to level out any steep change in column profile.

This behavior of the column can be visualized more easily by considering the strict steady-state simulation results. The results suggest that to ensure a steady-state operation of the plant, there

should be a steep temperature and concentration profiles in the middle section (stage 20 to 30) of the column as indicated in Figures 5.4 and 5.5. However, due to the pseudo-steady state condition of the actual column, and a significant liquid holdup on each tray, the effect of any change in vapor or liquid flow rate needs more time for temperature adjustment which ultimately results in the flattening of temperature profile. An additional factor for the smoothening of temperature profile may be the sluggish response of the resistance thermometer used in the seal-pot. A flatter actual temperature profile and a steep predicted mass flow rate and temperature profiles indicate that the stages between 20 and 30 are the most active region in the column from the separation point of view.

Yet another interesting feature of predicted liquid and vapor flow profiles, shown in Figure 5.5, is the existence of minima of liquid and vapor flow rates on stage numbers 28 and 29, respectively. The simulation results reveal that the vapor approaching the middle section of the column (stage 20 to 30) is much hotter than the liquid coming from the top (with a maximum vapor-liquid temperature difference of about 6.5°C on stage number 25) leading to higher rates of evaporation of liquid in comparison to condensation (see Tables A.1 and A.2 given in appendix A). This ultimately leads to the reduction in liquid flow rate as we move down the column and an increase in vapor flow rate as we move upward in the column. Due to this excess evaporation, the system deviates from near "equimolar overflow and vaporization" condition and hence reduces the well known "L/V ratio" from about 0.779 (between stage number 5 and 19) to about 0.704 on stage number 30. These indicate that stages 20 to 30 are the most active stages of the column from the hydrodynamic point of view. Therefore, maximum variation in component compositions, liquid and vapor flows, and temperature profiles in the column is expected in this region.

A peak of water concentration above the feed tray is observed in both predicted as well as plant data. This peak water concentration in this section of the column may be due to the relative volatility of water, which lies between the volatilities of ethyl acetate and acetic acid. Figure 5.4(d) shows a large relative error between the predicted and actual *EtOH* concentrations; however, absolute errors are less than 2% of the mass fraction. Such error is expected even during the experimental determination of concentration; nevertheless, there is consistent under-

prediction of *EtOH* concentration throughout the column but nature of concentration variation is similar to the plant data.

The predicted *EtAc* generation rate (kmol/hr.m^3) on each stage is plotted in Figure 5.6. On all the stages below the feed stage, the positive ethyl acetate generation is predicted due to the presence of the catalyst on these stages. On the other hand, the negative rate (backward reaction) predicted on the few stages above the feed stage is due to the presence of the catalyst and a significantly higher composition of water and *EtAc* on these stages that favors backward reaction (equation 4.1). On the rest of the stages in the column, negligible net backward reaction is predicted as the concentration of *HAc* on these stages is very low and there is no catalyst present. The predicted overall conversion in the RD column is 18.8%, which is comparable to the actual plant data.

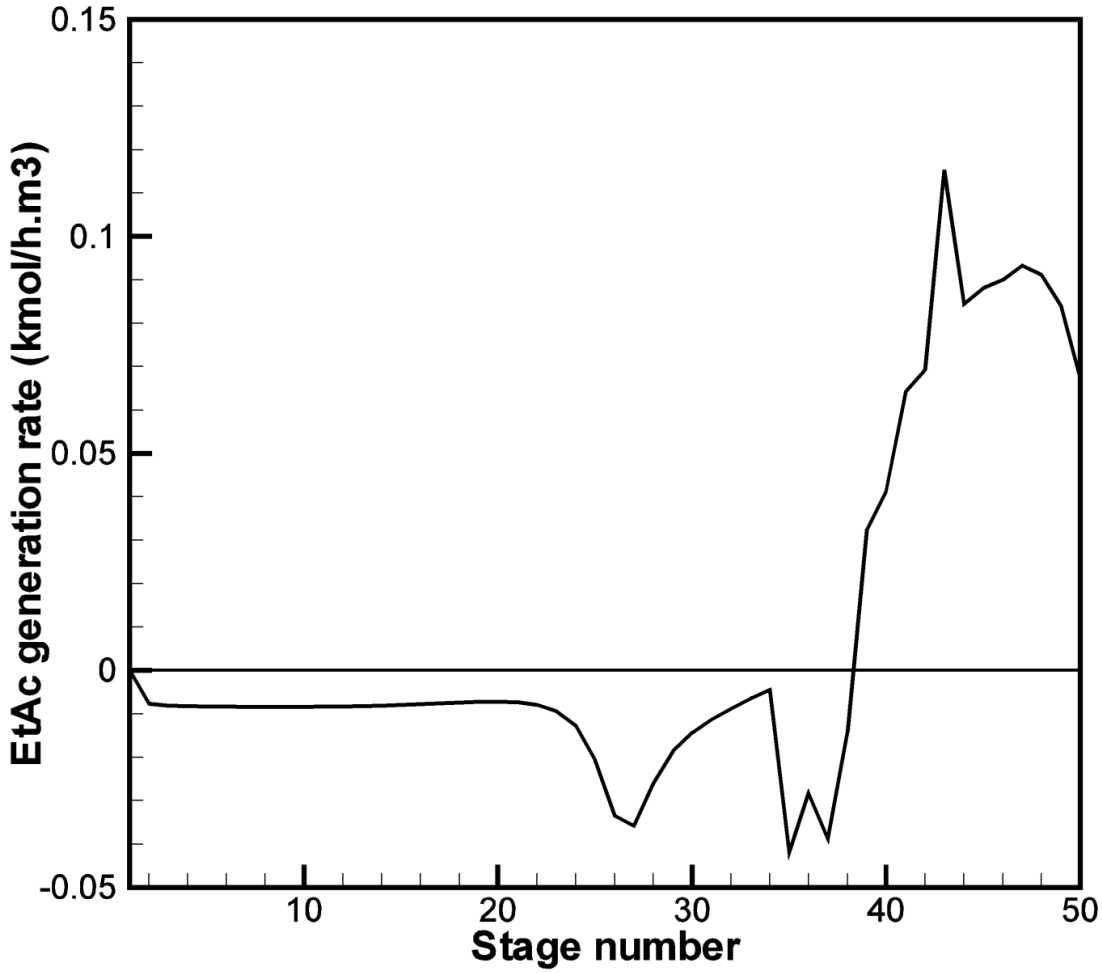

Figure 5.6: Ethyl acetate generation rate

The predicted surface tension of the liquid phase and the stage efficiency of each stage are shown in Figure 5.7. High surface tension between stages 20 to 40 may be associated with the similar trend of water content on these stages (Figure 5.4c), however, it is interesting to note that even when liquid phase surface tension is increasing on these stages, tray efficiencies estimated by the rate-based model of Aspen Plus^{TM} is considerably low. This is against the general observation that the tray efficiency increases with increasing surface tension. This indicates that the occurrence of reaction on a tray affects the relationship between point and tray efficiencies in a complex manner [Fisher and Rochelle, 2002]. The lower liquid flow (leading to less turbulence) on these trays may be the additional cause of lower efficiency in this section of the column. Efficiency attains a maximum value at the feed stage (stage 39) due to high liquid influx, leading to greater turbulence on the stage.

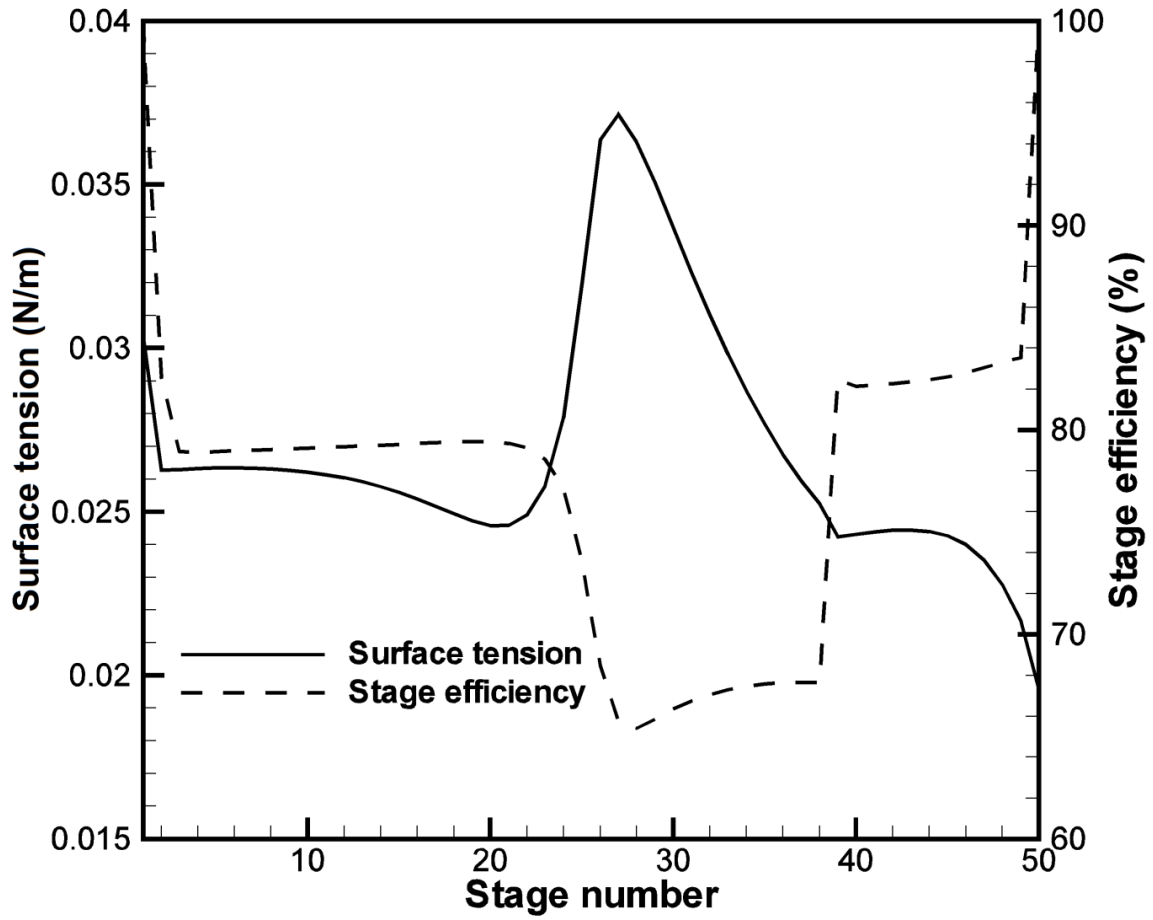

Figure 5.7: Predicted stage efficiencies and estimated liquid phase surface tension

Figure 5.8 shows the effect of the organic reflux flow rate from its lower limit of 13000 kg/h to 16000 kg/h on the *EtOH* conversion and *EtAc* purity. The simulations with a reflux rate less than 13,000 kg/h (i.e., below the standard reflux rate of the actual plant) do not converge. In such cases, lower reflux reduces separation in the column, thus the acetic acid composition in the condenser increases beyond the plait point which subsequently leads to no phase separation in the decanter and the simulator fails to converge.

Like a conventional distillation column, in this case too, an increase in organic reflux (keeping the distillate flow rate constant) causes an asymptotic increase in distillate purity (i.e., *EtAc* concentration). A linear increase in re-boiler duty (not shown in the figure) and decrease in ethanol conversion was also observed with an increase in reflux flow rate (Figure 5.9). The effect of the reflux flow rate on column profile is shown in Figure 5.9(a). The figure shows that the increasing reflux leads to higher *EtAc* concentration on more numbers of stages in the upper portion of the column. The composition changes are significant in the middle section which seems like a wave propagation phenomena observed during the dynamic simulation of an RD column [Kienle and Marquardt, 2003]. However, a higher *EtAc* concentration suppresses the forward reaction, thus, overall conversion in the column decreases. Also, the area under the ethanol mass fraction curve is decreasing with increasing reflux (Figure 5.9b) leading to a decrease in ethanol conversion.

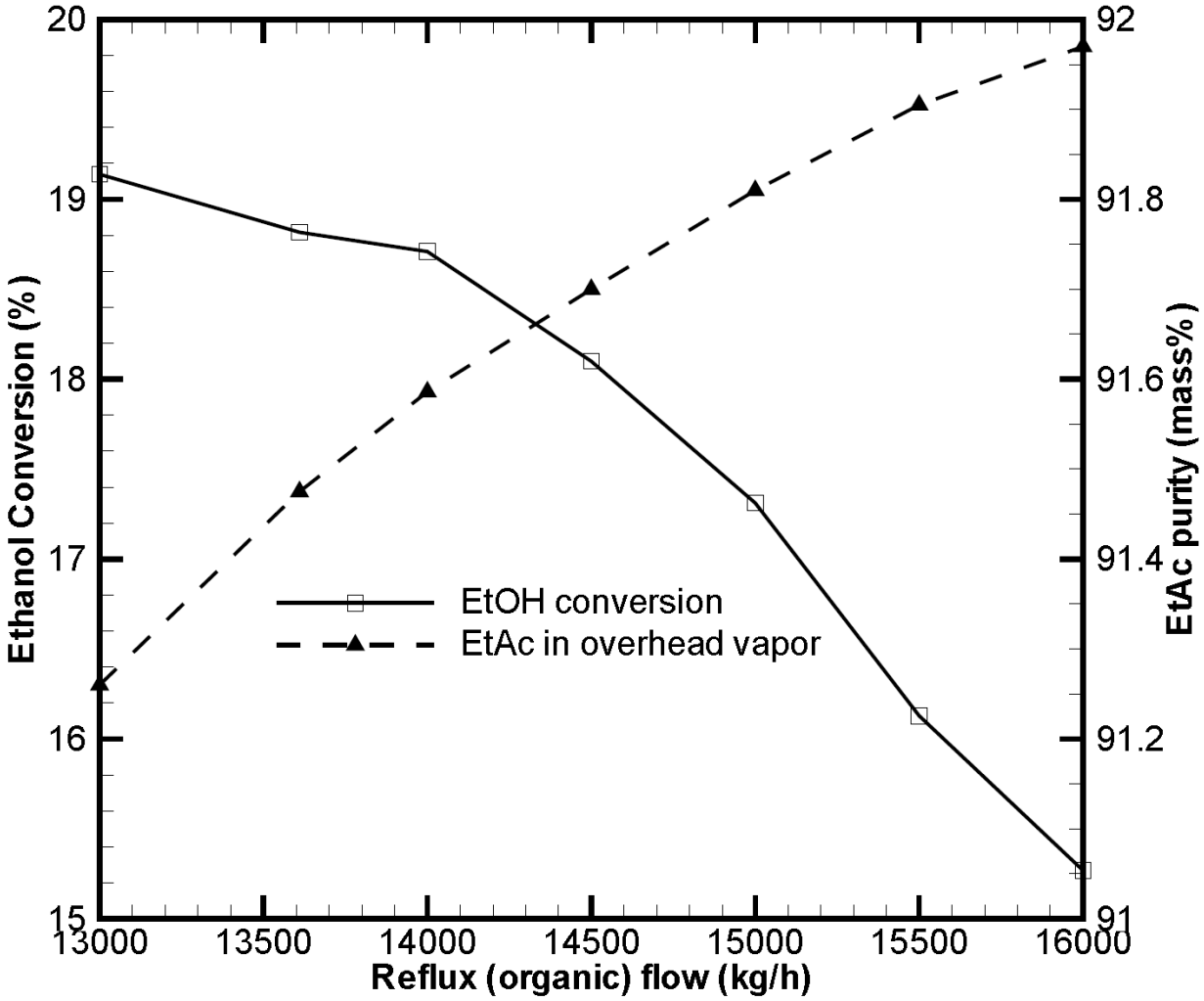

Figure 5.8: Effect of organic reflux flow on *EtOH* conversion and *EtAc* purity

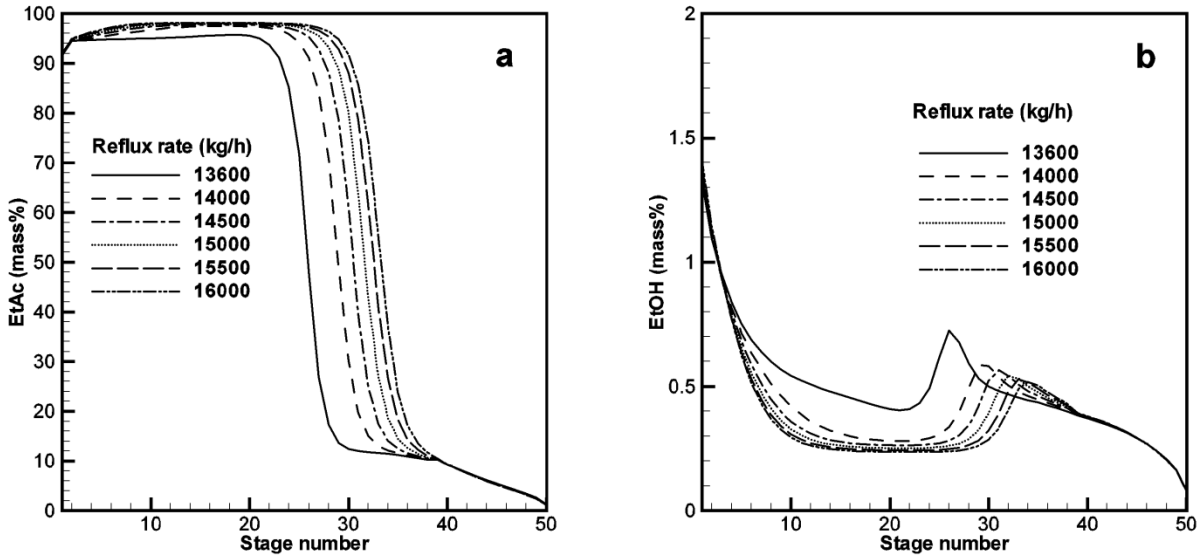

Figure 5.9: Effect of organic reflux flow on concentration profiles of (a) EtAc and (b) EtOH

5.4Comparison of equilibrium (EQ) and rate-based models

Many studies in the literature have advocated the use of rate-based models for the reactive distillation columns. The EQ (equilibrium) stage models assume phase equilibrium on all stages. In this section of the thesis, the RD column simulations using EQ model 'Radfrac' and the rate-based model of Aspen Plus^{TM}are compared with the plant data. The process parameters in both the cases of simulation are kept same as those for the plant. The same kinetic parameters and the regressed binary interaction parameters (Table 5.3) are used for both EQ and rate-based models.

The comparison of the column composition profiles, for liquid and vapor phases, with EQ, EQ model with stage efficiency from rate-based model, and rate-based model simulations is given in Figures 5.10-5.13. The figures clearly show that, for all the components, the rate-based model's predictions are far more superior to the EQ model predictions in both liquid and vapor phases. EQ model simulations using stage efficiency predicted by rate-based model also showed improved predictions (closer to plant data as compared to EQ model with ideal stages).

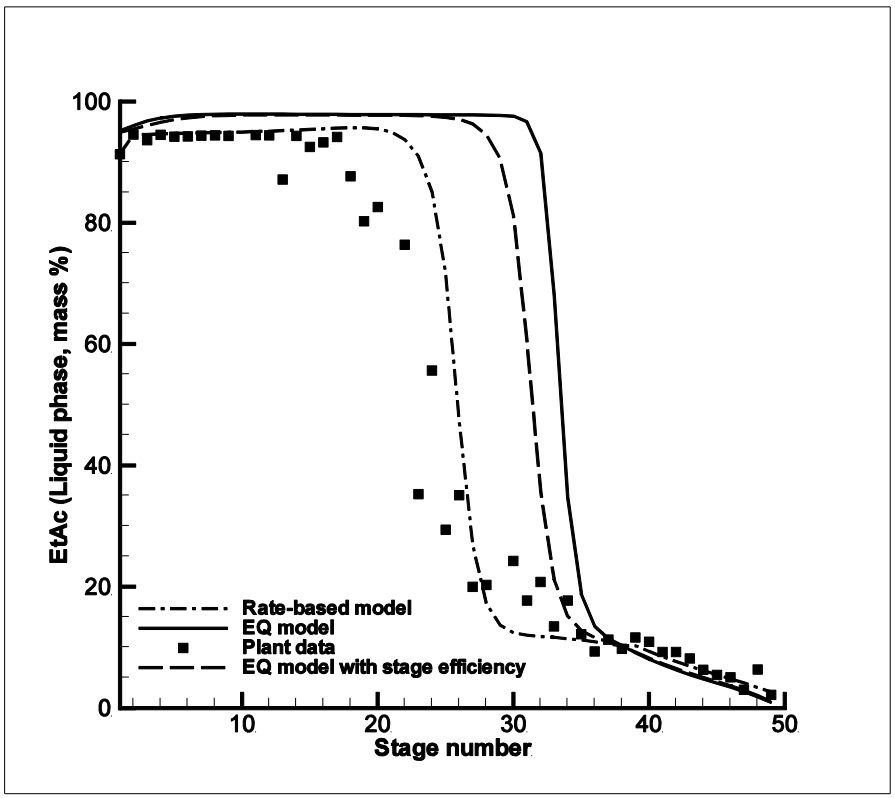

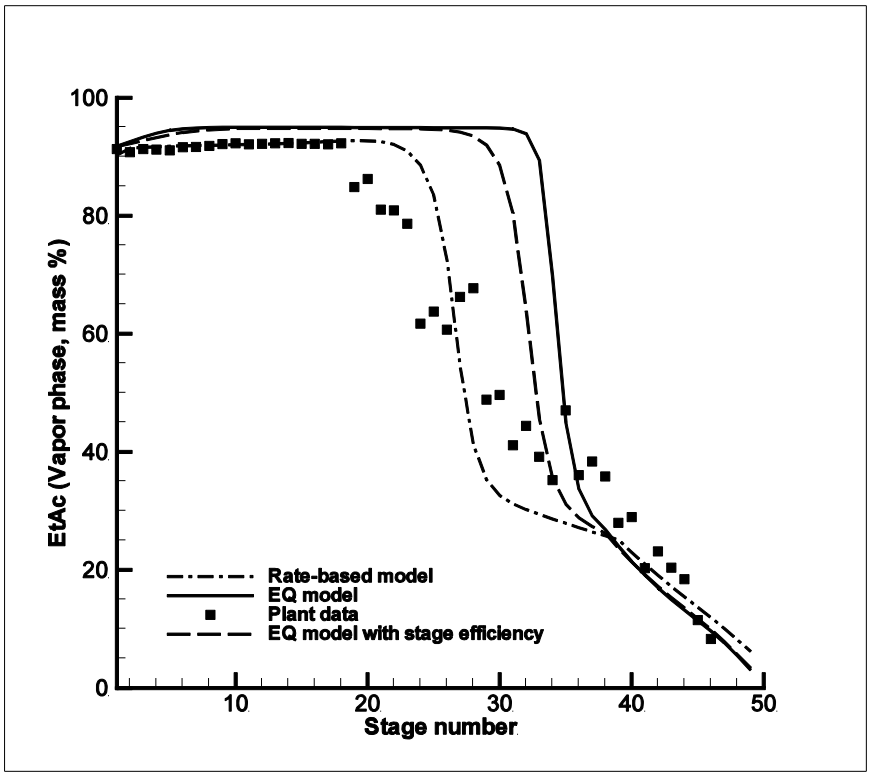

Figure 5.10: Comparison of *EtAc* composition profiles (a) liquid phase; (b) vapor phase

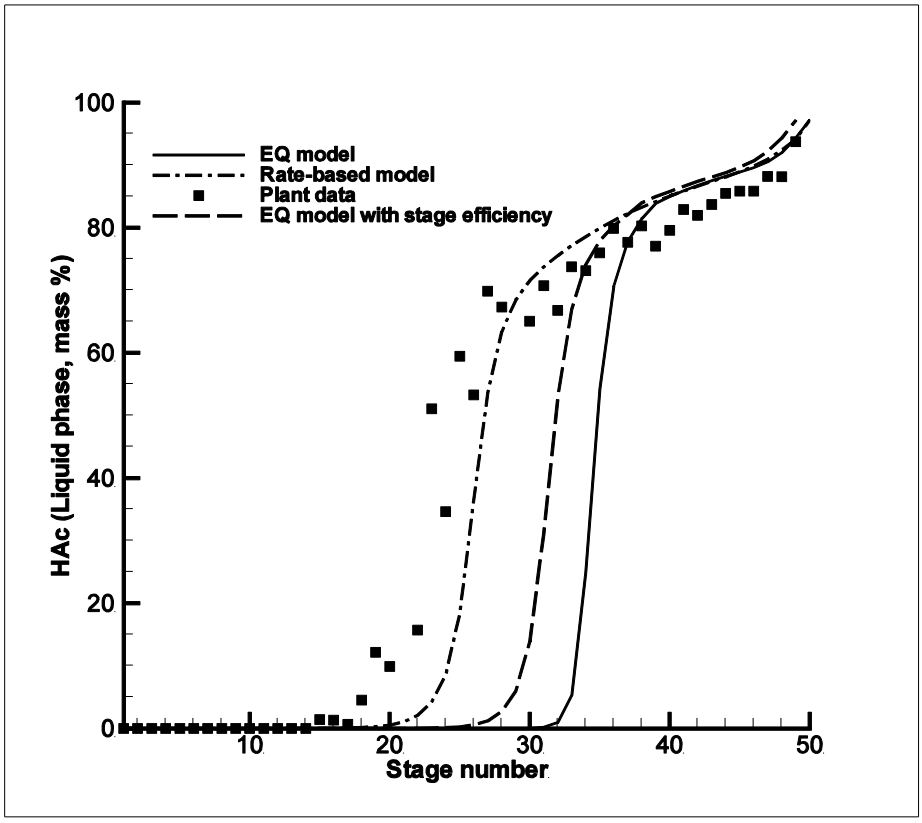

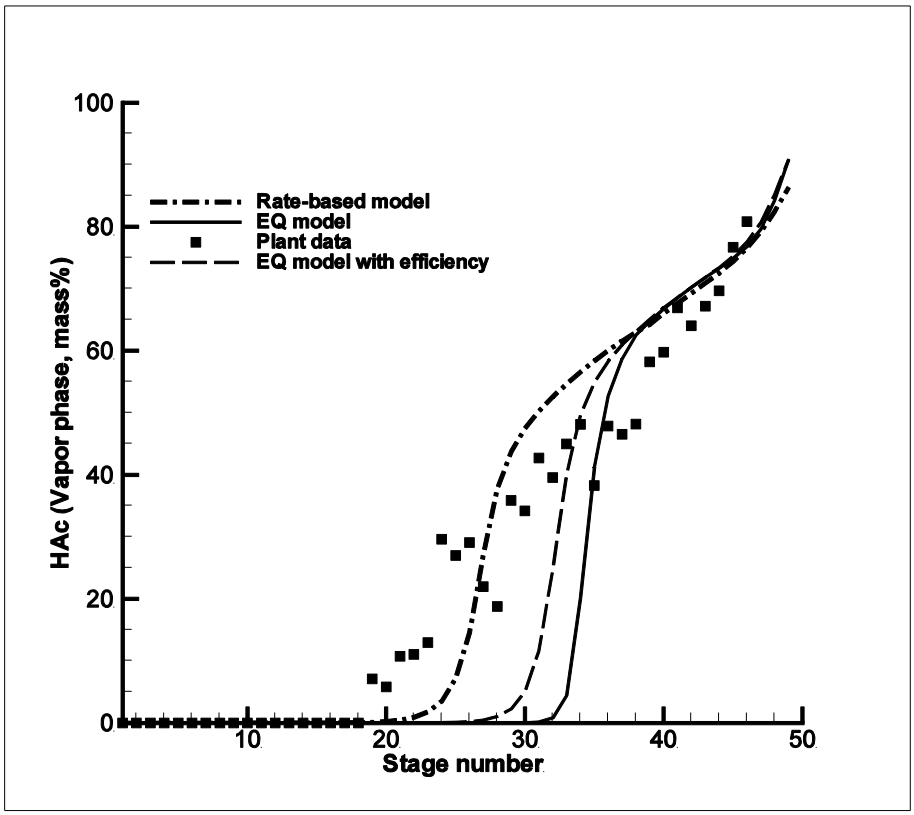

Figure 5.11: Comparison of *HAc* composition profiles (a) liquid phase; (b) vapor phase

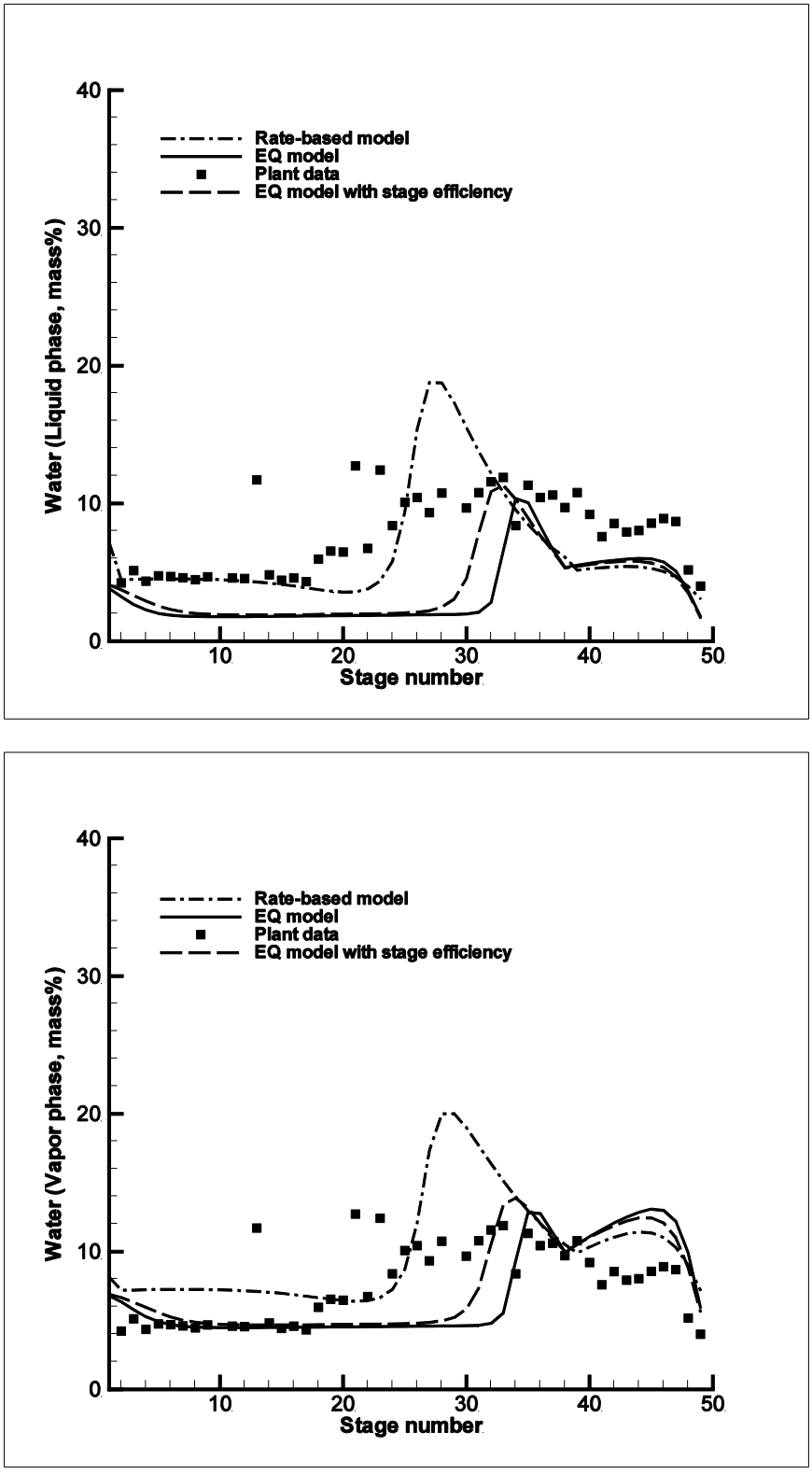

Figure 5.12: Comparison of water composition profiles (a) liquid phase; (b) vapor phase

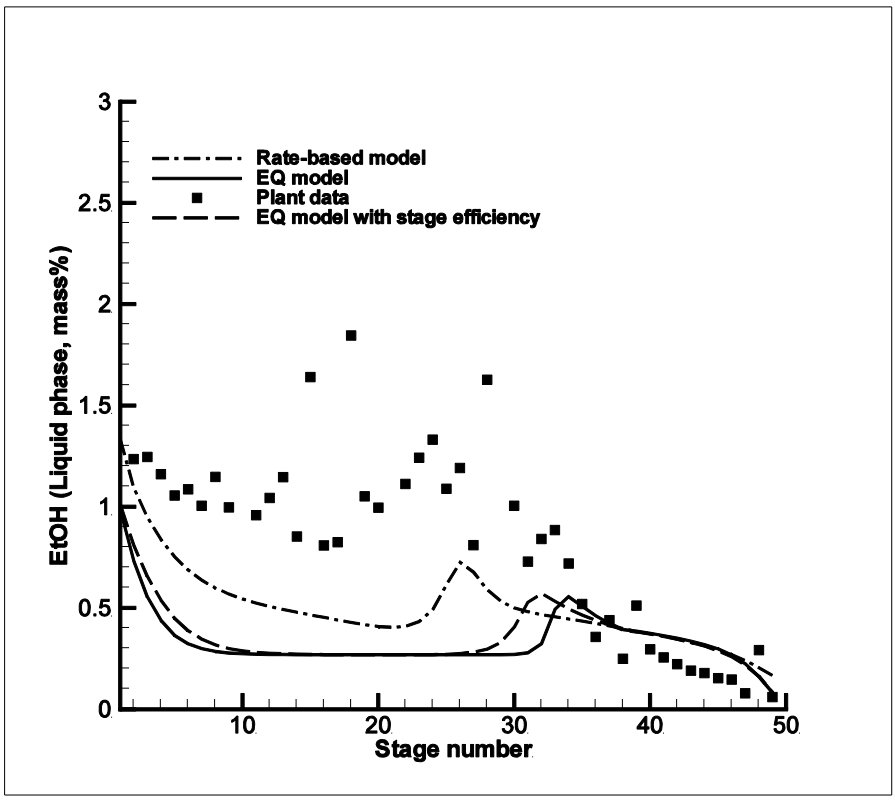

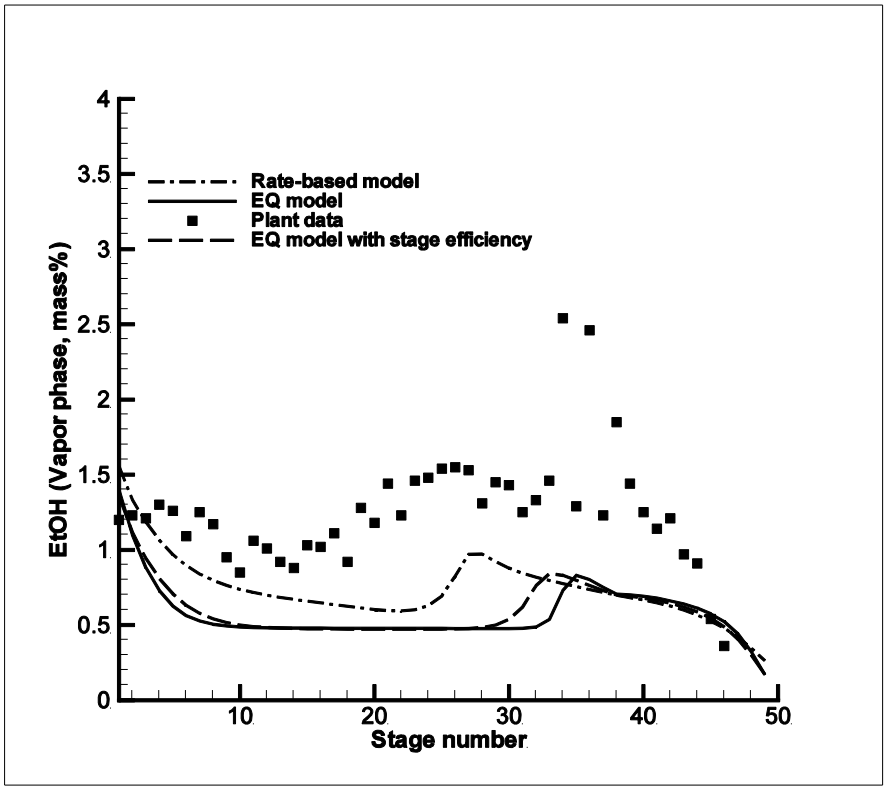

Figure 5.13: Comparison of *EtOH* composition profiles (a) liquid phase; (b) vapor phase

In the beginning of this research work, a sluggish response of the resistance-thermometer was observed [Singh *et al.*, 2015]. Considering this a second set of data (data set-2) was collected using more sensitive temperature probes with larger length and diameter. Figure 5.14 shows the comparison of column temperature profiles. The experimental temperature (data set-2) was generated by replacing the old temperature probe with a new probe (5 mm longer and 1.5 mm larger in diameter). The longer length reduces the error in the measurement and the larger diameter improves the response time. Significant improvement in the recorded temperature profile was observed. In this case too, the temperature profile predicted by rate-based model is close to the experimental (data set-2).

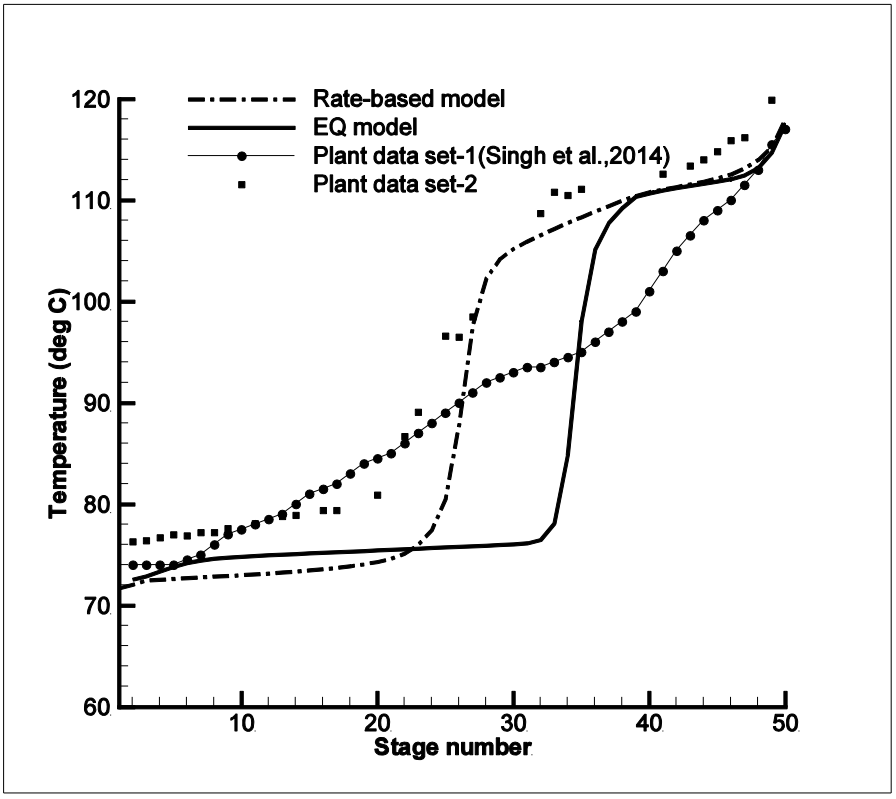

Figure 5.14: Column temperature profiles

The comparison of reaction rates for EQ and rate-based models (Figure 5.15) show that the EQ model predicts the reaction rates for ethyl acetate considerably different on some trays in the column. About 5 times higher negative reaction rates predicted on the stages 33-37 (Figure 5.15) for the EQ model are due to the over-prediction of *EtAc* liquid phase composition (Figure 5.10a) and under prediction of *HAc* liquid phase composition (Figure 5.11a) on these trays. Also, the slightly lower *EtAc* generation rates predicted on the stages 40-45 (Figure 5.15) for the rate-based model, are due to the introduction of mass transfer resistance in the rate-based model that leads to lower reaction rate.

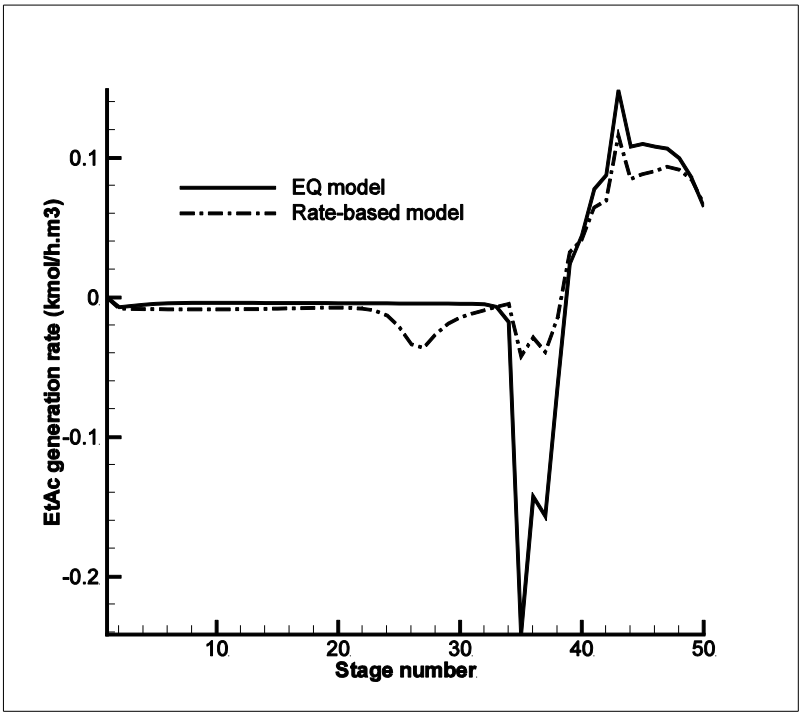

Figure 5.15: Ethyl acetate generation rate

5.5 **Effect of some design and operation parameters**

After the successful simulation of the RD column using rate-based model, the effect of some design (number of trays and feed stage location) and operation (fresh feed of *EtOH*) parameters on the performance of the column is studied.

Effect of number of trays:

As is evident from the ethyl acetate composition profile at the top (no change in composition is observed for the top 15 trays), there seems to be more number of trays in the column than that are required i.e. the column is overdesigned.

The effect of number of trays on the column performance is studied and the simulation results are shown in Figures5.16-5.19. These figures show the composition profiles of the four components for different number of trays in the RD column.

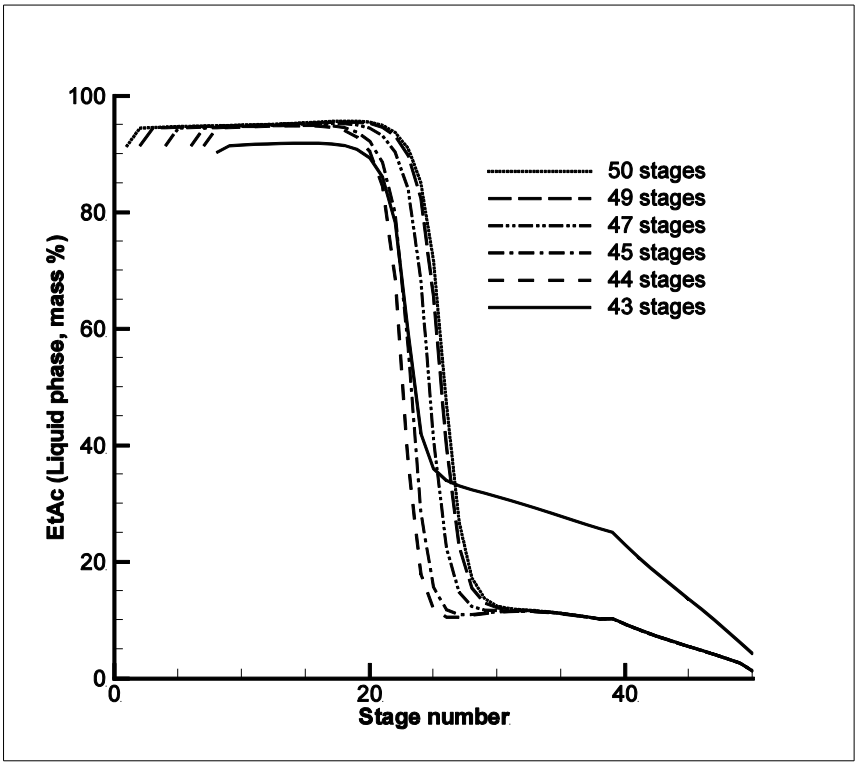

Figure 5.16: Comparison of *EtAc* composition profiles with varying number of stages

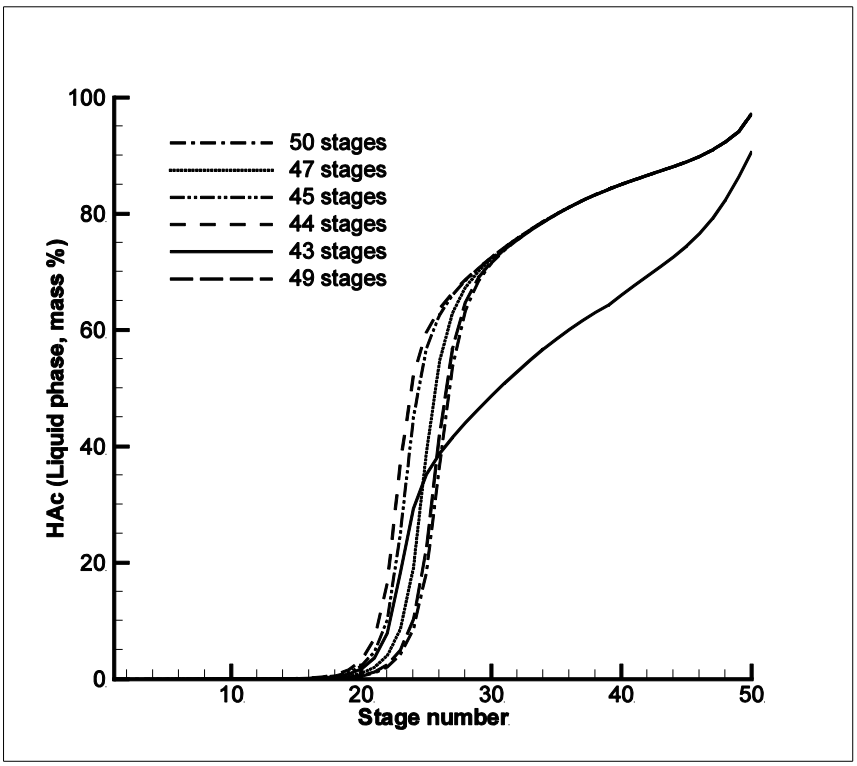

Figure 5.17: Comparison of *HAc* composition profiles with varying number of stages

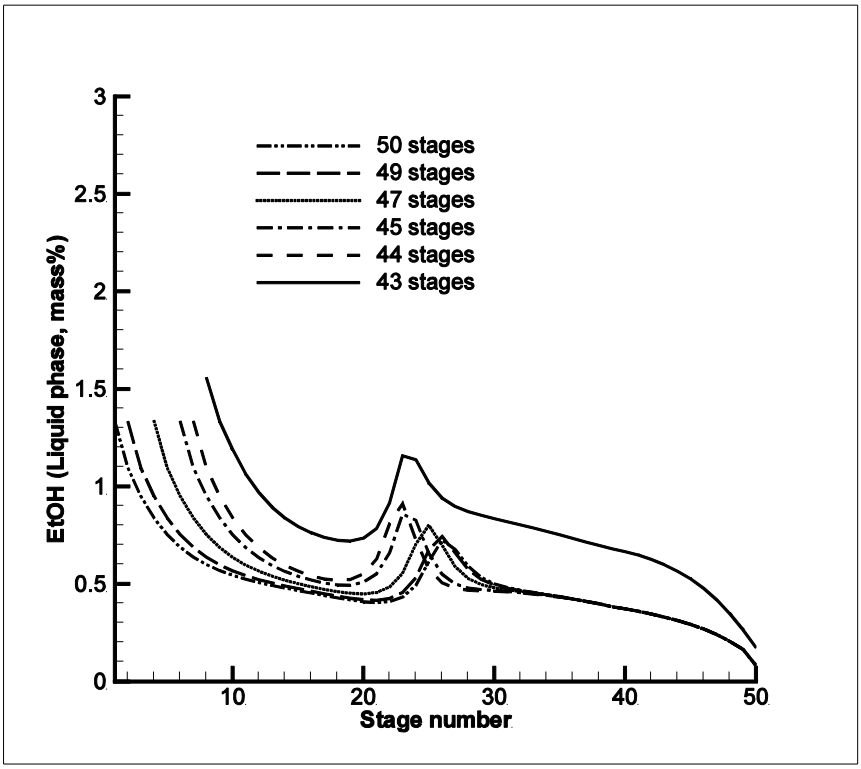

Figure 5.18: Comparison of *EtOH* composition profiles with varying number of stages

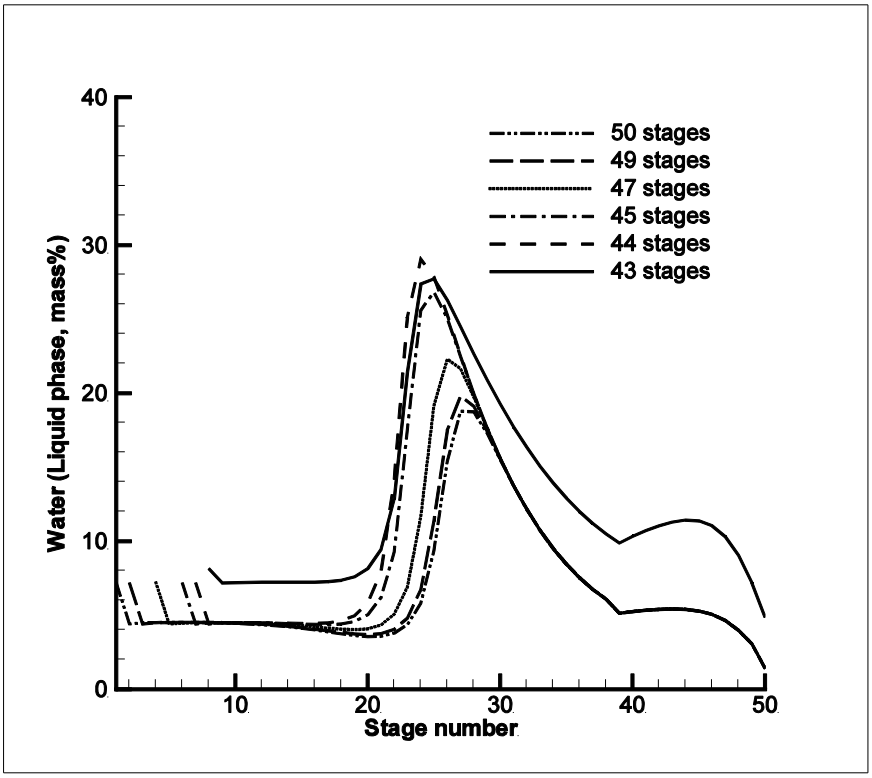

Figure 5.19: Comparison of H_2O composition profiles with varying number of stages

It is evident, that, reducing the number of trays in the column from 48 to 42 has no adverse effect on the components' composition profiles. Also, Table 5.6 shows that the composition of the streams remains same if the trays in the column are reduced from 48 to 42, which means that the product purity remains same even if a few trays from the upper section of the column are removed.

Table 5.6: Predicted stream compositions (mass fraction) with different number of stages

Number of stages	Component	Component mass fractions		
		Bottom product	Organic product	Water layer
44 stages	*EtAc*	0.01	0.95	0.09
	HAc	0.97	0.00	0.00
	EtOH	0.00	0.01	0.03
	H_2O	0.01	0.03	0.88
45 stages	*EtAc*	0.01	0.95	0.09
	HAc	0.97	0.00	0.00
	EtOH	0.00	0.01	0.03
	H_2O	0.01	0.03	0.88
47 stages	*EtAc*	0.01	0.95	0.09
	HAc	0.97	0.00	0.00
	EtOH	0.00	0.01	0.03
	H2O	0.01	0.03	0.88
49 stages	*EtAc*	0.01	0.95	0.09
	HAc	0.97	0.00	0.00
	EtOH	0.00	0.01	0.03
	H_2O	0.01	0.03	0.88
50 stages	*EtAc*	0.01	0.95	0.09
	HAc	0.97	0.00	0.00
	EtOH	0.00	0.01	0.03
	H_2O	0.01	0.03	0.88

Figure 5.20 (a &b) show that the ethyl acetate generation rate and conversion of ethanol are also not affected on reducing the number of stages from 48 to 42. Therefore, the bubble cap trays in the column may be safely reduced to 42 making the total stages 44 (including re-boiler and condenser).

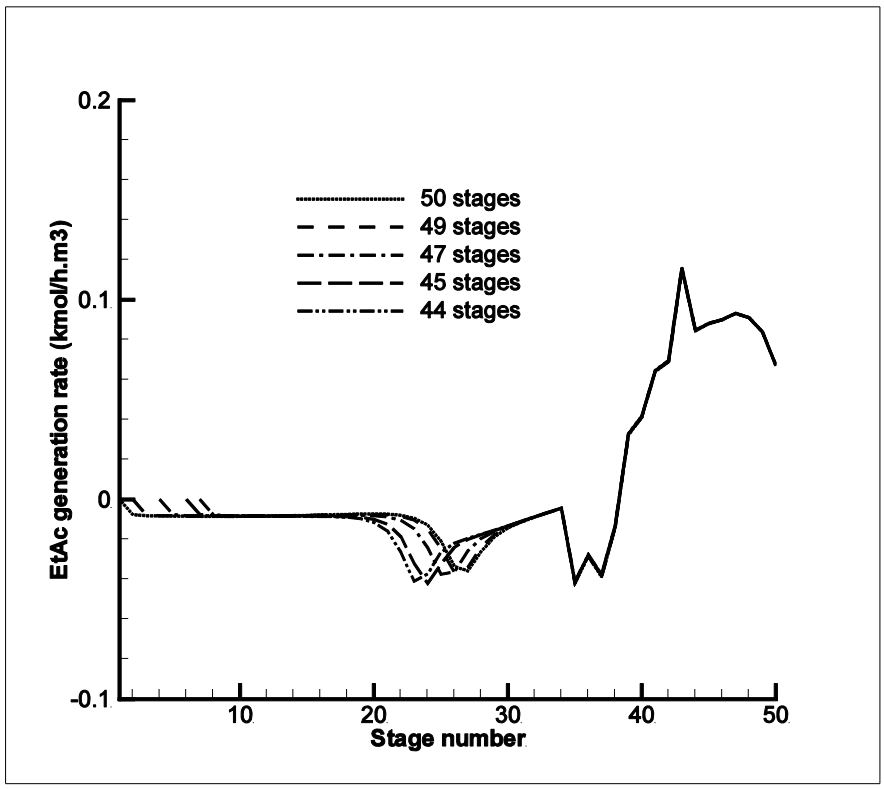

Figure 5.20(a): Comparison of *EtAc* generation rate profiles with different number of stages

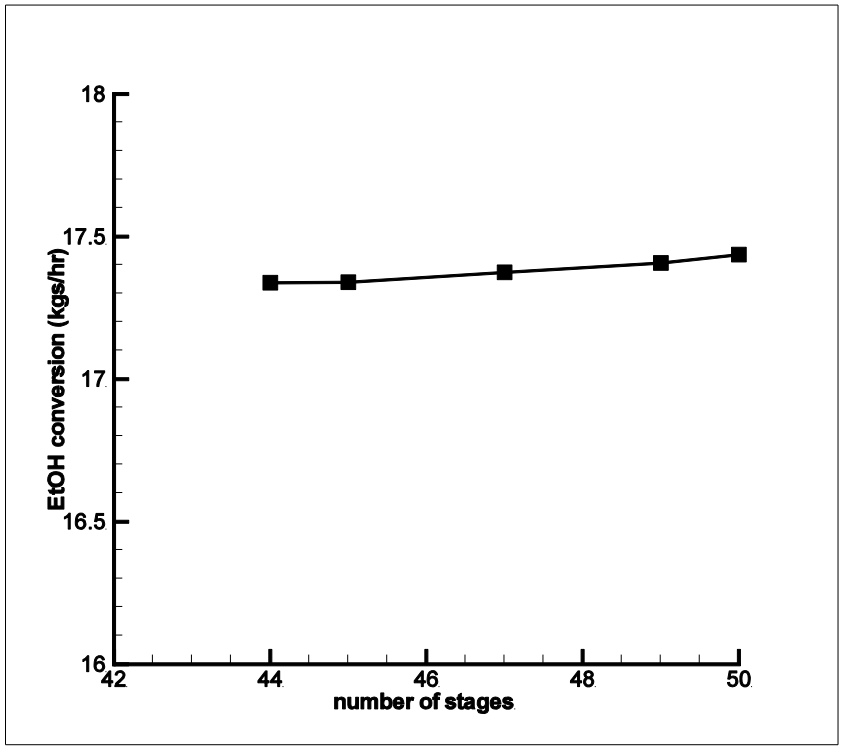

Figure 5.20(b): Comparison of *EtOH* conversion rate with varying number of stages

Effect of feed stage location:

The composition profile of ethyl acetate (Figure 5.21) is not much affected when the feed stage location is moved from stage 39 to stage 33 keeping the total number of stages same as the actual, i.e., 50stages. The purity of ethyl acetate in the organic product also remains same (Table 5.7).The Table 5.7 shows that re-boiler and condenser duties also decrease on moving the feed stage up in the column and the energy required on the downstream recovery of organic components from the water stream will also decrease on moving the feed stage up.

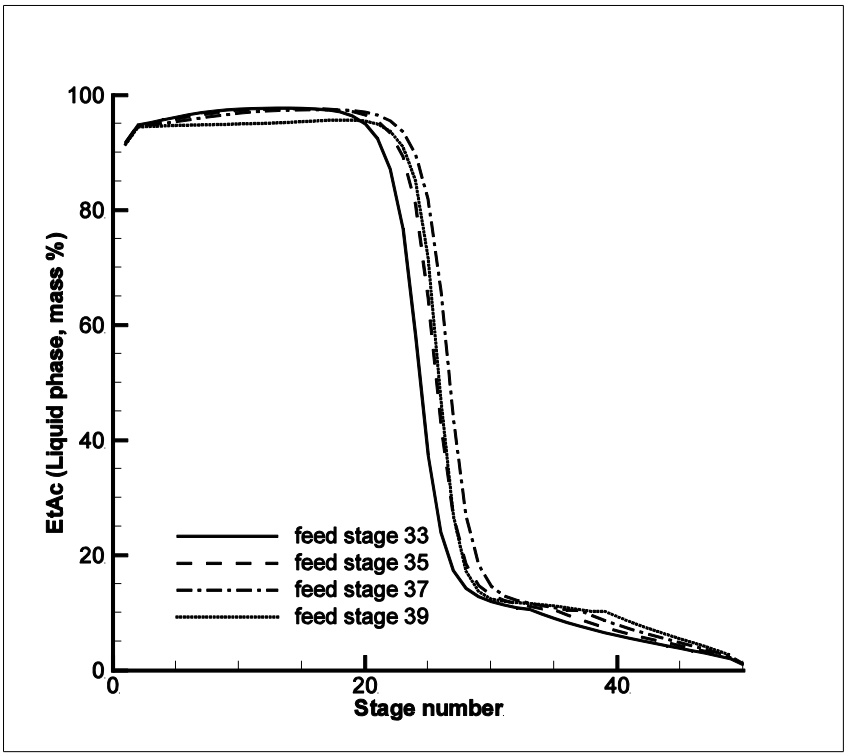

Figure 5.21: Comparison of *EtAc* composition profiles at different feed stage

Table 5.7: Predicted compositions, stream flows, re-boiler and condenser duty with change in feed stage location

		Feed at 39th stage	**Feed at 37th stage**	**Feed at 35th stage**	**Feed at 33rd stage**
Organic product composition (wt%)	*EtAc*	95.49	95.50	95.49	95.48
	HAc	0.00	0.00	0.00	0.00
	EtOH	1.24	1.23	1.24	1.25
	H_2O	3.27	3.27	3.27	3.27
Organic product stream (kg/hr)	*EtAc*	2507.44	2533.82	2555.86	2574.49
	HAc	0.00	0.00	0.00	0.00
	EtOH	32.48	32.71	33.18	33.64
	H_2O	85.86	86.74	87.54	88.23
	Total	**2625.78**	**2653.28**	**2676.59**	**2696.36**
Water layer (kg/hr)	*EtAc*	67.02	64.65	62.71	61.06
	HAc	0.00	0.00	0.00	0.00
	EtOH	25.85	24.87	24.24	23.73
	H_2O	693.34	669.20	648.57	630.86
	Total	**786.22**	**758.72**	**735.52**	**715.64**
Bottom flow (kg/hr)	*EtAc*	263.62	242.00	223.22	207.00
	HAc	20214.85	20213.16	20212.34	20211.77
	EtOH	17.16	16.68	16.22	15.81
	H2O	292.37	316.16	336.22	353.42
	Total	**20788**	**20788**	**20788**	**20788**
Re-boiler Duty(kcal/hr)		2795576	2771413	2751358	2734215
Condenser Duty(kcal/hr)		1715790	1707452	1700874	1695359
Re-boiler duty (kcal/kg *EtAC* in organic layer)		1115	1094	1076	1062
Condenser duty (kcal/kg *EtAC* in organic layer)		684	674	665	659

Effect of feed stage location on the ethyl acetate generation rate and ethanol conversion is shown in Figures 5.22 and 5.23 respectively. Figure 5.22 show more positive reaction as the feed stage is moved up. Also, the ethanol conversion increases as the reaction zone in the column increases with the shifting of feed stage from stage 39 to stage 33.

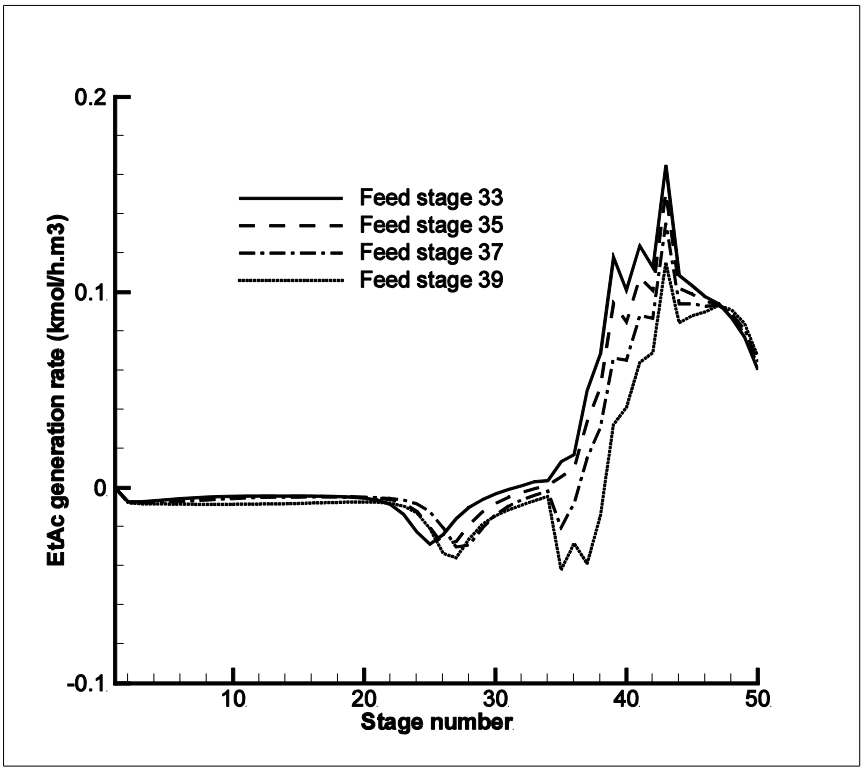

Figure 5.22: *EtAc* generation rate profiles for different feed stage location

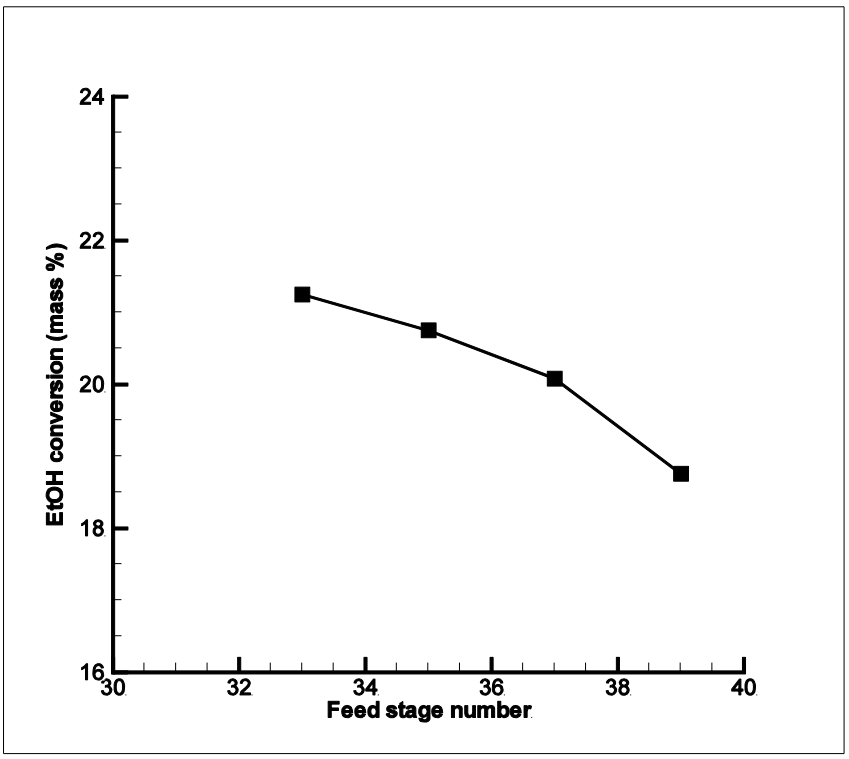

Figure 5.23: *EtOH* conversion for different feed stage location

Combined effect of feed location and addition of fresh ethanol:

As it was observed during simulation studies that the feed stage can be moved up in the column, it is also evident that the ethanol composition in the column is very low and conversion can be improved if ethanol can be added in the column. The extra stages can be utilized in a more effecting way by changing the feed location (moving the feed stage up in the column) so that reaction zone in the column increased; and by addition of a fresh feed of ethanol at stage 49 to improve the forward reaction.

Further simulation was run by adding a fresh feed of ethanol (150 kg/h) in the down-comer of 49^{th} stage. The feed from the pre-reactor was introduced at stage 34. The effect of these changes on the simulation show that the composition of ethyl acetate (Figure 5.24) remains close to the experimental data (obtained with feed at stage 39), suggesting a stable operation. The purity of ethyl acetate in the product remains same (Table 5.8). Effect of pre-reacted feed stage location and fresh feed of ethanol at stage 49 on the ethyl generation rate are shown in Figure 5.25 The ethanol conversion increases as the reaction zone in the column increases while feed is shifted

from stage 39 to stage 34 with addition of fresh feed of ethanol at stage 49. As shown in table 5.8 the ethanol conversion in the RD column increased from 17.43 kg/hr to 93.44 kg/hr. The ethanol conversion (wt%) increased to 39.94 % from 18.76%. Moreover, with the change in feed location and addition of fresh ethanol feed, the specific energy (kcal/kg of *EtAC*) requirement of the re-boiler reduced from1115 to1054 and condenser duty (kcal/kg of *EtAC*) requirement reduced from 684 to 654.

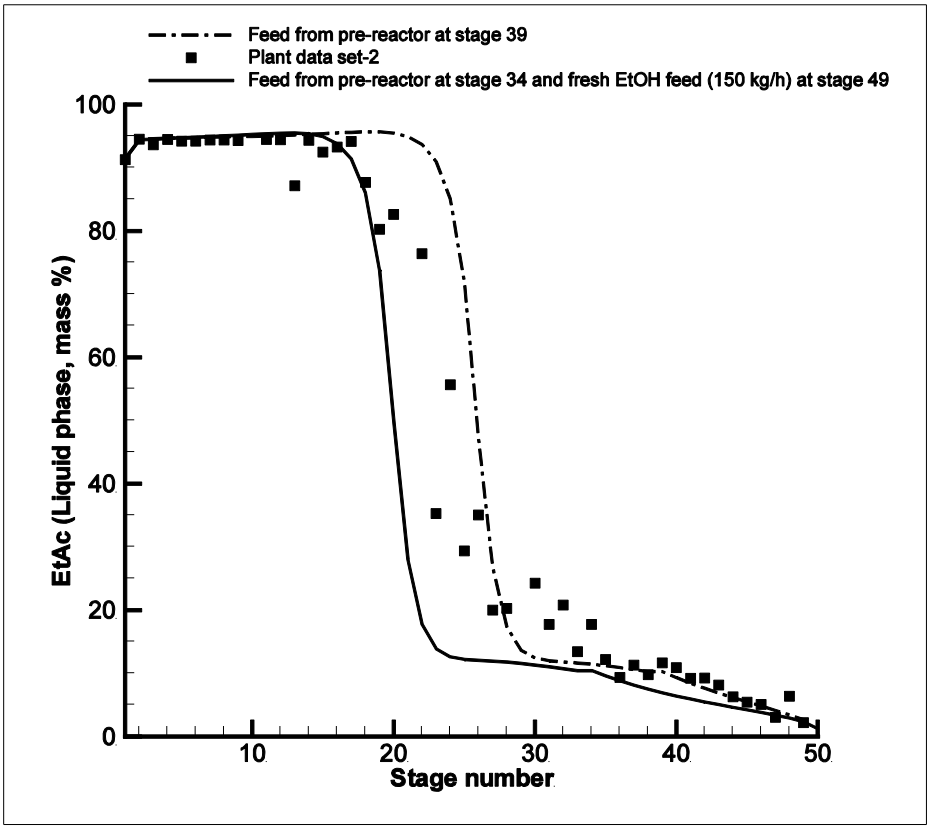

Figure 5.24: Comparison of EtAc composition profiles for combined effect of feed location and addition of fresh ethanol

Table 5.8: Predicted stream compositions and flows, re-boiler and condenser duties (feed from pre-reactor at stage 34 and a fresh ethanol feed at stage 49)

	34 and 49 feed stage	**39 feed stage**
Feed stream (kg/hr) at stage 34		
EtAc	2804.78	2804.78
HAc	20237.49	20237.49
EtOH	92.928	92.928
H_2O	1064.8	1064.8
Total	24200	
Feed stream (kg/hr) at stage 49		
EtOH	141	NA
H_2O	9	NA
Total	150	
Organic product composition (wt%)		
EtAc	95.43	95.49
HAc	0.00	0.00
EtOH	1.29	1.24
H_2O	3.28	3.27
Organic product stream (kg/hr)		
EtAc	2646.23	2507.44
HAc	0.00	0.00
EtOH	35.63	32.48
H_2O	90.95	85.86
Total	**2772.83**	**2625.78**
Water layer (kg/hr)		
EtAc	67.53	67.02
HAc	0.00	0.00
EtOH	26.92	25.85
H_2O	694.71	693.34
Total	**789.16**	**786.22**
Bottom flow (kg/hr)		
EtAc	269.72	263.62
HAc	20115.68	20214.85
EtOH	77.92	17.16
H2O	324.67	292.37

Total	**20788**	**20788**
Reboiler duty (kcal/hr)	2788408	2795576
Condenser duty (kcal/hr)	1731496.4	1715790
Reboiler duty (kcal/kg *EtAC* in organic layer)	1054	1115
Condenser duty (kcal/kg *EtAC* in organic layer)	654	684

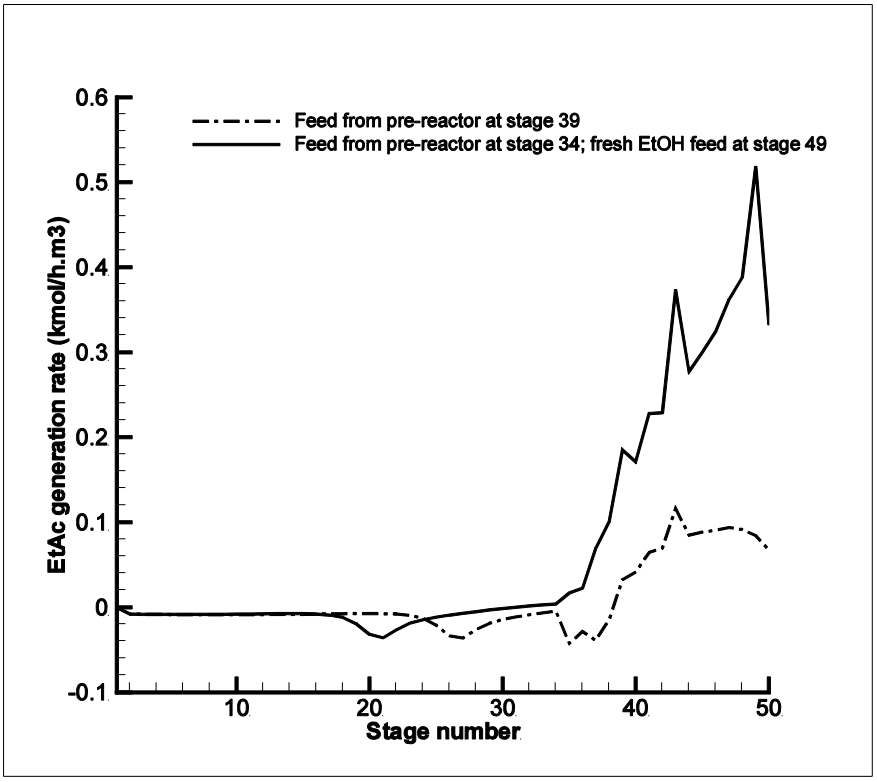

Figure 5.25: Comparison of EtAc generation rate profilesfor combined effect of feed location and addition of fresh ethanol

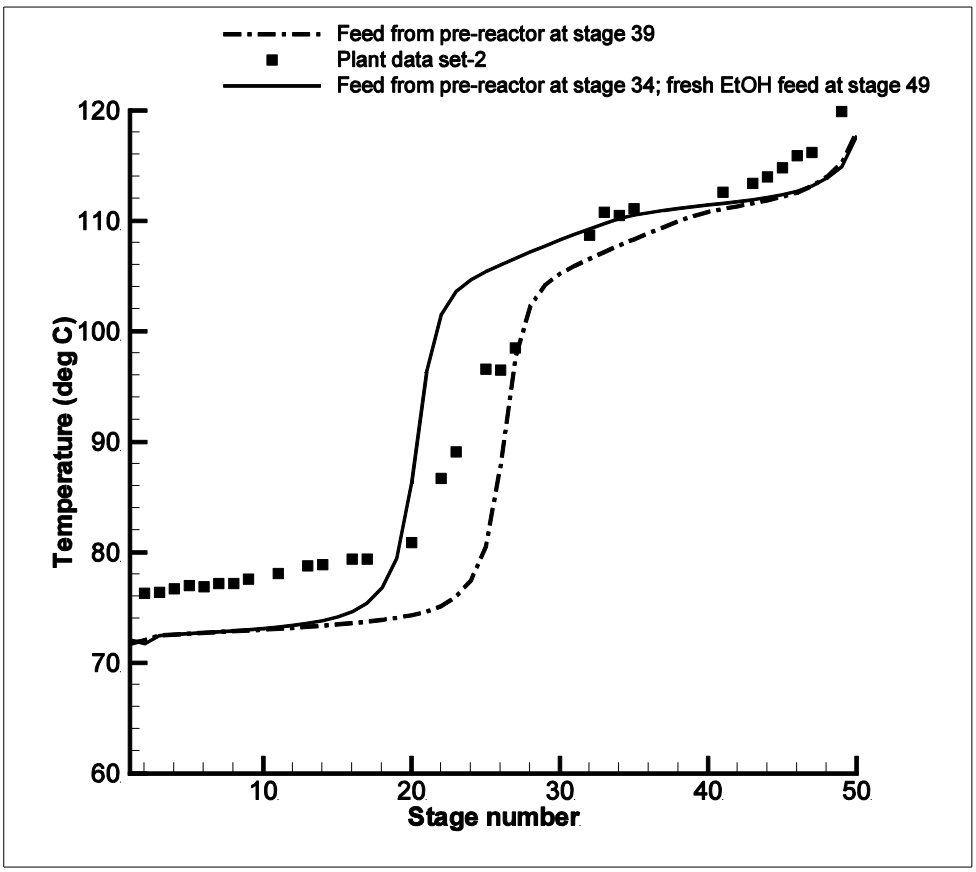

Figure 5.26: Comparison of column temperature profiles for *combined effect of feed location and addition of fresh ethanol*

Chapter 6

Conclusions and Recommendations

6.1 Conclusions

The much awaited experimental data of a large scale RD column is obtained. Results indicated many serious shortcomings in the conventional approach of simulation, particularly the difficulty in selecting proper thermodynamic model. An attempt was made to improve the binary parameters to be used for the esterification of acetic acid. In the present work a 50 stage plant scale RD column is simulated using rate-based model of Aspen Plus. A new set of binary interaction parameters is established for the NRTL model with a very good prediction of experimental vapor–liquid equilibrium data for the binary component pairs.

- The results are in agreement with the fact that the reactive distillation is more advantageous for equilibrium limited reactions, particularly when the favorable reaction temperature lies between boiling points of chemical species involved. Therefore, the RD process for esterification of ethanol is suitable not only for new plants but also for revamping of existing plants. For the existing units, excess ethyl acetate could be produced in the RD column in addition to the ethyl acetate produced in pre-reactor.
- For efficient designing and revamping of these columns, engineers need a sound theoretical basis for calculating parameters such as optimum reflux ratio, tray hold-ups of reactive zone (where acetic acid and ethanol concentration are high), variable and multiple feed injections in the reactive zone, etc. In addition to the available laboratory scale and pilot plant scale data, the industrial-scale data generated in the present study is expected to contribute significantly to further investigation.
- A multi-component system behaves differently from a binary system; particularly due to the fact that the thermodynamic activity of the components forming azeotropes get affected severely in the presence of a third and forth component. Therefore, either a quaternary activity model (which is not available so far) is required or the binary parameters are required to be improved for better predictability.
- Aspen simulation results using the NRTL model, with the established set of binary interaction parameters, in combination with plant design data closely predicted the observed composition profiles in the column. The compositions of outlet streams are also well predicted by the simulator. Simulation results show that the varying liquid flow rate and the presence of water in the column considerably affect the stage efficiency. The

increased reflux flow resulted in the increased purity (top product) as in case of a conventional distillation column, however, the ethanol conversion decreased with the increased reflux flow suggesting an additional variable in case of optimization of the RD column.

- Comparison of EQ and rate-based model simulations with the experimental data show that the rate-based model is better suited for the simulation of a RD column.
- It is also observed that increasing number of trays in the stripping section (reaction zone) increases ethanol conversion and reduces re-boiler and condenser duties. For revamped columns, like one studied in the present work, there are some extra stages in the stripping section. These extra stages can be utilized in a more effecting way by changing the feed location (moving the feed stage up in the column) so that reaction zone in the column is increased; and by addition of a fresh feed of ethanol at the bottom stage to improve the forward reaction.

6.2 Recommendations

On the basis of the present work, it was observed that there are some redundant trays in the rectification section of the finishing column. On the basis of the recommendations, the IOLCP has taken following actions:

- Another column in the same plant is having 54 stages (52 bubble cap trays, a condenser, a re-boiler) and diameter 2.5 m. In this column the feed was being introduced at stage 40th stage, the column had a provision for introducing the feed at 36st stage. After the present study, the feed was introduced at the 36st stage. An additional feed of Ethanol (150 kg/h)

With these, following improvements were observed:

- The average *EtAC* in organic layer from the column increased from 86 tons/day to 93 tons/day. Also, some steam consumption per ton of *EtAc* in organic layer was also reduced (1.95 tons from 2.05 tons).

As far as future research in the field is concerned, from components' concentration profiles it is clear that water concentration near the feed tray is significantly high which increases backward reaction. To further reduce this water concentration, some techniques such as use of a dividing wall (i.e., Divided Wall Reactive Distillation Column, DWRDC) can be tried (Hernandez *et al*.,

2009).Water removal can also be tried from the feed mixture from pre-reactor using some technique like pervaporation as proposed by [Lv *et al.*, 2012].

Also, the experimental data from plant scale complete RD processes should be generated to develop general design procedures for this process.

Further, the vapor-liquid equilibrium data for the quaternary system of ethyl acetate-acetic acid-ethanol-water system forming many azeotropes is not available. Efforts should be made to improve the thermodynamics of the quaternary system or NRTL parameters such that the thermodynamic correlations can be extended to wider range of operating conditions.

References

Alejski, K., Duprat, F. (1996). Dynamic simulation of the multi component reactive distillation. *Chemical Engineering Science, 51,* 4237-4252.

Alejski, K., Szymanowski, J., Bogacki, M. (1988). The application of a minimization method for solving reactive distillation problems. *Computers and Chemical Engineering*, 12, 833-839.

Alfradique, M.F., Castier, M. (2005). Modeling and simulation of reactive distillation columns using computer algebra. *Computers and Chemical Engineering.* 29, 1875-1884.

Aspen Plus (2010). Aspen physical property system-physical property models (V7.2). Aspen Tech.

Backhaus, A.A. (1921). Continuous processes for the manufacture of esters, US patent 1400849.

Barbosa, D., Doherty, M. F. (1987). Theory of phase diagrams and azeotropic conditions for two-phase reactive systems. *Proceedings of the Royal Society of London,* A413, 443-458.

Barbosa, D., Doherty, M. F. (1988a). Design and minimum-reflux calculations for single feed multi component reactive distillation columns. *Chemical Engineering Science*, 43, 1523-1537.

Barbosa, D., Doherty, M. F. (1988b). Design and minimum-reflux calculations for double feed multi component reactive distillation columns. *Chemical Engineering Science*, 43, 2377-2389.

Barbosa, D., Doherty, M.F. (1988c). The influence of equilibrium chemical reactions on vapor liquid-phase diagrams. *Chemical Engineering Science*, 43, 529-540.

Baur, R., Taylor, R., Krishna, R. (2000). Development of a dynamic non-equilibrium cell model for reactive distillation tray columns. *Chemical Engineering Science*, 55, 6139-6154.

Bessling, B., Schembecker, G., Simmrock, K.H. (1997). Design of processes with reactive distillation line diagrams. *Industrial and Engineering Chemistry Research*, 36, 3032-3042.

Bhargava, R., Hlavacek, V. (1984). Experience with adopting one-parameter imbedding methods towards calculation of counter current separation processes. *Chemical Engineering Communication,* 28, 165-179.

Bock, H., Wozny, G. (1997). Analysis of distillation and reaction rate in reactive distillation. *Distillation and Absorption '97. Institute of Chemical Engineers Symposium Series*, 142, 553-564.

Boston, J.F. (1970). A new class of quasi-Newton solution methods for multi component, multistage separation processes. Ph.D. Thesis, Tulane University.

Boston, J.F. (1978). Inside-out algorithms for multi-component separation process calculations, process symposium on computer applications to chemical engineering process design and simulations, *American Chemical Society* 178th meeting, Washington, DC.

Boston, J.F. (1980). Inside-out algorithms for multi component separation process calculations. *Computer Application to Chemical Engineering, American Chemical Society,* 135-151.

Byrne, G.D., Baird, L.A. (1985). Distillation calculations using a locally parameterized continuation method. *Computers and Chemical Engineering,*9, 593-599.

Calvar, N., Dominguez, A., Tojo, J. (2005). Vapor-liquid equilibria for the quaternary reactive system ethyl acetate + ethanol + water + acetic acid and some of the constituent binary systems at 101.3 kpa. *Fluid Phase Equilibria*, 235, 215-222.

Chang, Y.A., Seader, J.D. (1988). Simulation of continuous reactive distillation by a homotopy continuation method. *Computers and Chemical Engineering*, 12, 1243-1255.

Chimowitz, E.H., Anderson, T.F., Macchietto, S., Stutxman, L.F. (1983). Local models representing phase equilibria in multi-component, non-ideal vapour-liquid and liquid-liquid systems. 1. Thermodynamic approximation functions. *Industrial and Engineering Chemistry Process Design and Development*, 22, 217-225.

Chien, I.L., Teng, Y.P., Huang, H.P., Tang, Y.T., (2005). Design and control of an ethyl acetate process: coupled reactor/column configuration. *Journal of Process Control*, 15, 435-449.

Ciric, A.R., Spencer, J. (1995). Shortcut calculations in reactive distillation. *American Institute of Chemical Engineers National Meeting*, Miami Beach.

Dalaouti, N., Seferlis, P. (2006). A unified modeling framework for the optimal design and dynamic simulation of staged reactive separation processes. *Computers and Chemical Engineering*, 30, 1264-1277.

Davies, B., Jenkins, J.D., Dilfanian, S. (1979). Distillation with chemical reaction-distillation of formaldehyde solutions in a sieve plate column. *Institute of Chemical Engineers Symposium, Serial*, Number56, (4.2) 65-79.

De Nevers, N. (2012). Physical and chemical equilibrium for chemical engineers. 2nd ed., John Wiley & Sons, Inc., Hoboken, New Jersey.

Doherty, M.F., Buzad, G. (1992). Reactive distillation by design. *Chemical Engineering Research and Design, Transactions of the Institution of Chemical Engineers,* Part A, 70, 448-458.

Dutia, P. (2004). Ethyl acetate: A techno-commercial profile. *Chemical Weekly-Bombay*, *49*, 179-186. (Also available at: http://www.scribd.com/doc/48493833/Ethyl-Acetate)

Ellis, S.R.M., Garbett, R.D. (1960). A new equilibrium still for the study of partially miscible systems. *Industrial and Engineering Chemistry Research*, 52, 385-388.

Fisher, K.S., Rochelle, G.T. (2002). Effect of mixing on efficiencies for reactive tray contactors. *American Institute of Chemical Engineers Journal*, 48, 2537-2544.

Frey, T., Stichlmair, J. (1999).Thermodynamic fundamentals of reactive distillation. *Chemical Engineering Technology*, 22, 1, 11-18.

Fonyo, Z., Nishimura, H., Yamashita, Y. (1983). New simultaneous modular method for calculating multistage multi component separation processes. *American Institute of Chemical Engineers Journal*, 29, 538-544.

Giessler, S., Danilov, R.Y., Pisarenko, R.Y., Serafimov, L.A., Hasebe, S., Hashimoto, I. (2001). Systematic structure generation for reactive distillation processes. *Computers and Chemical Engineering*, 25, 49-60.

Hangx, G., Kwant, G., Maessen, H., Markusse, P., Urseanu, I. (2001). "Reaction kinetics of the esterification of ethanol and acetic acid towards ethyl acetate," *Deliverable 22, Intelligent Column Internals for Reactive Separations (INTINT), Technical Report to the European Commission,* 2001. *(*Also available at:http://www.cpi.umist.ac.uk/intint/NonConf_Doc.asp.)

Harmsen, G.J. (2007). Reactive distillation: The front-runner of industrial process intensification a full review of commercial applications, research, scale-up, design and operation. *Chemical Engineering and Processing*, 46, 774-780.

Hernandez, S., Sandoval-Vergara, R., Borroso-Munoz, F.O., Murrieta-Duenas, R., Hernandez-Escoto, H., Segovia-Hernandez, J.G., Rico-Ramirez, V. (2009). Reactive dividing wall distillation columns: Simulation and implementation in pilot plant. *Chemical Engineering and Processing*, 48, 250-258.

Hirata, M., Komatsu, H. (1966). Vapor-Liquid equilibrium of quaternary system; Acetic acid, Ethanol, water and Ethyl acetate. *Journal of Chemical Engineering of Japan*, Kagaku Kogaku, 30, 989-997.

Higler, A.P., Taylor, R., Krishna, R. (1998). Modeling of a reactive separation process using a non-equilibrium stage model. *Computers and Chemical Engineering*, 22, S111-S118.

Higler, A.P., Taylor, R., Krishna, R. (1999a). The influence of mass transfer and mixing on the performance of a tray column for reactive distillation. *Chemical Engineering Science*, 54, 2873-2881.

Higler, A.P., Taylor, R., Krishna, R. (1999b). Non-equilibrium modeling of reactive distillation: Multiple steady states in MTBE synthesis. *Chemical Engineering Science*, 54, 1389-1395.

Hiwale, R.S., Bhate, N.V., Mahajan, Y.S., Mahajani, S.M. (2004). Industrial applications of reactive distillation: recent trends. *International Journal of Chemical Reactor Engineering*, 2, 1-52.

Holland, C. D. (1963). Multi component Distillation. Englewood Cliffs, New Jersey: Prentice-Hall.

Holland, C.D. (1981). Fundamentals of Multi component Distillation. New York: McGraw-Hill.

Indian Pharmacopoeia (2010). Indian Pharmacopoeia Commission, Delhi.

Ishii Y., Otto, F.D. (1973). A general algorithm for multistage multi component separation calculations. *Canadian Journal of Chemical Engineering*, 51, 601-606.

Izarraraz, A., Bentzen, G.W., Anthony, R.G., Holland, C.D. (1980). Solve more distillation problems: Part 9-when chemical reactions occur. *Hydrocarbon Processing*, 59, 195-203.

Jelinek, J., Hlavacek, V. (1976). Steady state counter current equilibrium stage separation with chemical reaction by relaxation method. *Chemical Engineering Communication*, 2, 79-85.

J&W GC and GC/MS Column Selection Guide. Agilent Technologies: Santa Clara, CA. (Also available at: http://www.chem.agilent.com/Library/catalogs/Public/5990-9867EN_GC_CSG.pdf)

Kang, Y.W., Lee, Y.Y., Lee, W.K. (1992).Vapor-liquid equilibria with chemical reaction equilibrium systems containing acetic acid, ethyl alcohol, water, and ethyl acetate. *Journal of Chemical Engineering of Japan*, 25, 6, 649-655.

Kaymak, D.B., Luyben, W.L. (2004). Effect of the chemical equilibrium constant on the design of reactive distillation columns. *Industrial and Engineering Chemistry Research*,43, 3666-3671.

Keller, T., Gorak, A. (2013). Modeling of homogeneously catalysed reactive distillation processes in packed columns: Experimental model validation. *Computers and Chemical Engineering*, 48, 74-88.

Keller, T., Holtbruegge, J., Gorak, A. (2012). Transesterification of dimethyl carbonate with ethanol in a pilot-scale reactive distillation column. *Chemical Engineering Journal*, 180, 309-322.

Kenig, E.Y., Bader, H., Gorak, A., Beβling, B., Adrian, T., Schoenmakers, H. (2001). Investigation of ethyl acetate reactive distillation process. *Chemical Engineering Science*, 56, 6185-6193.

Kenig, E.Y., Pyhalahti, A., Jakobsson, K., Gorak, A., Aittamaa, J., Sundmacher, K. (2004). Advanced rate-based simulation tool for reactive distillation. *American Institute of Chemical Engineers Journal*, 50, 332-342.

Ketchum R.G. (1979). A combined relaxation-Newton method as a new global approach to the computation of thermal separation processes. *Chemical Engineering Science, 34,* 387-395.

Keyes, D.B. (1932). Esterification processes and equipment. *Industrial and Engineering Chemistry Research*, 24, 1096-1103.

Kiatkittipong, W., Intaracharoen, P., Laosiripojana, N., Chaisuk, C., Praserthdam, P., Assabumrungrat, S. (2011). Glycerol ethers synthesis from glycerol etherification with tert-butyl alcohol in reactive distillation. *Computer and Chemical Engineering,* 35, 2034-2043.

Kienle, A., Marquardt, W. (2002). Nonlinear dynamics and control of reactive distillation processes. In reactive distillation: Status and future directions. Sundmacher, K., & Kienle, A. Eds., Wiley-VCH Verlag.

King, C.J. (1980). Separation Processes. New York: McGraw-Hill.

Kinoshita, M., Hashimoto, I., Takamatsu, T. (1983). A new simulation procedure for multi component distillation column processing non-ideal solutions or reactive solutions. *Journal of Chemical Engineering of Japan,*16, 5, 370-377.

Khaledi, R., Bishnoi, P.R. (2006). A method for modeling two- and three-phase reactive distillation columns. *Industrial and Engineering Chemistry Research*,45, 6007-6020.

Kloker, M., Kenig, E.Y., Gorak, A., Markusse, A.P., Kwant, G., Moritz, P. (2004). Investigation of different column configurations for the ethyl acetate synthesis via reactive distillation. *Chemical Engineering and Processing: Process Intensification*, 43, 791-801.

Komatsu, H. (1977). Application of the relaxation method for solving reacting distillation problems. *Journal of Chemical Engineering of Japan*, 10, 200-205.

Komatsu, H., Holland, C.D. (1977). A new method of convergence for solving reacting distillation problems. *Journal of Chemical Engineering of Japan*, 10, 292-297.

Komatsu, H., Suzuki, I., Ishikawa, T., Hirata, M. (1970). Distillation accompanied by esterification of acetic acid-ethyl alcohol systems. Kagaku Kogaku, 34, 45-52. (Also available at: http://www.jstage.jst.go.jp/article/kakoronnbhunshu1953/34/1/34_1_45/_article)

Kreul, L.U., Gorak, A., Barton, P.I. (1999). Modeling of homogeneous reactive separation processes in packed columns. *Chemical Engineering Science*, 54, 19-34.

Kumar, V., Sharma, A., Chowdary, I.R., Ganguly, S., Saraf, D.N. (2001). A crude distillation unit model suitable for online applications. *Fuel Processing Technology*, 73, 1, 1-21.

Lai, I.K., Liu Y.C., Yu C.C., Lee M.J., Huang H.P. (2008). Production of high-purity ethyl acetate using reactive distillation: Experimental and start-up procedure. *Chemical Engineering and Processing*, 47, 1831–1843.

Lee, J.H., Dudukovic, M.P. (1998). A comparison of the equilibrium and non-equilibrium models for a multi component reactive distillation column. *Computers and Chemical Engineering*, 23, 159-172.

Lewis W.K., Matheson, G.L. (1932). Studies in distillation design of rectifying columns for natural and refinery gasoline. *Industrial and Engineering Chemistry Research*, 24, 494.

Liang, X., Gao, S., Gong, G., Wang, Y., Yang, J.G. (2008). Synthesis of a novel hetrogeneous strong acid catalyst from p-toluene sulfonic acid (PTSA) and its catalytic activities. *Catalysis Letter*, 124, 352-356.

Lv, B., Liu, G., Dong, X., Wei, W., Jin, W. (2012). Novel reactive distillation pervaporation coupled process for ethyl acetate production with water removal from reboiler and acetic Acid recycle. *Industrial and Engineering Chemistry Research*, 51, 8079−8086.

Macarron, A. (1959). Vapor-Liquid equilibria of binary mixtures methanol-acetic acid, ethanol-acetic acid, n-propanol-acetic acid, n-butanol acetic acid. *Chemical Engineering Science,* 10, 105-111.

Mahajani, S.M., Kolah, A.K. (1996). Some design aspects of reactive distillation columns (RDC). *Industrial and Engineering Chemistry Research*, 35(12), 4587-4596.

Malone, M.F., Doherty, M.F. (2000). Reactive distillation, commentary. *Industrial and Engineering Chemistry Research*, 39, 3953-3957.

Murthy, A.K.S. (1984). Simulation of distillation column reactors. *Proceedings of Summer Computer Simulation Conference,* Boston, MA, 630-635.

Nagata, I., Nakajima, J. (1991). Modification of the NRTL model for ternary and quaternary liquid-liquid equilibrium calculations. *Fluid Phase Equilibria,* 70, 275-292.

Naphtali, L.M., Sandholm, D.P. (1971). Multi component separation calculations by linearization. *American Institute of Chemical Engineers Journal*, 17, 148-153.

Nelson, P.A. (1971). Countercurrent equilibrium stage separation with reaction. *American Institute of Chemical Engineers Journal*, 17, 1043-1049.

Okur, H., Bayramoglu, M. (2001). The effect of the liquid-phase activity model on the simulation of ethyl acetate production by reactive distillation. *Industrial and Engineering Chemistry Research*, 40, 3639-3646.

Pearce, C.J. (1954). Extraction of acetic acid from water. *Chemical Engineering Science,* 3, 48-54.

Perez-Cisneros, E., Schenk, M., Gani, R., Pilavachi, P.A. (1996). Aspects of simulation, design and analysis of reactive distillation operations. *Computers and Chemical Engineering*, 20, S267-S272.

Pilavachi, P.A., Schenk, M., Perez-Cisneros, E., Gani, R. (1997). Modeling and simulation of reactive distillation operations. *Industrial and Engineering Chemistry Research*, 36, 3188-3197.

Roat, S.D., Downs, J.J., Vogel, E.F., Doss, J.E. (1986). The integration of rigorous dynamic modeling and control system synthesis for distillation columns: An industrial approach. In *Chemical process control-CPC III*. Morari, M. & McAvoy, T. J. Eds., New York: Elsevier.

Rose, A., Sweeny, R.F., Schrodt, V.N. (1985). Continuous distillation calculations by relaxation method. *Industrial and Engineering Chemistry Research*, 50, 737-740.

Russell, R.A. (1983). A flexible and reliable method solves single tower and crude-distillation-column problems. *Chemical Engineering Science,*90, 53-59.

Saeger, R.B., Bishnoi, P.R. (1986). A modified inside-out algorithm for simulation of multistage multi-component separation processes using the UNIFAC group-contribution method. *Canadian Journal of Chemical Engineering,*64, 759-767.

Salgovic, A., Hlavacek,V., Ilavsky, J.(1981). Global simulation of countercurrent separation processes via one-parameter imbedding techniques. *Chemical Engineering Science*, 36, 1599-1604.

Savković-Stevanović, J., Misic-Vukovic, M., Boncic-Caricic, G., Trisovic, B., Jezdic, S. (1992). Reaction distillation with ion exchangers. *Separation Science and Technology*, 27, 613-630.

Schoenmakers, H.G., Bessling, B. (2003). Reactive and catalytic distillation from an industrial perspective. *Chemical Engineering and Processing*, 42, 145–155.

Seader, J.D. (1989). The rate-based approach for modeling staged separations. *Chemical engineering progress,* 41-49.

Seader, J.D., Henley, E.J. (2006). Separation process principle. John Wiley & Sons Inc., New Jersey, U.S.A.

Seader, J.D., Henley, E.J., Roper, D.K. (2011). Separation process principle: chemical and biochemical operations. John Wiley & Sons Inc., New Jersey, U.S.A.

Sharma, M.M., Mahajani, S.M. (2002). Industrial applications of reactive distillation. In: Reactive Distillation: Status and Future Directions. K. Sundmacher and A. Kienle Eds. Weinheim, Wiley-VCH.

Sharma, N., Singh, K. (2010). Control of reactive distillation column: a review. *International Journal of Chemical Reactor Engineering*, 8, 1, R5.

Siirola, J.J. (1995). An industrial perspective on process synthesis. *American Institute of Chemical Engineers Symposium Series,* 91(304), 222-233.

Simandl, J. (1988). Simulation of distillation towers with chemical reactions. Ph.D. Thesis, University of Calgary.

Simandl, J., Svrcek, W.Y. (1991). Extension of the simultaneous solution and inside-outside algorithms to distillation with chemical reactions. *Computers and Chemical Engineering*, 15, 337-348.

Simandl, J., Svrcek, W. Y. (1985).Simulation of multi-stage reaction towers. P*roceedings of Summer Computer Simulation Conference,* Chicago, IL, 347-352.

Simandl, J., Svrcek, W.Y. (1987). Simulation of reactive distillation by the inside-outside method. *Proceedings of 37th Chemical Engineering Conference,* Montreal, Canada, 365-367.

Singh, D., Gupta, R.K., Kumar, V. (2014) Experimental studies of industrial-scale reactive distillation finishing column producing ethyl acetate. *Industrial and Engineering Chemistry Research*, 53, 10448−10456.

Singh, D., Gupta, R.K., Kumar, V. (2015). Simulation of a plant scale reactive distillation column for esterification of acetic acid. *Computers and Chemical Engineering*, 73, 70−81.

Singh, A., Tiwari, A., Bansal, V., Gudi, R. D., Mahajani, S.M. (2007). Recovery of acetic acid by reactive distillation: Parametric study and nonlinear dynamic effects. *Industrial and Engineering Chemistry Research***,** 46, 9196-9204.

Smejkal, Q., Kolena, J., Hanika, J. (2009). Ethyl acetate synthesis by coupling of fixed-bed reactor and reactive distillation column: Process integration aspects. *Chemical Engineering Journal*, 154, 236-2244.

Sneesby, M.G., Tade, M.O., Datta, R., Smith, T.N. (1998). Detrimental influence of excessive fractionation on reactive distillation. *American Institute of Chemical Engineers Journal*, 44, 388-393.

Spes, H. (1966). Katalytische reaktionen in ionenaustaucherkolonnen unter erschiebung des chemische geleichgewichts. *Chemiker Atg*/*Chemische Apparatur*, 90, 443-446.

Steinigeweg, S., Gmehling, J.(2002). n-butyl acetate synthesis via reactive distillation: Thermodynamic aspects, reaction kinetics, pilot-plant experiments and simulation studies. *Industrial and Engineering Chemistry Research*, 41, 5483–5490.

Steinigeweg, S., Gmehling,J. (2003). Esterification of a fatty acid by reactive distillation. *Industrial and Engineering Chemistry Research,* 42, 3612-3619.

Sundmacher, K., Kienle, A, Eds. (2002). *Reactive distillation: status and future directions*, Weinheim: Wiley-VCH.

Suzuki, I., Komatsu, H., Hirata, M. (1970). Formulation and prediction of quaternary vapor-liquid equilibria accompanied by esterification. *Journal of Chemical Engineering of Japan*, 3, 152-156.

Suzuki, I., Yagi, H., Komatsu, H., Hirata, M. (1971). Calculation of multi component distillation accompanied by chemical reaction. *Journal of Chemical Engineering of Japan*, 4, 26-33.

Tang, Y.T., Huang, H.P., Chien, I.L. (2003). Design of a complete ethyl acetate reactive distillation system. *Journal of Chemical Engineering of Japan*, 36, 11, 1352-1363.

Tang, Y.T., Hun, S.B., Chen, Y.W., Huang, H.P., Lee, M.J., Yu, C.C. (2005). Design of reactive distillations for acetic acid esterification with different alcohols. *American Institute of Chemical Engineers Journal*, 51, 1683-1699.

Taylor, R., Krishna, R. (1993). *Multi component Mass Transfer*. New York: Wiley.

Taylor, R., Krishna, R. (2000). Modeling reactive distillation. *Chemical Engineering Science*, 55, 5183-5229.

Taylor, R., Krishna, R., Kooijman, H. (2003). Real-world modeling of distillation. *Reactions and Separations*, 7, 28-39.

Thiele, E.W. Geddes, R.L. (1933). Computation of distillation apparatus for hydrocarbon mixtures. *Industrial and Engineering Chemistry Research*, 25, 289-295.

Tiemey, J. W., Riquelme, G. D. (1982). Calculation methods for distillation systems with reaction. Chemical *Engineering Communication*, 16, 91-108.

Tomich, J.F. (1970). A new simulation method for equilibrium stage process. *American Institute of Chemical Engineers Journal*,16, 229-232.

Tsai, Y.C., (2007). Kinetic study on synthesis of ethyl acetate via heterogeneous catalytic reaction, master thesis, department of chemical engineering, National Taiwan University of Science and Technology.

Tun, L.K., Matsumoto, H. (2013). Application methods for genetic algorithms for the search of feed positions in the design of a reactive distillation process. *Procedia Computer Science*, 22, 623 -632.

Ung, S., Doherty, M.F. (1995a). Necessary and sufficient conditions for reactive azeotropes in multi-reaction mixtures. *American Institute of Chemical Engineers Journal*, 41, 2383.

Ung, S., Doherty, M.F. (1995b). Vapor-liquid phase equilibrium in systems with multiple chemical reactions. *Chemical Engineering Science*, 50, 23-48.

Venimadhavan, G., Buzad, G., Doherty, M. F., Malone, M.F. (1994). Effect of kinetics on residue curve maps for reactive distillation. *American Institute of Chemical Engineers Journal*, *40*, 1814-1824.

Venimadhavan, G., Malone, M.F., Doherty, M.F. (1999a). Bifurcation study of kinetic effects in reactive distillation. *American Institute of Chemical Engineers Journal*, 45, 546-556.

Venkataraman, S., Chan, W.K., Boston, J.F. (1990). Reactive distillation using Aspen plus. *Chemical Engineering Progress*, 86, 8, 45-54.

Vickery, D.J. Taylor, R. (1986). Path-following approaches to the solution of multi component, multistage separation process problems. *American Institute of Chemical Engineers Journal*, 32, 547-556.

Vogel, A. I., Mendham, J., Denney, R. C. (1989). Vogels Textbook of Quantitative Chemical Analysis, 5th ed., Longman Scientific and Technical: London.

Vora, N., Daoutidis, P. (2001). Dynamics and control of an ethyl acetate reactive distillation column. *Industrial and Engineering Chemistry Research*, 40, 833–849.

Wang J.C., Henke, G.E. (1966). Tridiagonal matrix for distillation. *Hydrocarbon Process,* 45, 155-163.

Wayburn T.L. (1983). Modelling interlinked distillation columns by differential homotopy-continuation. Ph.D. Thesis. The University of Utah.

Wayburn, T.L., Seader, J.D. (1987). Homotopy-continuation methods for computer aided process design. *Computers and Chemical Engineering*, 11, 7-25.

Weng, K. C., Lee, H. Y. (25-27 June,2013). Feasibility analysis of ethyl acetate reactive distillation with different catalysts in low tray efficiencies. Proceedings of the 6th International Conference on Process Systems Engineering (PSE ASIA), Kuala Lumpur.

Wilson, G. M. (1964). Vapor–liquid equilibrium XI. A new expression for the excess Gibbs free energy of mixing. *Journal of the American Chemical Society*, *86*, 127.

Wu, K.C., Chen, Y.W. (2003). An efficient two-phase reaction process for the production of ethyl acetate. *Industrial and Engineering Chemistry Research,* 42, 5775-5781.

Appendix A

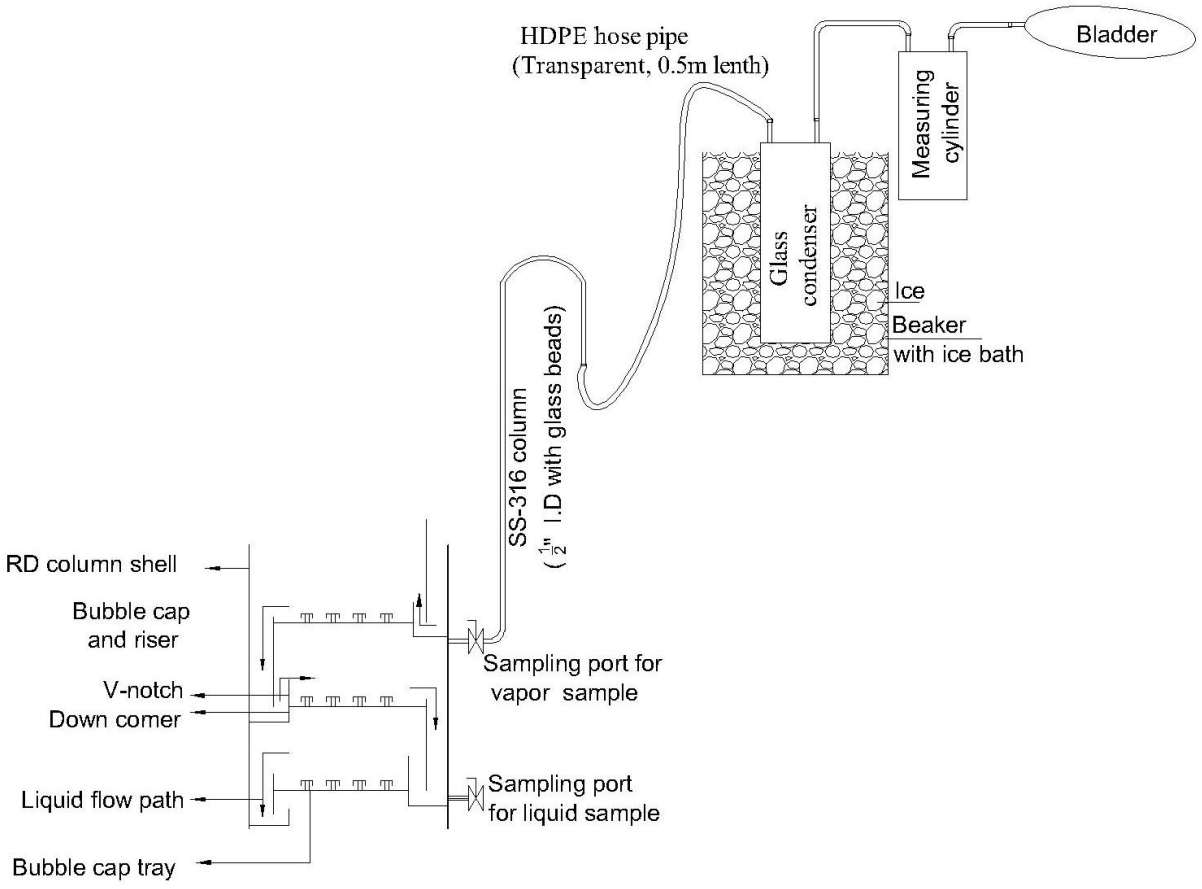

Figure A.1: Drawing of sampling device

Table A.1: Liquid and vapor phase mass percent of ethyl acetate (*EtAc*), acetic acid (*HAc*), ethanol (*EtOH*), and water (H_2O) at all stages counted from top (condenser being the first stage) for Case-1.

Stage No.	**Liquid phase (mass%)**				**Vapor phase (mass%)**				**Temp. (°C)**	**Gauge Pressure (atm)**
	EtAc	***HAc***	***EtOH***	***H_2O***	***EtAc***	***HAc***	***EtOH***	***H_2O***	**Liquid phase**	**Vapor phase**
1	NR	NR	NR	NR	90.68	0.00	1.32	8.00	NA	0.22
2	94.12	0.00	1.05	4.83	90.39	0.00	1.20	8.41	74	0.22
3	93.37	0.00	0.93	5.70	NR	NR	NR	NR	74	0.22
4	94.09	0.00	0.96	4.95	90.93	0.00	1.07	8.00	74	0.23
5	93.78	0.00	0.92	5.30	90.96	0.00	0.94	8.10	74	0.23
6	93.75	0.00	0.96	5.29	91.07	0.00	1.02	7.91	74.5	0.24
7	93.96	0.00	0.79	5.25	91.56	0.00	1.04	7.40	75	NR
8	93.79	0.00	1.14	5.07	91.33	0.00	1.10	7.57	76	0.25
9	93.23	0.00	1.47	5.30	91.54	0.00	1.07	7.39	77	NR
10	NR	NR	NR	NR	91.19	0.00	1.42	7.39	78	0.25
11	90.49	3.43	0.90	5.18	91.48	0.00	1.20	7.32	79	0.26
12	93.96	0.00	0.88	5.16	89.52	1.47	1.66	7.35	80	0.26
13	79.31	14.02	1.42	5.25	86.43	4.57	1.67	7.32	81	0.26
14	78.84	14.30	1.44	5.42	85.28	5.80	1.64	7.29	82	0.26
15	60.79	32.21	1.87	5.13	78.37	12.11	2.24	7.28	83	0.26
16	37.66	54.60	2.64	5.10	75.65	14.78	2.28	7.29	84	0.26
17	50.39	42.70	2.00	4.91	NR	NR	NR	NR	85	0.26
18	11.81	80.97	0.67	6.55	65.26	24.14	2.51	8.10	86	0.26
19	34.54	56.59	1.76	7.10	54.90	34.97	2.86	7.27	87	0.26
20	NR	NR	NR	NR	60.10	30.08	2.82	7.00	88	0.26
21	27.44	63.89	1.47	7.20	55.07	35.04	2.60	7.28	89	0.26
22	20.37	71.11	1.18	7.34	40.86	49.34	2.48	7.32	90	0.26
23	13.82	77.39	0.79	8.00	34.06	56.15	2.32	7.48	91	0.26
24	12.94	77.36	0.69	9.00	38.12	52.04	2.24	7.60	91.5	0.26
25	12.22	76.47	0.63	10.68	32.57	57.38	1.85	8.20	91.8	0.27
26	11.92	76.98	0.60	10.50	40.23	48.57	2.05	9.15	91.9	0.27
27	10.84	79.03	0.20	9.93	32.25	54.86	2.04	10.85	92	0.27
28	11.17	77.46	0.02	11.35	41.09	43.76	2.50	12.65	92	NR
29	NR	NR	NR	NR	35.65	48.88	1.14	14.33	93	0.27

30	11.76	77.58	0.40	10.26	37.18	46.27	1.32	15.23	93	0.27
31	10.31	78.18	0.21	11.30	31.45	51.50	1.65	15.40	94	0.27
32	9.65	78.16	0.02	12.17	33.45	49.38	1.68	15.50	94	0.27
33	8.55	77.97	0.99	12.49	32.81	50.50	1.80	14.89	94	0.27
34	13.53	76.92	0.57	8.98	33.25	50.52	1.63	14.60	95	0.27
35	7.79	79.94	0.37	11.90	33.18	51.27	1.70	13.85	96	0.27
36	9.27	79.35	0.35	11.02	32.27	50.91	2.52	14.31	97	0.28
37	12.61	75.40	0.46	11.53	26.82	57.53	1.28	14.36	98	0.28
38	15.44	73.85	0.41	10.30	36.56	48.19	0.83	14.42	99	0.28
39	11.56	76.54	0.51	11.39	38.79	47.92	0.94	12.34	100	0.28
40	13.02	76.84	0.34	9.80	28.45	59.96	1.07	10.52	101.5	0.29
41	9.63	81.91	0.27	8.19	19.36	66.96	1.56	12.12	103	0.29
42	9.72	80.84	0.30	9.14	20.84	66.17	0.97	12.01	105	0.29
43	7.63	83.65	0.20	8.52	8.75	78.56	0.75	11.93	107	0.3
44	6.86	83.83	0.71	8.60	6.35	81.43	0.52	11.70	108	0.3
45	5.04	85.67	0.13	9.16	3.36	85.79	0.20	10.66	110.5	0.31
46	5.06	85.26	0.16	9.51	4.11	85.18	0.22	10.50	111	0.32
47	2.39	88.33	0.03	9.25	2.92	90.88	0.00	6.20	112	0.33
48	2.93	91.19	0.18	5.70	NR	NR	NR	NR	113	0.34
49	2.54	93.93	0.03	3.5	NR	NR	NR	NR	115	0.34
50	NR	NR	NR	NR	NR	NR	NR	NR	116	0.22

Table A.2: Liquid and vapor phase mass percent of ethyl acetate (*EtAc*), acetic acid (*HAc*), ethanol (*EtOH*), and water(H_2O) at all stages counted from top (condenser being the first stage) for Case-2.

Stage No.	**Liquid phase (mass%)**				**Vapor phase (mass%)**				**PTSA (wt%)**	**Temp. (°C)**	**Gauge Pressure (atm)**
	EtAc	***HAc***	***EtOH***	***H_2O***	***EtAc***	***HAc***	***EtOH***	***H_2O***	**Liquid phase**	**Liquid phase**	**Vapor phase**
1	NA	NA	NA	NA	91.30	0.00	1.20	7.50	NA	NA	0.23
2	94.53	0.00	1.24	4.23	90.76	0.00	1.23	8.01	NA	74	0.23
3	93.63	0.00	1.25	5.12	91.29	0.00	1.21	7.50	NA	74	0.23
4	94.49	0.00	1.16	4.35	91.20	0.00	1.30	7.50	NA	74	0.23
5	94.20	0.00	1.06	4.74	91.08	0.00	1.26	7.66	NA	74	0.25
6	94.22	0.00	1.09	4.69	91.60	0.00	1.09	7.31	NA	74.5	0.25
7	94.38	0.00	1.01	4.61	91.65	0.00	1.25	7.10	NA	75	NR
8	94.40	0.00	1.15	4.46	91.86	0.00	1.17	6.97	NA	76	0.26
9	94.32	0.00	1.00	4.68	92.15	0.00	0.95	6.89	NA	77	NR
10	NR	NR	NR	NR	92.30	0.00	0.85	6.85	NA	77.5	0.26
11	94.46	0.00	0.96	4.58	92.12	0.00	1.06	6.82	NA	78	0.26
12	94.42	0.00	1.04	4.54	92.19	0.00	1.01	6.81	NA	78.5	0.27
13	87.15	0.00	1.15	11.70	92.28	0.00	0.92	6.79	NA	79	0.27
14	94.34	0.00	0.85	4.81	92.33	0.00	0.88	6.79	NA	80	0.27
15	92.50	1.43	1.64	4.43	92.19	0.00	1.03	6.78	NA	81	0.27
16	93.28	1.33	0.81	4.58	92.20	0.00	1.02	6.78	NA	81.5	0.27
17	94.17	0.69	0.82	4.31	92.12	0.00	1.11	6.77	NA	82	0.27
18	87.69	4.51	1.85	5.95	92.31	0.00	0.92	6.77	NA	83	0.27
19	80.27	12.15	1.05	6.53	84.86	7.09	1.28	6.77	NA	84	0.27
20	82.61	9.92	1.00	6.47	86.25	5.81	1.18	6.77	NA	84.5	0.27
21	NR	NR	NR	12.72	81.03	10.75	1.44	6.78	NA	85	0.27
22	76.41	15.74	1.11	6.74	80.92	11.04	1.23	6.82	NA	86	0.27
23	35.27	51.07	1.24	12.42	78.65	12.96	1.46	6.93	NA	87	0.27
24	55.66	34.63	1.33	8.38	61.72	29.63	1.48	7.17	NA	88	0.27
25	29.38	59.45	1.09	10.08	63.79	26.99	1.54	7.69	NA	89	0.27
26	35.08	53.31	1.19	10.42	60.72	29.08	1.55	8.65	NA	90	0.27
27	20.01	69.85	0.81	9.33	66.27	22.00	1.53	10.20	NA	91	0.28
28	20.29	67.34	1.63	10.75	67.73	18.81	1.31	12.15	NA	92	NR
29	NR	NR	NR	NR	48.86	35.87	1.45	13.83	NA	92.5	0.28

30	24.27	65.06	1.01	9.66	49.66	34.18	1.43	14.73	NA	93	0.28
31	17.74	70.75	0.73	10.78	41.13	42.72	1.25	14.90	NA	93.5	0.28
32	20.79	66.80	0.84	11.57	44.40	39.58	1.33	14.70	NA	93.5	0.28
33	13.44	73.78	0.89	11.89	39.17	44.98	1.46	14.39	0.001	94	0.28
34	17.74	73.16	0.72	8.38	35.22	48.14	2.54	14.10	0.002	94.5	0.28
35	12.17	76.00	0.52	11.31	47.05	38.30	1.29	13.35	0.009	95	0.28
36	9.33	79.89	0.36	10.42	36.07	47.86	2.46	13.61	0.009	96	0.28
37	11.28	77.68	0.44	10.60	38.35	46.56	1.23	13.86	0.025	97	0.29
38	9.77	80.28	0.25	9.70	35.85	48.18	1.85	14.12	0.031	98	0.29
39	11.64	77.06	0.51	10.79	27.98	58.23	1.44	12.34	0.050	99	0.3
40	10.91	79.59	0.30	9.20	28.97	59.76	1.25	10.02	0.040	101	0.31
41	9.23	82.93	0.26	7.58	20.29	66.95	1.14	11.62	0.047	103	0.31
42	9.25	81.98	0.22	8.54	23.13	64.04	1.21	11.61	0.041	105	0.32
43	8.17	83.72	0.19	7.92	20.41	67.19	0.97	11.43	0.059	106.5	0.33
44	6.30	85.49	0.18	8.03	18.41	69.68	0.91	11.00	0.037	108	0.34
45	5.45	85.84	0.15	8.56	11.52	76.68	0.54	11.26	0.034	109	0.34
46	5.09	85.85	0.15	8.91	8.30	80.84	0.36	10.50	0.031	110	0.35
47	3.04	88.19	0.08	8.69	NR	NR	NR	NR	0.029	111.5	0.35
48	6.37	88.17	0.29	5.17	NR	NR	NR	NR	0.026	113	0.36
49	2.19	93.76	0.06	4.00	NR	NR	NR	NR	0.023	115.5	0.36
50	NR	NR	NR	NR	NR	NR	NR	NR	0.025	117	NR

Appendix B

Table B.1:Statistics for *EtAc-H_2O* binary pair regression

x	y (lit)	y (regressed)	Error	Error square
0.0006	0.0405	0.0545595	-0.01406	0.00019767
0.0011	0.1256	0.0965819	0.029018	0.00084205
0.0459	0.71	0.695989	0.014011	0.000196308
0.69	0.707	0.6891493	0.017851	0.000318647
0.775	0.699	0.7050774	-0.00608	3.69348E-05
0.8737	0.765	0.7524153	0.012585	0.000158375
0.9444	0.865	0.846526	0.018474	0.000341289
0.9807	0.9411	0.9374231	0.003677	1.35196E-05
Bias = 0.009435 Standard deviation = 0.014106 RMSE = 0.016220331				

y(lit) = experimental data from literature; y (regressed) = regressed values; Error = [(y (lit)-y(regressed)]; Std. dev. = standard deviation; R. std. dev. = relative standard deviation

Table B.2: Statistics for *EtAc-HAc* binary pair regression

x	y (lit)	y (regressed)	Error	Error square
0.0238	0.0825	0.09136	-0.00886	7.84996E-05
0.0366	0.1189	0.1241732	-0.00527	2.78066E-05
0.0476	0.1518	0.1551554	-0.00336	1.12587E-05
0.0776	0.2443	0.238674	0.005626	3.16519E-05
0.0907	0.2718	0.2759159	-0.00412	1.69406E-05
0.117	0.3265	0.3324631	-0.00596	3.55586E-05
0.141	0.3795	0.3831491	-0.00365	1.33159E-05
0.1657	0.4297	0.4289284	0.000772	5.95367E-07
0.2203	0.5369	0.5158394	0.021061	0.000443549
0.2661	0.6113	0.5820559	0.029244	0.000855217
0.3085	0.6739	0.6390266	0.034873	0.001216154
0.3924	0.7621	0.7240544	0.038046	0.001447468
0.4617	0.8215	0.7855222	0.035978	0.001294402
0.4924	0.8463	0.8025648	0.043735	0.001912768
0.5332	0.8702	0.8310073	0.039193	0.001536068
0.5559	0.882	0.8456686	0.036331	0.001319971
0.6068	0.9074	0.8727751	0.034625	0.001198884
0.6568	0.9266	0.8925035	0.034097	0.001162571
0.6986	0.9439	0.9106341	0.033266	0.00110662
0.7426	0.9571	0.9292658	0.027834	0.000774743
0.7974	0.971	0.9461213	0.024879	0.00061895
0.8415	0.9769	0.9597088	0.017191	0.000295537
0.8644	0.9811	0.9675639	0.013536	0.000183226
0.9197	0.9898	0.9818681	0.007932	6.2915E-05
0.9482	0.9938	0.9895854	0.004215	1.77629E-05
0.9809	0.9968	0.9966798	0.00012	1.4448E-08
Bias = 0.017359 Standard deviation = 0.017694 RMSE = 0.024543875				

y(lit) = experimental data from literature; y (regressed) = regressed values; Error = [(y (lit)-y(regressed)]; Std. dev. = standard deviation; R. std. dev. = relative standard deviation

Table B.3:Statistics for *HAc-H_2O* binary pair regression

X	y (lit)	y (regressed)	Error	Error square
0.0901	0.2253	0.2282844	-0.00298	8.90664E-06
0.1414	0.3177	0.3050252	0.012675	0.000160651
0.1934	0.3954	0.3678336	0.027566	0.000759906
0.2593	0.4654	0.4424054	0.022995	0.000528752
0.3241	0.5311	0.4988686	0.032231	0.001038863
0.3627	0.5622	0.5340644	0.028136	0.000791612
0.4454	0.6371	0.6006484	0.036452	0.001328719
0.47	0.6593	0.6247036	0.034596	0.001196911
0.5071	0.6844	0.648404	0.035996	0.001295712
0.5337	0.7047	0.6718154	0.032885	0.001081397
0.5698	0.7271	0.6949887	0.032111	0.001031136
0.6046	0.7536	0.7255786	0.028021	0.000785199
0.6546	0.7961	0.763392	0.032708	0.001069813
0.68	0.82	0.7858659	0.034134	0.001165137
0.7057	0.8394	0.8007553	0.038645	0.001493413
0.73	0.8566	0.8155642	0.041036	0.001683937
0.7789	0.8819	0.8521798	0.02972	0.00088329
0.8287	0.9064	0.8880506	0.018349	0.0003367
0.8557	0.9183	0.9091051	0.009195	8.45462E-05
0.8963	0.9419	0.9160368	0.025863	0.000668905
0.914	0.9515	0.9498066	0.001693	2.8676E-06
0.9391	0.9651	0.9628539	0.002246	5.04497E-06
0.9653	0.9809	0.9818329	-0.00093	8.70302E-07
0.9902	0.9951	0.9940417	0.001058	1.12E-06
Bias = 0.0231 Standard deviation = 0.014137 RMSE = 0.026928461				

y(lit) = experimental data from literature; y (regressed) = regressed values; Error = [(y (lit)-y(regressed)]; Std. dev. = standard deviation; R. std. dev. = relative standard deviation

Table B.4:Statistics for *HAc-EtOH* binary pair regression

x	y (lit)	y (regressed)	Error	Error square
0.055	0.107	0.110036	-0.00304	9.21608E-06
0.073	0.144	0.152197	-0.0082	6.71908E-05
0.103	0.197	0.213412	-0.01641	0.000269341
0.133	0.274	0.27216	0.00184	3.3845E-06
0.166	0.312	0.328412	-0.01641	0.00026936
0.207	0.393	0.399492	-0.00649	4.21409E-05
0.233	0.437	0.44984	-0.01284	0.000164873
0.28	0.526	0.528103	-0.0021	4.42177E-06
0.347	0.597	0.612738	-0.01574	0.000247697
0.46	0.75	0.742252	0.007749	6.00393E-05
0.516	0.793	0.799534	-0.00653	4.26932E-05
0.587	0.854	0.855275	-0.00127	1.62537E-06
0.659	0.9	0.900016	-1.5E-05	2.4025E-10
0.728	0.934	0.93489	-0.00089	7.91922E-07
0.816	0.966	0.967209	-0.00121	1.46241E-06
0.924	0.99	0.991332	-0.00133	1.77396E-06
1.0	1.0	1.0	0	0
Bias = -0.00488 Standard deviation = 0.00699 RMSE = 0.008352568				

y(lit) = experimental data from literature; y (regressed) = regressed values; Error = [(y (lit)-y(regressed)]; Std. dev. = standard deviation; R. std. dev. = relative standard deviation

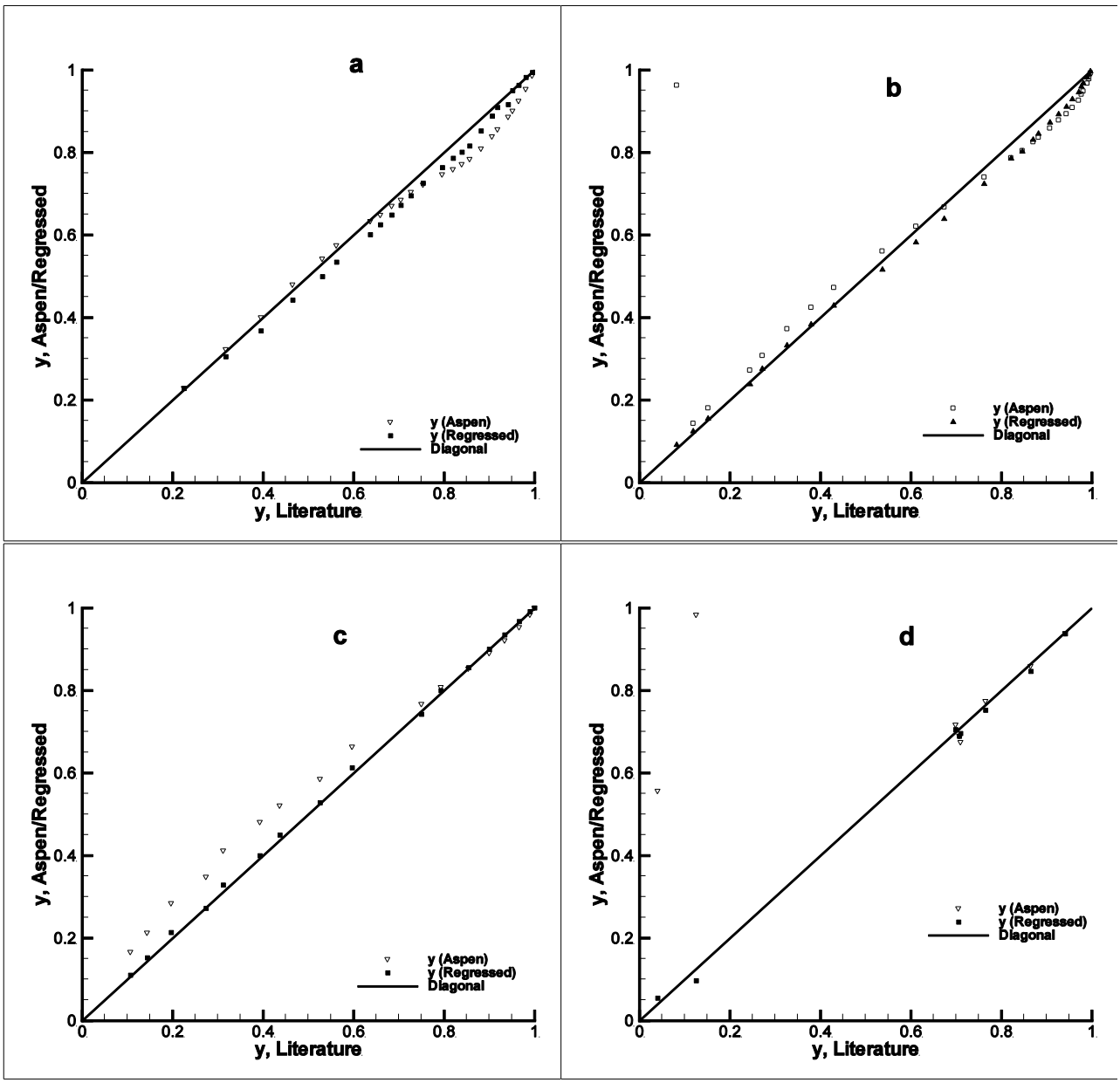

Figure B.1: Parity plots for regressed and Aspen Plus parameters of binary pairs(a)*HAc-H_2O*; (b) *EtAc-HAc*; (c) *HAc-EtOH*; (d) *EtAc-H_2O*

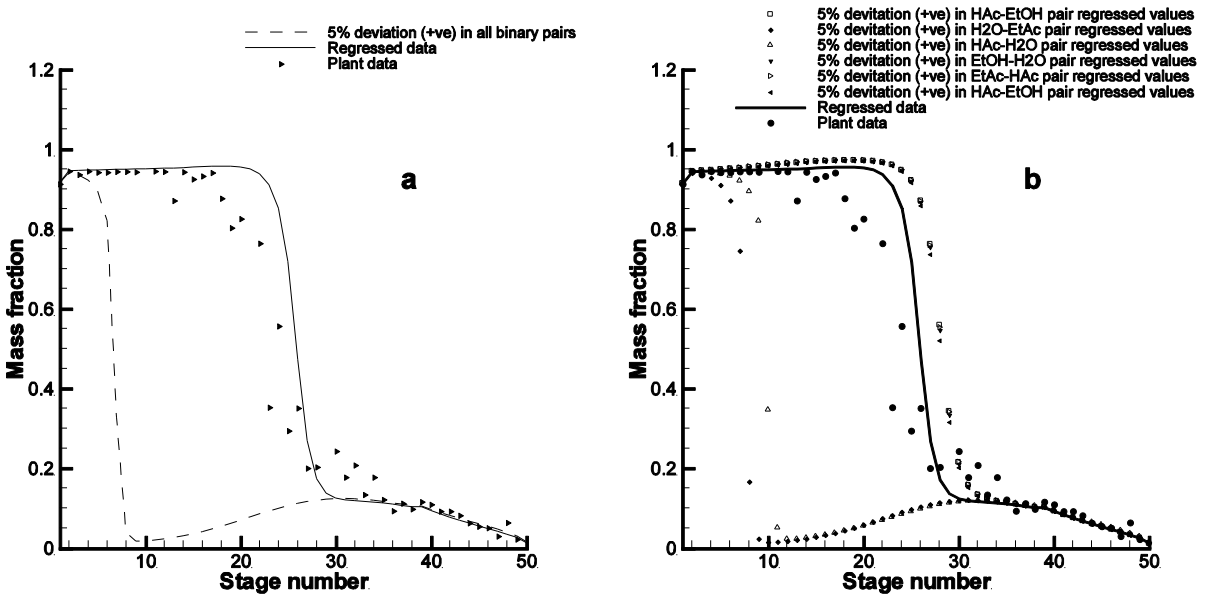

Figure B.2: Sensitivity of *EtAc* composition profile to (a) 5% decrease in the values of parameters of all binary pairs; (b) 5% decrease in the value of parameters of one binary pair at a time

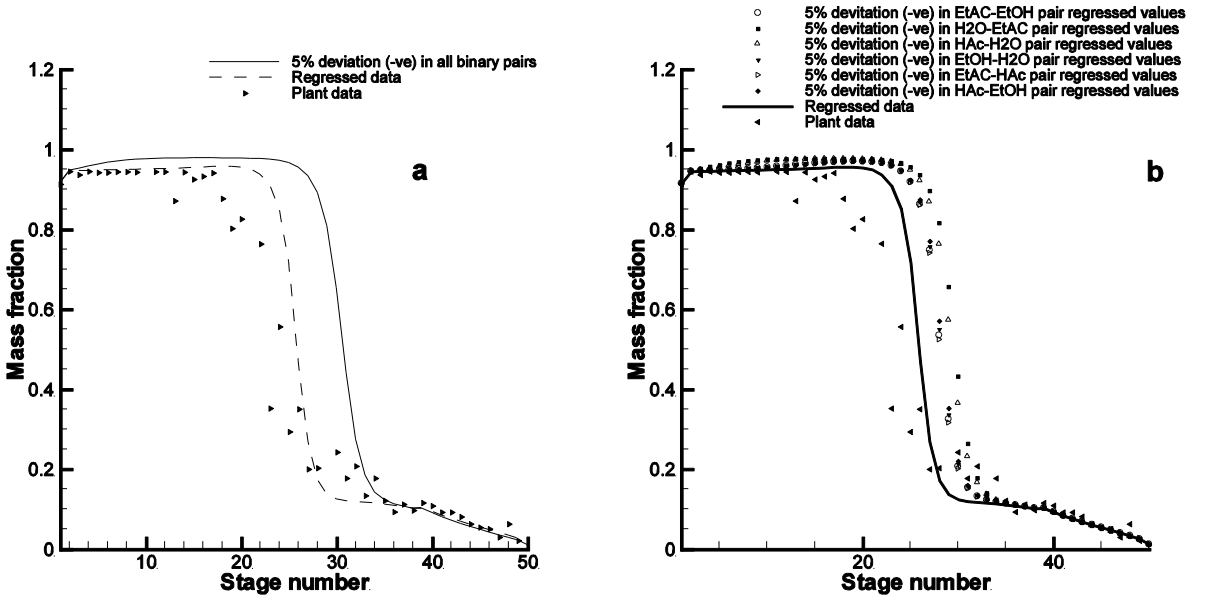

Figure B.3: Sensitivity of *EtAc* composition profile to (a) 5% decrease in the values of parameters of all binary pairs; (b) 5% decrease in the value of parameters of one binary pair at a time

Appendix C

Table C.1: Various models for the liquid and vapor phase properties, with NRTL as base property method, used for Aspen Plus simulation

Property	**Model name**
PHIVMX	ESIG
GAMMA	GMRENON
WHNRY	WHENRY
PL	PL0XANT
PHIV	ESIG0
PHILPC	PHILPC00
HNRY	HENRY1
HNRYPC	HNRYPC00
DHVMX	ESIG
VLPM	VL1BROC
DHVL	DHVLWTSN
DHV	ESIG0
DHLPC	DHLPC00
DGVMX	ESIG
DSVMX	ESIG
VVMX	ESIG
VLMX	VL2RKT
MUVMXLP	MUV2WILK
MUVLP	MUV0CEB
MULMX	MUL2ANDR
KVMXLP	KV2WMSM
KVLP	KV0STLP
KLMX	KL2SRVR
DVMX	DV1CEWL
DLMX	DL1WCA
SIGLMX	SIG2HSS
DGV	ESIG0
DSV	ESIG0
VV	ESIG0
VL	VL0RKT
MUL	MUL0ANDR
KVPC	KV0STPC
VV	ESRK0
KL	KL0SR
DV	DV0CEWL
DL	DL0WCA
SIGL	SIG0HSS
GAMMA	GMIDL
PS	PS0ANT
PHISPC	PHISPC00
HS	HS0POL1
GS	GS0POL1
VSMX	VS2IS
VS	VS0POLY
KSMX	KS2IDL
KS	KS0POLY
SS	SS0POL1
WSL	WSL001
HCSL	HCSOL1